3-iodothyronamine (T_1AM) effects on glutamatergic postsynaptic signaling pathway

Doctoral programme of Biochemistry and Molecular Biology – Bibim 2.0

Candidate
Lavinia Bandini

Supervisor
Prof. Riccardo Zucchi

Abstract

Thyroid hormones (TH), namely thyroxine (T_4) and 3,5,3'-triiodothyronine (T_3), are crucial regulators of multiple growth processes and control systems of energy metabolism. T_4 and T_3 undergo a complex metabolism *in vivo,* by several enzymes encompassing deiodinases, amine transferases, amine oxidases, decarboxylases and several classes of conjugating enzymes, particularly sulfotransferases and UDP-glucuronosyltransferases.

T_4 or T_3 metabolites can produce significant functional effects when administered via interaction either with Thyroid Hormone Receptor (TR), or with other receptors. They are considered as chemical messengers further enriching TH signaling, and have become known as "novel thyroid hormones" or "active thyroid hormones metabolites". These novel hormones include: T_2; Thyronamines (TAMs), mostly 3-iodothyronamine (T_1AM) and non-iodinated thyronamine (T_0AM); thyroacetic acids, mostly 3,5,3',5'-thyroacetic acid (TA_4), 3,5,3'-thyroacetic acid (TA_3), and 3-thyroacetic acid (TA_1).

Recently, it emerged that 3-iodothyronamine (T_1AM), a derivative of decarboxylation and deiodination of thyroid hormones, has pro-learning and anti-amnestic effects, modulates pain threshold, sleep pattern and food intake. It also counteracts beta-amyloid toxicity in mice.

Glutamatergic neurotransmission, the major excitatory system in the brain, plays a key role in regulating neuroplasticity, learning and memory, and it is often compromised in neurological disorders. T_1AM reduced availability might results in some disorders associated with thyroid hormones. T_1AM binds to the trace amine-associated receptor 1 (TAAR1) a G-protein coupled receptor with a putative role in neurotransmission.

In the present work, firstly we characterized the gene expression profile of two different brain cell lines and then we evaluated the effects of T_1AM on the expression of proteins involved in the glutamatergic postsynaptic pathway.

A hybrid line of cancer cells of mouse neuroblastoma and rat glioma (NG 108-15) and a human glioblastoma cell line (U-87 MG) were used. We first characterized the *in vitro* model by analyzing gene expression of several proteins involved in the glutamatergic postsynaptic cascade by real time PCR (RT-PCR), and cellular uptake and metabolism of T_1AM by HPLC coupled to mass spectrometry (HPLC MS-MS).

The cell lines were then treated with T_1AM, ranging from 0.1 to 10 μM, alone or in combination with 10 μM resveratrol (RSV) and/or 10 μM amyloid β peptide (25-35). Cell viability, glucose

consumption, protein expression, cAMP production and calcium concentration in cell lysates were assessed.

Our results indicated that both cell lines expressed receptors implicated in glutamatergic pathway, namely AMPA, NMDA and EphB2, but only U-87 MG cells expressed TAAR1 and they took up T_1AM which was catabolized to TA_1 and might be used as biochemical model to study its post synaptic signaling cascade.

At micromolar concentration T_1AM had a slightly but significant cytotoxic effect, that is completely blunted if incubated with RSV and it was able to induce different post-translational modification in neuronal cell lines.

T_1AM reduced glucose consumption and decreased intracellular calcium concentration in NG 108-15 cell line, while increased cAMP concentration, albeit at different doses.

At pharmacological concentrations, the major effect highlighted in both cell lines was an increase in the phosphorylation of proteins involved in the glutamatergic postsynaptic signaling.

In the NG 108-15 cells an increase in phosphorylation of ERK extracellular signal-regulated kinases (ERKs) (pERK/ total ERK) and CaMKII Ca-calmodulin-dependent protein kinase (CaMK) II (pCaMKII/total CaMKII).

In U-87 MG cells, T_1AM induced the phosphorylation of the transcriptional factor cAMP response element-binding protein (CREB) and increase the expression of cFOS. Expression or post-translational modifications of other proteins were not affected.

We then extend investigation on the effects of 3-iodothyroacetic acid TA_1, a catabolite of T_1AM and of thyroid hormone, on brain cell lines focusing on the glutamatergic postsynaptic pathway that we explored by infusion with T_1AM, assuming that TA_1 may either strengthen T_1AM effects or exert parallel actions, especially in brain tissue.

First, we assessed uptake and metabolism of TA_1. Cell lines were treated with TA_1 for 24h, at concentration ranging from 0.1 to 10 μM. Uptake, cell viability, cAMP production and protein expression were assessed.

TA_1 was taken up by cells, even though only a slight reduction in medium concentration was recorded upon 24h of incubation. Cell viability was significantly increased by TA_1 10 μM in U-87 MG cell line, while NG 108-15 cells were unaffected.

Western blot analysis indicated that, upon infusion of pharmacological doses of TA_1, neither the expression of Sirtuin 1, (p=NS) nor the post-translational modifications of ERK (pERK/total ERK, p=NS) were affected in U-87 MG. Instead TA_1 induced the phosphorylation of the transcriptional factor cAMP response element-binding protein (CREB) (pCREB/total).

In NG 108-15 cell line, preliminary analysis on protein expression and post-translational modification after TA_1 infusion, indicated that no modifications of ERK (pERK/total ERK) were occurred.

In conclusion our results indicated that NG 108-15 and U-87 MG cells express receptors implicated in the glutamatergic system and, at pharmacological concentrations, T_1AM can affect glutamatergic signaling.

Therefore, our preliminary results suggest that, in our experimental models, TA_1 does not seem to mimic T_1AM effects.

Abbreviations

ADR	Alfa Adrenergic receptor
AMPA	α-amino-3-hydroxy-5-methyl-4-isoxazolepropionate
ADHD	Attention Deficit Hyperactivity Disorder
ApoB	Apolipoprotein B
ATP	Adenosine Triphosphate
BBB	Blood-Brain Barrier
Ca^2	Calcium
cAMP	Cyclic adenosine monophosphate
CaMKII	Calcium/calmodulin-dependent protein kinase II
CREB	cAMP response element-binding protein
CSF	Cerebrospinal Fluid
DEHAL-1	Iodotyrosine Dehalogenase1
DIO	Iodothyronine deiodinase
DIT	Diiodotyrosine
ERK	Extracellular Signal–Regulated Kinase
EphB2	Ephrin type-B receptor 2
EPSP	Excitatory postsynaptic potential
FBS	Fetal bovine serum
fTH	Free TH
GLUT	Glucose Transporter
GPCR	G-protein-coupled receptors
H^+	Hydrogen
HIF-1	Hypoxia-inducible factor 1
HPLC	High performance liquid chromatography
HPLC-MS-MS	HPLC coupled to tandem mass spectrometry
HPT	Hypothalamic-pituitary-thyroid axis
HSA	Human Serum Albumin

I	Iodine
I^-	Iodide
K^+	Potassium
LDL	Low density protein
LTP	Long-term potentiation
MAO	Monoamine oxidases
MAPK	Mitogen-activated protein kinase
MCT	Monocarboxylate Transporter
MIT	Monoiodotyrosine
MS	Mass spectrometry
MS-MS	Tandem mass spectrometry
MTT	3-(4,5-dimethylthiazol-2-yl)-2,5-diphenyltetrazolium bromide
Na^+	Sodium
NMDA	N-methyl-D-aspartate
ODC	Ornithine decarboxylase
PIK-3	Phosphatidylinositol 3-kinase
PMSF	Phenylmethylsulphonyl fluoride
PKA	Protein kinase A
PKC	Protein kinase C
PLC	Phospholipase C
rT_3	3,3',5'-triiodothyronine or reverse T_3
RQ	Respiratory quotient
RT-PCR	Real Time - Polymerase Chain Reaction
T_0AM	Thyronamine
T_1AM	3-Iodothyronamine
T_2	Diiodothyronine
T_2AM	Diiodothyronamine
T_3	3,5,3'-Triiodo-L-Thyronine
T_3AM	Triiodothyronamine
T_4	3,5,3',5'-Tetraiodo-L-Thyronine or Thyroxine
TA_1	3-Iodothyroacetic Acid

TA_3	3,5,3’-thyroacetic acid
TA_4	3,5,3’,5’-thyroacetic acid
TAAR1	Trace-Amine Associated Receptor 1
TAM	Thyronamine
TBG	Thyroid Binding Globulin
Tetrac	3,5,3’,5’-tetraiodothyroacetic acid
TG	Thyroglobulin
TH	Thyroid Hormones
TPO	Thyroperoxidase
TR	Thyroid Hormone Receptor
TRE	Thyroid hormone response element
TRH	Thyrotropin-Releasing Hormone
TRPM	Transient Receptor Potential Cation Channel Subfamily M
TSH	Thyroid-Stimulating Hormone
Triac	3,5,3’-triiodothyroacetic acid
TTR	Transthyretin
UDP	Uridine diphosphate

Summary

List of figures

List of tables

Introduction

1.1 Thyroid hormones

Thyroid hormones (TH) are required for normal development as well as regulating metabolism. TH crucially control many processes in all vertebrates, including humans, regulating many homeostatic processes such as growth, reproduction and energy balance (Mullur 2014). Their action is essential for the biological function of all tissues, including brain development; regulation of cardiovascular, bone, and liver function; food intake; and energy expenditure among many others (Fekete 2014).

The role of TH in regulating metabolic pathways has led to several new therapeutic targets for metabolic disorders. Hyperthyroidism, excess thyroid hormone, promotes a hypermetabolic state characterized by increased resting energy expenditure, weight loss, reduced cholesterol levels, increased lipolysis, and gluconeogenesis. Conversely, hypothyroidism, reduced thyroid hormone levels, is associated with hypometabolism characterized by reduced resting energy expenditure, weight gain, increased cholesterol levels, reduced lipolysis, and reduced gluconeogenesis (Mullur 2014).

Moreover, thyroid hormones orchestrate many aspects of neurodevelopment, including cell cycle progression, fate choice, migration, differentiation, axo- and synaptogenesis, and myelination (Vancamp 2020).

In humans, derangements of TH function in the foetus result in multi-organ complications. Epidemiological evidence in areas of iodine deficiency and data from children born to women with thyroid disorders indicate that maternal TH deficiency dramatically alter neurodevelopment in the progeny, leading to physical and mental disturbances. These include cretinism, deafness, schizophrenia, attention deficit hyperactive disorder (ADHD) and autism (de Escobar 2007; Hetzel 2000; Zimmermann 2008).

Although THs may exert their effects on a number of intracellular loci, their primary effect is on the transcriptional regulation of target genes. Early studies showed that the effects of TH at the genomic level are mediated by nuclear TRs, which are intimately associated with chromatin and bind TH with high affinity and specificity. Like steroid hormones that also bind to nuclear receptors, TH enter the cell and proceeds to the nucleus (Yen 2001).

1.1.1 Biosynthesis and metabolism of T_3 and T_4

With the term thyroid hormones (TH), we refer to the iodinated tyrosine-based molecules 3,3',5,5'-tetra-iodothyronine (T_4 or Thyroxine) and 3,5,3'-tri-iodothyronine (T_3) (Figure 1).

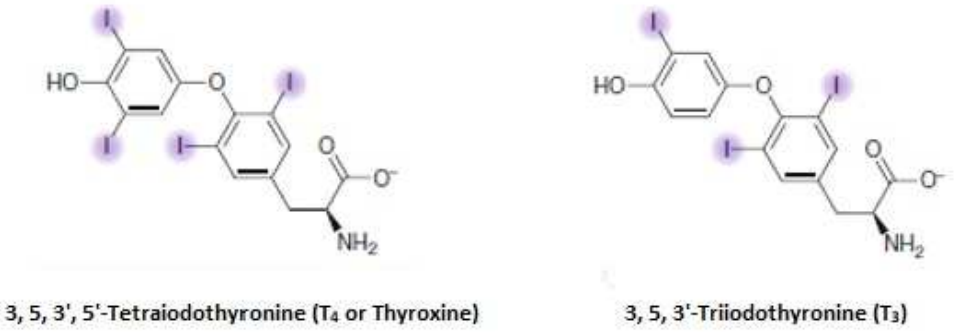

Figure 1. Chemical structure of T_4 and T_3. The two tyrosinic rings containing 4 and 3 atoms of iodine, respectively, are coupled together through an ether bridge.

Thyroid hormones are produced and secreted by the thyrocytes, the follicular cells of the thyroid gland, into the circulation in two forms, the inactive prohormone (T_4), and the biologically active form of thyroid hormone (T_3), differing in the number of bound iodine atoms. Only ~20% is secreted as T_3, the remaining derived from T_4 to T_3 deiodination by type 1 and 2 deiodinases (Dio1 and Dio2) (Gereben 2015, Luongo 2019).

Synthesis of T_4 consists of two sequential steps and relies on iodide availability, which is taken up as iodide (I^-) across the basolateral membrane of thyrocytes by the sodium/iodide (Na^+/ I^-) symporter, and then moved across the apical membrane into the follicle colloid. The transport of iodide inside the follicles is the first phase of the thyroid hormone biosynthesis and it is also the main limiting factor (Di Jeso 2016) (Figure 2).

Pendrin then allows the exit of the iodides through the apical plasma membrane, into the colloid. Here, thyroperoxidase (TPO) oxidizes iodide to an iodinating form and this reactive iodide is covalently linked to selected tyrosines of thyroglobulin (Tg), a large homodimeric glycoprotein synthesized by the follicular cells and then secreted into the follicular lumen by exocytosis. This results in either single or double-iodinated residues of tyrosine, named "Monoiodotyrosine (MIT)" and "Diiodotyrosine (DIT)", respectively.

Under these oxidizing conditions, MIT/DIT are coupled to form thyroid hormones T_3 and T_4 on thyroglobulin supports. Follicular cells then absorb the colloid globules by endocytosis, and these vesicles fuses with the lysosomes releasing T_4, T_3, DIT, and MIT into the cytoplasm. The iodide from uncoupled to MIT and DIT is recycled by tyrosine dehalogenase (Dehal1) (Di Jeso 2016).

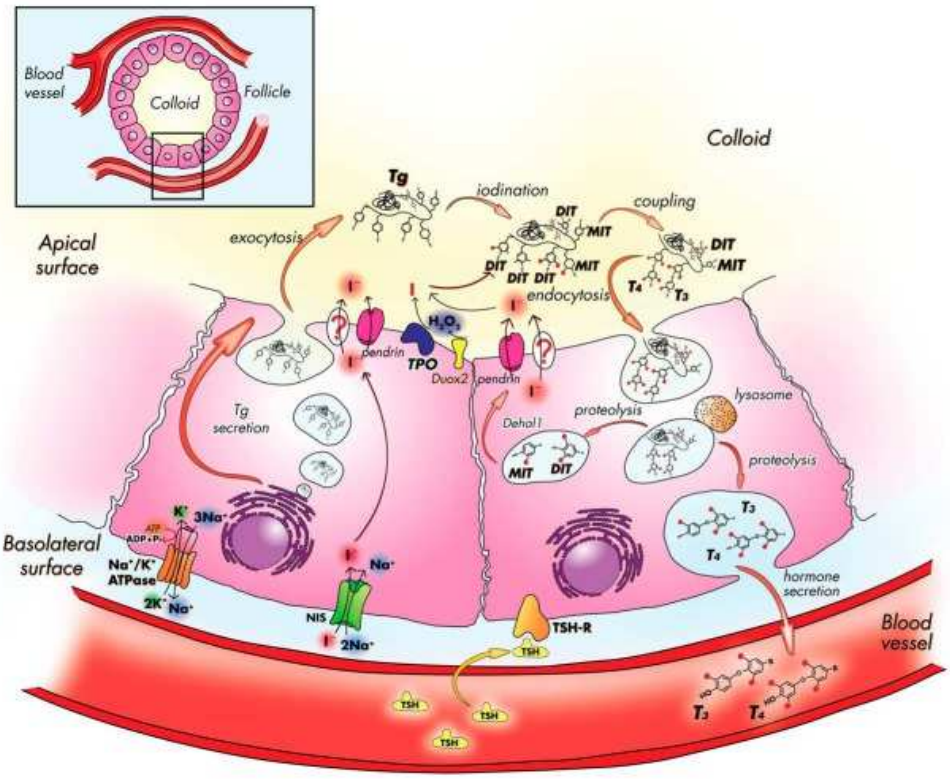

Figure 2. Schematic representation of all the steps of the thyroid hormone biosynthesis and its secretion between thyroid follicles and blood vessels (Di Jeso 2016).

Normal thyroid function is the result of defensive mechanisms that avoid over-supply of TH to tissues/organs, modulating their availability in target cells, their circulating concentrations and therefore they mediate synthesis, secretion and metabolism (Luongo 2019).

First, the production of T_3 and T_4 is regulated by the pituitary thyroid-stimulating hormone TSH (thyrotropin), whose release is in turn stimulated by the hypothalamic thyrotropin-releasing hormone TRH (thyrotropin-releasing factor) (Fekete 2014).

Levels of TH control the secretion of TRH and TSH at hypothalamus and pituitary gland, respectively, by a negative feedback mechanism, to maintain physiological levels of the main hormones of the hypothalamic-pituitary-thyroid axis (HPT axis) (Ortiga 2016, Hoermann 2015, Fekete 2014).

In addition to TRH/TSH regulation by TH feedback, there is central modulation by nutritional signals, such as leptin, as well as peptides regulating appetite. The nutrient status of the cells provides feedback on TH signaling pathways through some epigenetic modification of histones. Integration of TH signaling with the adrenergic nervous system occurs peripherally, in liver, white fat, and brune adipose tissue, but also centrally, in the hypothalamus (Fekete 2014).

Reduction of circulating TH levels, due to primary thyroid failure, results in increased TRH and TSH production, whereas the opposite occurs when circulating TH are in excess. Thus, the hypothalamus, the pituitary, and the thyroid form the HPT axis, which regulates the circulating concentration of TH (Ortiga 2016) (Figure 3).

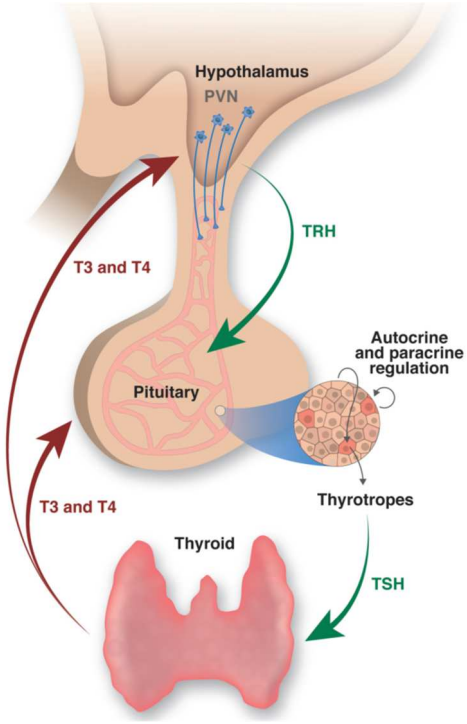

Figure 3. Schematic illustration of the machinery involved in negative feedback regulation of the HPT axis by thyroid hormone (Ortiga 2016).

The second system operates at the intracellular level, where the concentration of thyroid hormone is tightly controlled by three members of the thioredoxin enzyme family namely iodothyronine deiodinase (Dio1, Dio2 and Dio3), which are responsible for the regulation of levels and the activity of thyroid hormones, catalysing the removal of iodine atoms.

Dio1 and Dio2 catalyse the removal of the iodine at the outer ring (phenolic ring) of T_4 to form T_3, in a process resulting as its activation, whereas Dio3 is responsible for the removal of the iodine at the inner ring (tyrosyl ring) to form the inactive metabolite rT_3 (3,3',5'-triiodothyronine or reverse T_3) (Luongo 2019) (Figure 4).

The three isoforms possess different biochemical and regulatory features, exhibiting different tissue localization. Dio1 is an homodimeric selenocysteine-containing integral membrane enzyme expressed mainly in the liver, kidney, thyroid and pituitary gland and, as a matter of fact, it is not expressed in the central nervous system. It catalyses the conversion of T_4 to T_3 and supplies a significant fraction of the active thyroid hormone in human plasma (Köhrle 2000).

Dio2 is the isoforms responsible of the production of the nuclear T_3 in the brain (Köhrle 2000) and it is also expressed in skeletal and cardiac muscle, pituitary gland, brown adipose tissue, placenta and thyroid (Bianco 2002).

Dio3 is present in the brain, skin, placenta and some foetal tissues.

Approximately 80-85% of T_3 is generated by Dio1, primarily in the liver and kidneys (Moreno 2008). As already introduced above, most of the human circulating T_3 is not produced by the thyroid gland, but it is the result of the deiodination activity in the extrathyroidal tissues, catalysed mainly by Dio2 and, with a minor extent, by Dio1 (Bianco 2002).

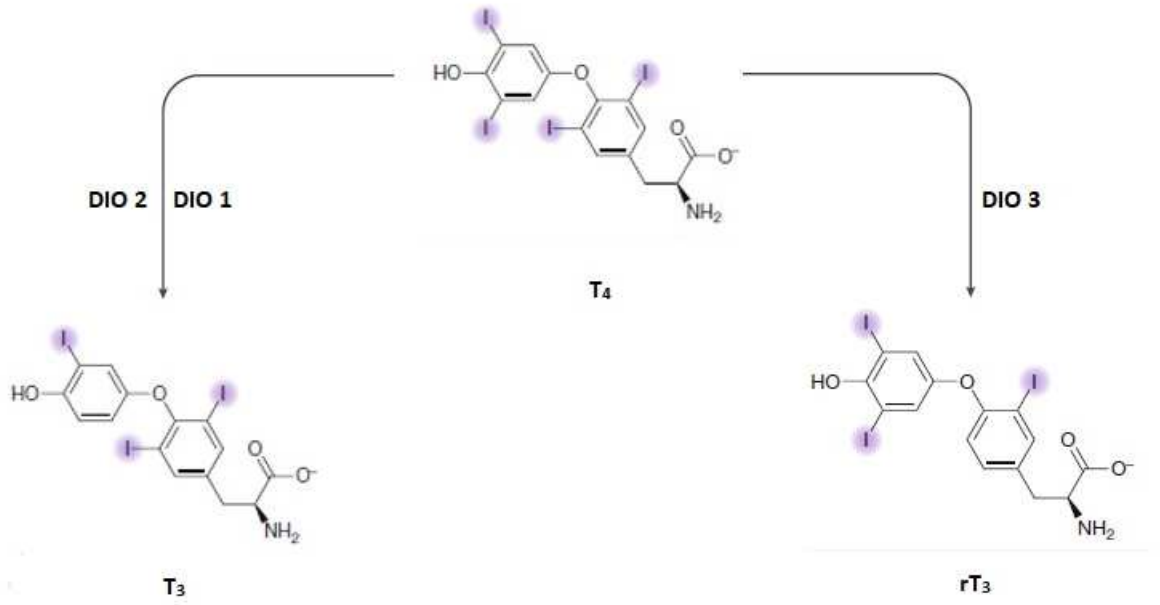

Figure 4. TH deiodination reactions. T_4 is activated by the catalytic activity of Dio1 and Dio2 to form T_3 whereas the inactivation reaction leading to rT_3 is catalysed by Dio3.

1.1.2 Transport of T_3 and T_4

In order to produce their effects on nuclear and cytoplasmic receptors and to be metabolized, TH need to be released into the bloodstream, through a series of transporters present on the basolateral plasma membrane of thyrocytes. The details of the mechanism of transport of TH to the circulation haven't been elucidated completely; however, monocarboxylate transporter 8 (MCT8), and possibly MCT10, seem to play a pivotal role in this process (Wirth 2011).

They belong to a family of proteins with 12 transmembrane domains. They are not specific for TH and they are widely expressed among many tissues in addition to thyroid (liver, heart, kidney, placenta, intestine, thyroid, and brain) and in distinct areas within the brain with an important role for

T_3 transport across the blood-brain barrier (BBB). Pathogenic mutations of mtc8 gene have been detected in several diseases, indicating a pathophysiological role for TH transport (Bernal 2015).

Since TH are highly hydrophobic molecules, several carrier proteins are responsible for their transport and distribution through the bloodstream and cellular compartments. The main plasma proteins that bind TH in humans are thyroxine-binding globulin (TBG), transthyretin (TTR or thyroxine-binding pre-albumin) and human serum albumin (HSA). A small amount of plasma TH is bound to minor carrier proteins, like lipoproteins or, with a minor extent, can be available in the circulation as free TH (fTH) (Khorle 2000).

TBG is a glycoprotein synthetized in the liver, consisting of a single 56 KDa polypeptide chain with one binding site for TH. Notably, the binding of T_4 to TBG induces conformational changes that increase its stability. Since it carries a major part of TH (~70%), qualitative and quantitative abnormalities of TBG have a significant impact on total circulating TH levels (Bartalena 1993, Feldt-Rasmussen 2007).

TTR, formerly known as thyroxine-binding pre-albumin, is a 55 KDa protein that circulates in blood as a stable homotetramer where the 4 subunits organize themselves to form a central channel that contains two binding sites for T_4. Just one of these two sites is used physiologically, since the binding of the hormone to a site causes a reduction in affinity for the other one trough a negative cooperative effect (Refetoff 2000). TTR carries 10 to 15 % of protein bound T_4 and it is mostly synthetized in liver and, with a minor extent, in the central nervous system. It has an important role in the transport and delivery of T_4 in the cerebrospinal fluid (CSF), where it is the main TH transporting protein (Palha 2002).

HSA binds ~5% of circulating TH with a lower affinity respect to TBG and TTR (Rassmussen 2007). Despite these low affinities, the related contribution in TH transport is still significant because of the high amount of albumin that circulates in human serum. An albumin role has been proposed as a fast TH resource during the rapid exchange in capillary transits (Schussler 2000).

Blood binding proteins can be seen as a reservoir and a buffering system that ensure a constant availability of TH to cells and tissues; they increase TH solubility and their half-life in plasma, reducing their hepatic and renal degradation and excretion. Therefore, TH binding proteins may protect the organism against the abrupt changes of TH plasma levels that can occur because of altered production, degradation or increased loss. In addition, they may also play a role in modulating TH delivery to specific tissues (Khorle 2000).

1.1.3 Mechanism of action

TH are involved in the regulation of cell functions through two mechanisms: a genomic one, consisting in a transcriptional regulation, trough the binding of nuclear thyroid hormone receptors (TR) (Yen 2001), and a non-genomic one, depending on the binding of TH to plasma membrane and intracellular receptors (Davis 2005).

TR are nuclear receptors that act as ligand-dependent transcription factors, able to modulate the transcription of target genes when activated by TH. In fact, the binding of T_3 to TR can increase or decrease the transcription rate of target genes. In the nucleus, TR can constitutively bind to specific regions located in the promoter region of TH target genes, known as thyroid hormone response element (TRE) (Ortiga 2014).

It has been shown that TR are still bound to TRE even in the absence of TH, repressing or silencing the basal transcription of the positive regulated target genes (Oetting 2007, Ortiga 2016) (Figure 5).

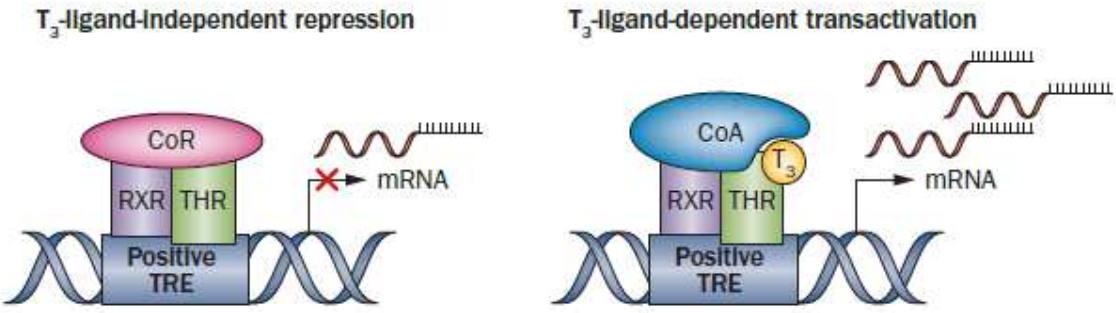

Figure 5. Mechanism of gene regulation by TH. In the absence of T_3 a co-repressor represses target gene expression. When T_3 binds to the receptor, the co-repressor is released and co-activators are recruited, resulting in activation of gene expression (Ortiga 2016).

TR belong to a larger superfamily of receptors that also includes receptors for retinoic acid, vitamin D, steroid hormones and, peroxisomal proliferator receptors. The core common structural characteristic of these receptors is represented by a central DNA-binding domain that contains two zinc-fingers and a carboxyl-terminal ligand-binding domain. TR A and TR B are the genes that encode for TRα and TRβ isoforms, respectively. Through alternative splicing they give rise to a variety of proteins. Only four of these proteins are functional receptors, namely TRα1, β1, β2, and β3 (Chiamolera 2012).

The tissue expression of the four functional TR has been demonstrated to not be homogenous. TRα1 and TRβ1 are expressed in almost every tissue, however, TRα1 is more abundant in the skeletal and cardiac muscles and in brown adipose tissue, whereas TRβ1 expression is higher in the kidney, liver and brain. TRβ2 is predominantly expressed in specific areas of the hypothalamus, in the anterior

pituitary gland, inner ear and in the developing brain; whereas TRβ-3 is mainly expressed in kidney, liver, and lung (Yen 2001; Oetting 2007; Brent 2012).

TRβ is the responsible of most of TH effects on metabolism and, from a pharmacological point of view, also an ideal target to treat metabolic disorders, mainly lipid-related, or brain diseases. An ideal thyromimetic drug, should possess a high TRβ selectivity, to avoid any adverse effects on bone and heart (Saponaro 2020).

Nongenomic effects of TH do not involve the classical concept of TR mediated TH action. They do not require gene transcription and protein synthesis but can include modulation of gene transcription. The mechanisms of several non-genomic actions depend upon signal transduction system and can involve novel TH membrane receptors, extranuclear TRβ or truncated isoforms of TRα (Davis 2016; Davis 2008).

One of the putative non-genomic TH receptors is the integrin αVβ3 expressed at the plasma membrane (Bergh 2005; Davis 2005). TH interaction with the integrin receptor activates proteins might be involved in modulation of transcription of specific genes and in cell proliferation. These pathways depend on activation of phospholipase C (PLC), protein kinase C (PKC), mitogen activated protein kinase (MAPK)1 and 2. The activation of MAPK leads to phosphorylation of the tumour protein p53 with a final decrease of its transcriptional activity (Davis 2005; Davis 2016).

T_3 is also responsible of many non-genomic actions on plasma membrane proteins, contributing to basal activity of some ion pumps such as Ca^{2+}-ATPase, Na^{+}/K^{+}-ATPase and Na+/H+ antiporter (Davis 2011).

Furthermore, TH can stimulate phosphatidylinositol 3-kinase (PIK-3) and Rac activity on the plasma membrane through the interaction with TRβ, that in turn are involved in the activation of voltage-dependent potassium channels. The activation of PIK-3 mediated by T_3 has also direct and indirect effects on the transcriptional increase transcription of hypoxia-inducible factor 1 (HIF-1) gene and glucose transporter 1 (GLUT-1) (Oetting 2007).

Recent studies demonstrated the involvement of truncated TRα isoforms in the regulation of actin cytoskeleton modelling which has a key role in the developmental program of the brain (Davis 2008). In response to T_3, truncated TRα isoforms have shown to be imported into mitochondrial inner membrane where they are able to directly stimulate oxidative phosphorylation processes (Oetting 2007).

1.1.4 Peripheral metabolism

Once TH have reached peripheral tissues, T_4 and T_3 undergo a complex metabolism in vivo, by several enzymes encompassing deiodinases, amine transferases, amine oxidases, decarboxylases and several classes of conjugating enzymes, particularly sulfotransferases and UDP-glucuronidases (van der Spek 2017).

These enzymes are important in the control of TH levels; TH are subjected to tissue-specific metabolism that includes: deiodination, conjugation, sulfonation, oxidative deamination and decarboxylation reactions (Figure 6).

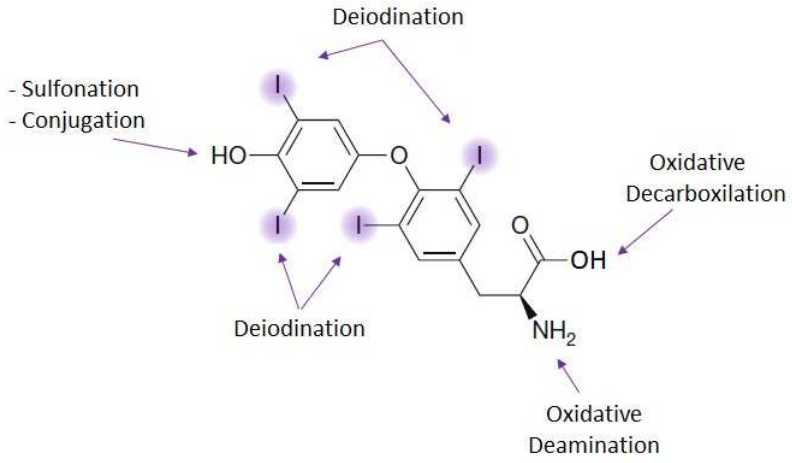

Figure 6. Schematic overview of the metabolism of TH.

T_3 and rT_3 can be subjected to additional deiodination reactions, to form 3,5-diiodothyronine (3,5-T_2), 3,3'-diiodothyronine (3,3'-T_2), 3',5'-diiodothyronine (3',5'-T_2) and 3-iodo-L-Thyronine (3-T_1). 3,3'-T_2 and 3',5'-T_2 demonstrated no remarkable activities, whereas 3,5-T_2 proved the ability to bind to TR and have been studied for a long time by researchers. 3,5-T_2 actions are mediated by the TR classical interaction but also through rapid effects at the cell membrane and mitochondria (Moreno 2017).

The alanine side chain of TH can also undergo oxidative deamination and decarboxylation. These metabolic pathways can lead to the production of iodothyroacetic acids; 3,5,3',5'-tetraiodothyroacetic acid (TETRAC), 3,5,3'-triiodothyroacetic acid (TRIAC) and thyronamines. Tetrac is produced by oxidative deamination of T_4, while TRIAC can be produced by deiodination of Tetrac or by deamination of T_3.

They are both transported by TTR in serum, and they act as thyromimetic compounds lowering TSH concentrations. Tetrac binds to TR onto integrin αVβ3 and elevated concentrations of this compound have been found in Grave's disease patients. Triac has a potent T_3-mimetic activity showing a high affinity for TRβ and it has been described to be a substrate for MCT8 transporter (Köhrle 2019).

1.2 Thyronamines and the emerging role of T_1AM 3-iodothyronamine

Thyronamines are decarboxylated metabolites of TH detected in blood and tissues of humans and several animals (Scanlan 2004; Saba 2010; Hoefig 2011; Hackenmueller 2012; DeBarber 2008; Chiellini 2012; Galli 2012; Assadi-Porter 2018). They represent a new class of endogenous signaling compounds, derived from their aromatic amino acid TH precursors and have been postulated to act as neurotransmitters (Dratman 1974).

1.2.1 Structure and endogenous concentration of Thyronamines

The structure of thyronamines is identical to that of thyroid hormone and deiodinated thyroid hormone derivatives, except that TAMs do not possess a carboxylate group of the alanine side chain (Figure 7). They differ for the number and the location of the iodine atoms and their nomenclature is analogous to the one used for TH; T_XAM, with x indicating the number of iodine atoms per molecule (Piehl 2011).

Scanlan et al. in 2004 (Scanlan 2004) discovered that, among all thyronamines, the 3-iodothyronamine (3-T_1AM) was the one with more physiological effects (Figure 7).

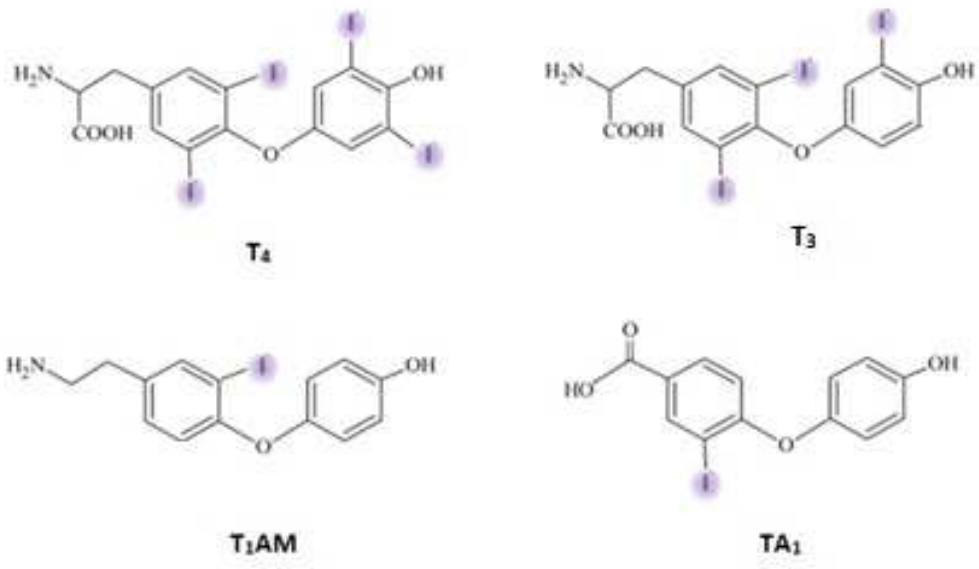

Figure 7. Structure of TH Thyroxine (T_4) and T_3 and a thyronamine, T_1AM with his major metabolite TA_1.

T_1AM as an endogenous molecule, whose pharmacological administration results in dose-dependent reversible effects on body temperature (Scanlan 2004; Doyle 2007; Braulke 2008), cardiac function (Scanlan 2004; Chiellini 2007; Frascarelli 2014; Ghelardoni 2009), energy metabolism (Braulke

2008; Manni 2012; Ghelardoni 2014) and neurological functions (Scanlan 2004; Saba 2010; Zucchi 2014).

Interestingly, many of the effects attributed to T_1AM or its major metabolite 3-iodothyroacetic acid (TA_1) appear to oppose those of the classical thyromimetic effects exerted by T_3 (Piehl 2011) as a potent hypothermia, a decrease in heart rate and cardiac output (Scanlan 2004) and the induction of a shift from carbohydrates to fatty acids as preferential metabolic source (Braulke 2008). Alternatively, many neurologic and metabolic effects of T_1AM appear to be at least in part synergic with those of T_3 as far as compared in detail.

It was also demonstrated that the rapid onset of T_1AM effects was not compatible with the classical TH nuclear mechanisms, but evidence has been provided that T_1AM may activate G-coupled receptor (GPCR) (Dinter 2015), besides TAAR1 (Scanlan 2004; Hart 2006, Dinter 2015) and additional targets such some transient receptor potential (TRP) channels (Lucius 2016; Khajavi 2015) and intracellular binding sites (Cumero 2012; Venditti 2011). Therefore, some investigators consider T_1AM as a multitarget ligand, but the patho-physiological role of the individual receptors and binding sites is presently under debate (Scanlan 2004; Phiel 2011; Köhrle 2019).

While TH is routinely determined via chromatographical or immunological methods, liquid chromatography-tandem mass spectrometry (HPLC-MS/MS) has been initially used for the unequivocal detection of endogenous TAMs. The first report of the endogenous presence of T_1AM dates back to 2004, and was obtained using LC-MS/MS (Scanlan 2004).

However, it must be noted that these initial reports were only qualitative in nature. Few years later, a significant technological improvement was achieved with the development of a novel LC-MS/MS method, which allowed the quantitation of T_1AM, jointly with TH and/or putative T_1AM catabolites in blood and tissue homogenates (Saba 2010). This method confirmed that T_1AM is present in virtually every rodent blood and tissue with a widespread distribution (brain, heart, and liver) (Scanlan 2004, Chiellini 2007, Hoefig 2016) and in human blood for the first time (Saba 2010).

T_1AM tissue levels in rodents are on the order of a few pmol/g (0.3-0.03 pmol/mL), reaching the highest values in rat liver and kidney (92.92-28.46 and 36.08-10.42 pmol/g, respectively) (Saba 2010) comparable or even superior with tissue T_3/T_4 levels (64.4-141.6 and 0.8-3.072 pmol/mL, respectively) (Tai 2002, Tai 2004).
When the same technique was used human blood, T_1AM concentration was found to be very similar between human and rodent serum, namely about 0.15-0.30 pmol/mL (Saba 2010).

Therefore, an immunoassay has been developed to allow T_1AM quantitation in human serum. With this approach, human serum T_1AM concentration was measured in the range of 14–66 nmol/l (Hoefig 2011), meaning about two orders of magnitude higher than previously reported in most studies using HPLC-MS/MS (Table 1).

Compartment		Concentration Range of T_1AM	Method	Reference
Human and rat serum		0.15-0.30 pmol/mL	HPLC MS-MS	Saba et al. 2010
		14-66 pmol/mL	CLIA	Hoefig et al. 2011
Rat tissues	Lung	5.61 ± 1.53 pmol/g	HPLC MS-MS	Saba et al. 2010
	Heart	6.60 ± 1.36 pmol/g		
	Stomach	15.46 ± 6.93 pmol/g		
	Muscle	25.02 ± 6.93 pmol/g		
	Kidney	36.08 ± 10.42 pmol/g		
	Liver	92.92 ± 28.46 pmol/g		

Table 1. 3-Iodothyronamine (T_1AM) tissue concentrations in human and rodents.

These discrepancies might be caused by strong binding of the highly hydrophobic T_1AM to lipoprotein particles, particularly apolipoprotein ApoB100 (Roy 2012), speculating that less than 1% of circulating T_1AM is free, and that protein-bound T_1AM is lost during the extraction procedures (Lorenzini 2017).

1.2.2 Biosynthesis and metabolism

Even though T_1AM was recognized as being an endogenous compound in 2004 (Scanlan 2004), the exact mechanism of endogenous T_1AM biosynthesis is still uncertain.

T_1AM could be produced in two main metabolic pathways: thyroidal synthesis and secretion of T_1AM or it may be the result of sequential deiodination by deiodinase (Dio) selenoenzymes and decarboxylation by ornithine decarboxylase (ODC) (Khorle 2019).

Up to now, *de novo* biosynthesis of T_1AM would require partial oxidative iodination and ether-bond coupling of two tyrosyl rings resembling the biosynthesis of TH which solely occurs bound to their precursor protein thyroglobulin (Dunn 2001). Alternatively, *de novo* biosynthesis of T_1AM from T_0AM would require iodination of T_0AM. So far, both the iodination and the coupling reactions of tyrosyl residues have been described only within the thyroid gland, in specific compartments of the thyroidal follicles and involve thyroperoxidase (TPO) and dual oxidase (Song 2010).

However, there are no reports in the literature that suggest that the production of thyronamines or thyronines with lower iodination grade than T_4 and T_3 occurs in the thyroid gland, nor direct secretion of T_1AM from the thyroid gland has been reported, supporting the hypothesis of an extrathyroidal TAM biosynthesis from TH (Hoefig 2011).

According to the second hypothesis thyronamines are produced from T_3 or T_4. The biosynthesis would require a step of deiodination to form T_2 and then the decarboxylation of the phenylalanine side chain to form di-iodo-thyronamine (T_2AM), in combination with deiodination by removing up to three iodine atoms to form T_1AM (Zucchi 2019) (Figure 8).

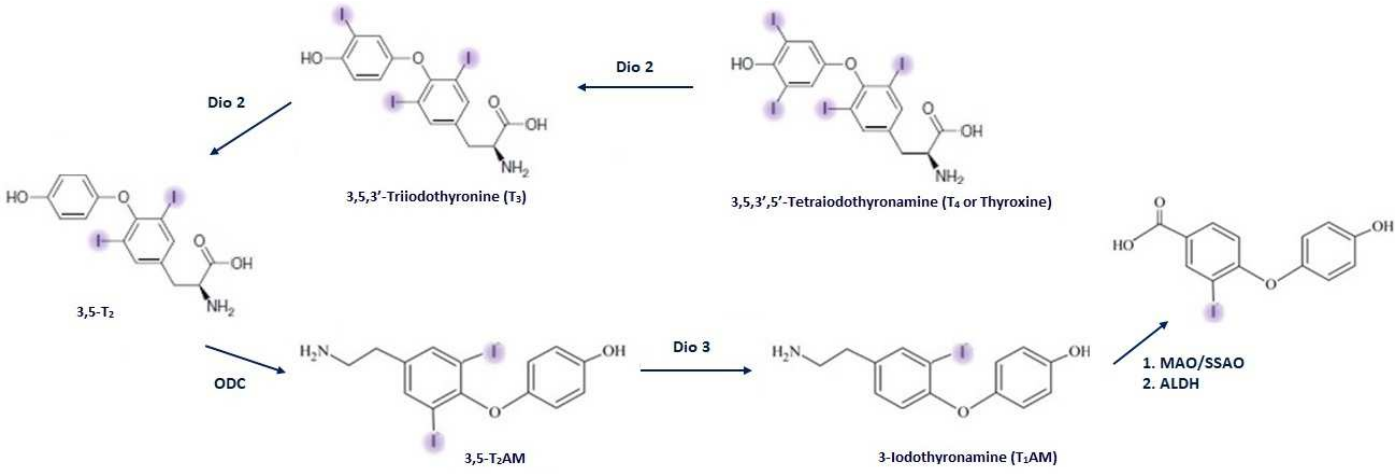

Figure 8. Hypothetical pathway of T_1AM and TA_1 production from TH, T_3 or T_4. Dio isoenzyme catalyze reductive sequential removal of iodide. Ornithine decarboxylase ODC decarboxylates iodothyronines to generate TAMs.

A systematic *in vitro* screen of all possible TAM deiodination reactions revealed that thyronamines are isozyme-specific substrates of deiodinases Dio 1, Dio 2 and Dio 3 (Piehl 2008), whose transcripts have been found in mice intestinal tissue.

Using the mouse everted gut sac model in combination with LC-MS/MS, it was demonstrated that T_1AM production from T_4 is possible in mouse intestine via several deiodination and decarboxylation steps. Gene expression analysis confirmed the expression of all three deiodinases as well as the ornithine decarboxylase (ODC) in mouse intestine, demonstrating that the intestine expresses the entire molecular machinery required for T_1AM biosynthesis from T_4 (Hoefig 2016). However, since these results were only obtained in the mice intestine, it is unclear whether this is the only biosynthetic pathway or whether T_1AM synthesis from TH may occur in other tissues.

Once produced, T_1AM does not bind the same serum proteins as TH, who result strongly bind to TBG, TTR, albumin and only at minor extent to lipoproteins (Hoefig 2016), but is mainly present bound reversibly to Apolipoprotein B-100 (ApoB-100) with a 1:1 stoichiometry and a KD of 17 nM

(Roy 2012). ApoB-100 is a polypeptide that is a fundamental component of Low Density Lipoprotein (LDL), Very Low Density Lipoprotein (VLDL), IDL and Lipoprotein(a) Lp(a).

T_1AM is equally distributed between LDL and VLDL particles. The physiological role of the strong binding of T_1AM to ApoB100 may be to provide a mechanism for transportation and entry of T_1AM into target cells via LDLR mediated endocytosis (Roy 2012).

With regard to T_1AM distribution, after intraperitoneal (i.p.) injection, T_1AM is rapidly cleared from the plasma with an half-life of 8 minutes during the first hour, after this a lower elimination process takes place (half-life of 50 minutes approximately) (DeBarber 2008).

The rapid disappearance of T_1AM is related to cell uptake and metabolism. To identify putative T_1AM transporters, a systematic large-scale screening analysis of the solute carrier transporter family was performed. No single specific TAM transporter was identified from this screen, however, sodium- and chloride- independent, pH-dependent, TAM-specific cellular uptake, may involve multiple transporters (Ianculescu 2009, Ianculescu 2010). However, an apparent sodium-dependent T_1AM uptake has been shown in cardiac H9c2 cells (Saba 2010).

The uptake of exogenous radiolabeled 125I-3-T_1AM from the blood stream revealed that T_1AM is systemically distributed to various mouse tested organs: adipose tissue, blood, bone, brain, gallbladder, heart, intestine, kidney, liver, lung, muscle, pancreas, skin, spleen, stomach, and thyroid (Chiellini 2012).

It was demonstrated that T_1AM liver, muscle and adipose tissues might be regarded as T_1AM storage sites through a sodium and chloride-independent transport mechanism (Ianculescu 2009; Saba 2010; Agretti 2011; Ghelardoni 2014).

T_1AM and its metabolites are excreted via the biliary and urinary tracts (Chiellini 2012; Lee 2013).

It has been demonstrated that T_1AM and thyronamines can undergo several metabolic reactions that leads to a variety of derivatives (Köhrle 2019). The major oxidative metabolite of T_1AM seems to be TA_1. T_1AM can undergo the oxidative deamination of phenylethylamine side chain of T_1AM forming an aldehydic intermediate which then can be further oxidized to 3-iodothyroacetic acid (TA_1) by the ubiquitously expressed NAD-dependent aldehyde dehydrogenase (Lorenzini 2017).
The biological role of TA_1 is still unknown, even if an activity on the histaminergic system has been reported (Musilli 2014, Laurino 2015).

Moreover, T_1AM can be substrate of sulfotransferases (SULT), enzymes which are able to catalyze the sulfation of different endogenous compounds generating T_1AM-sulfate (Pietsch 2007). Also,

glucuronidation seems to contribute to thyronamines metabolism and elimination, indeed the formation of T_1AM-glucuronide (Hackenmueller 2012). Enzymes involved in TAM glucuronidation or release of TAMs from these conjugates via glucuronidase activity are still unknown. Sulfonation and glucuronidation are part of the so-called phase II detoxification reactions and they are involved in the inactivation and excretion of TH. The general aim of these reactions is to increase the solubility of TH in water and facilitate their excretion through bile and/or urine (Visser 1988).

1.2.3 Signal transduction pathways

Given the structural similarity of thyronamines with thyroid hormones and the identification of endogenous TAM in blood of experimental animals and humans, as well as in tissues of experimental animals, it was hypothesized that these biogenic amines derived form, might represent "hormones" (Khorle 2019).

T_1AM acts as rather promiscuous ligand for several molecular target with a variety of GPCR targets, showing different effects, depending on cell type or tissue: members of the trace amine-associated receptor (TAAR) G protein–coupled receptor (GPCR) family for example, Taar1, Taar5, or the α2a adrenergic receptor (ADRAα2a) (Hoefig 2016) (Figure 9).

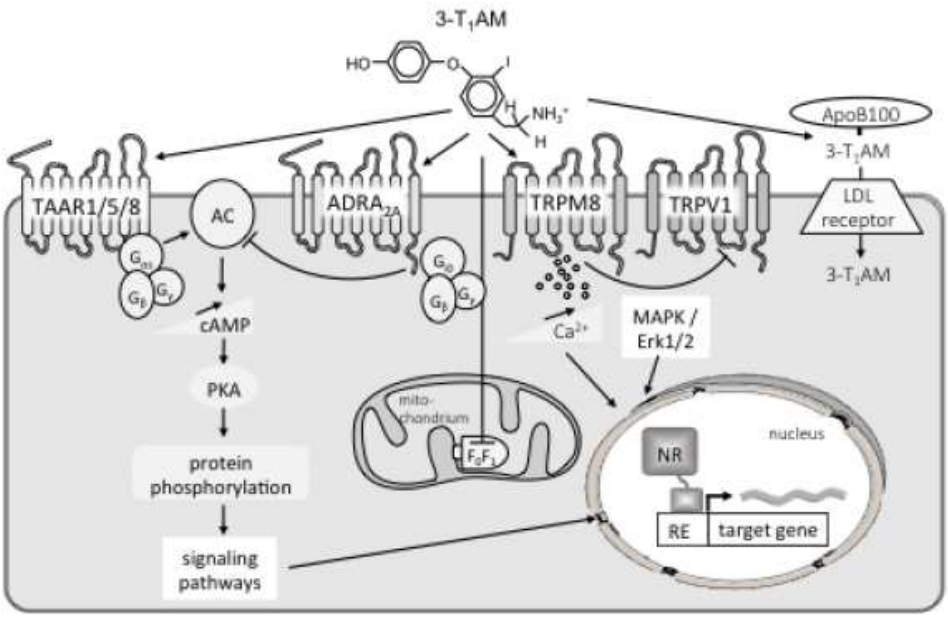

Figure 9. Summary of known cellular targets and signaling pathways for T_1AM (Hoefig 2016).

However, exogenous administration of T_1AM leads to multiple effects, raising the possibility that not only GPCRs are target of its action, but also other membrane proteins (Khajavi 2017) as well as transient receptor potential channels TRP receptor as TRPM8 (Khajavi 2017) and intracellular targets including F_0F_1-ATP synthase located on mitochondria (Venditti 2011, Cumero 2012).

Beyond intracellular targets, T_1AM interact with ApoB-100, a component of VLDL and LDL lipoproteins, the latter probably accounting for high affinity protein binding in serum (Hoefig 2016, Khorle 2019).

The subfamily of TAARs has been discovered as a group of receptors able to bind trace amines, such as b-phenylethylamine, octopamine, tyramine, and volatile amines, with TAAR1 as the most important member of this subfamily (Hackenmueller 2012). A great variety of different tissues expresses TAAR1 and may be able to respond to T_1AM stimulation (Rutigliano 2018).

The first reports on the effects of T_1AM suggested that they were mediated by TAAR1, as T_1AM interaction with TAAR1 resulted in activation of the Gs/adenylyl cyclase pathway stimulating the production of cAMP (Scanlan 2004).

A later study (Chiellini 2007) demonstrated that the cardiovascular effects identified by Scanlan et al (hypothermia, negative chronotropic and inotropic effects) may not be related to increased intracellular cAMP reactions and in 2010, Panas et al. observed that one main action of T_1AM, that is, the reversible and marked decreased of body temperature after administration of high doses of this agent, is still present in the TAAR1 knockout mouse (Panas 2010).
This led to the first indication of several target structures and signaling pathways for T_1AM, that could potentially mediate its physiological and pharmacological effects.

Adrenergic receptors (ADR) are already earlier recognized as promising candidate as targets of T_1AM (Regard 2007). The main effect reported after binding of T_1AM to ADRα2A is a reduction of insulin secretion in pancreatic β cells (Regard 2007). Then, in vitro findings confirmed that T_1AM activates the G_i/G_o signaling pathway at ADRα2A nearly as efficiently as other neurotransmitters; mediating some of the metabolic effects of T_1AM (hyperglycaemia, reduced insulin secretion and increased glucagon) (Regard 2007, Dinter 2015b).
For the β2-adrenergic receptor (ADRβ2), but not for ADRβ1, a modulatory effect of T_1AM was observed on isoproterenol-induced activation of the Gs/adenylyl cyclase pathway in human embryonic kidney cells. In human conjunctival epithelial cells (IOBA-NHC), a T_1AM challenge increases Ca^{2+} influx, which can be blocked by timolol, an unspecific blocker of adrenergic receptors (Dinter 2015b).

Laurino et al. performed binding experiments and demonstrated that T_1AM can also act as a competitive ligand of all muscarinic receptor 3 (M_3R) and act as antagonist by blocking the action of carbachol, the endogenous M_3R agonist (Laurino 2016).

T_1AM can also activate other membrane proteins, not also GPCR. It was demonstrated that T_1AM activates the transient receptor potential channels 8 (TRPM8), in different cell types, as neoplastic cells, where significantly increases cytosolic Ca^{2+} (Khajavi 2015).
Its activation prevents the activation of the TRP vanilloid 1 (TRPV1) ion channel that is known to be associated with inflammation (Khajavi 2015, Lucius 2016). Thus, T_1AM might also exert beneficial local anti-inflammatory activity (Khajavi 2015; Hoefig 2016).

Besides targeting cell membrane proteins, T_1AM function in energy metabolism indicates the existence of intracellular targets. These are not nuclear receptors (Scanlan 2004), but a direct influence of mitochondrial function might occur (Scanlan 2004).
To exert such action, T_1AM in a first step has to enter the cell. If no intracellular production and subsequent intracellular action (intracrine) occur in case of T_1AM three ways of entry are likely: specific transmembrane transporters for T_1AM or its distributor protein ApoB100 containing bound T_1AM (a Trojan horse–like mode of entry) or via internalization of a T_1AM/GPCR complex. For the latter, so far, no indications exist; however, classical TH transmembrane transporters recently identified in a pancreatic β cell line might mediate cellular uptake of T_1AM (Ianculescu 2009; Lemphul 2018) (Figure 10).

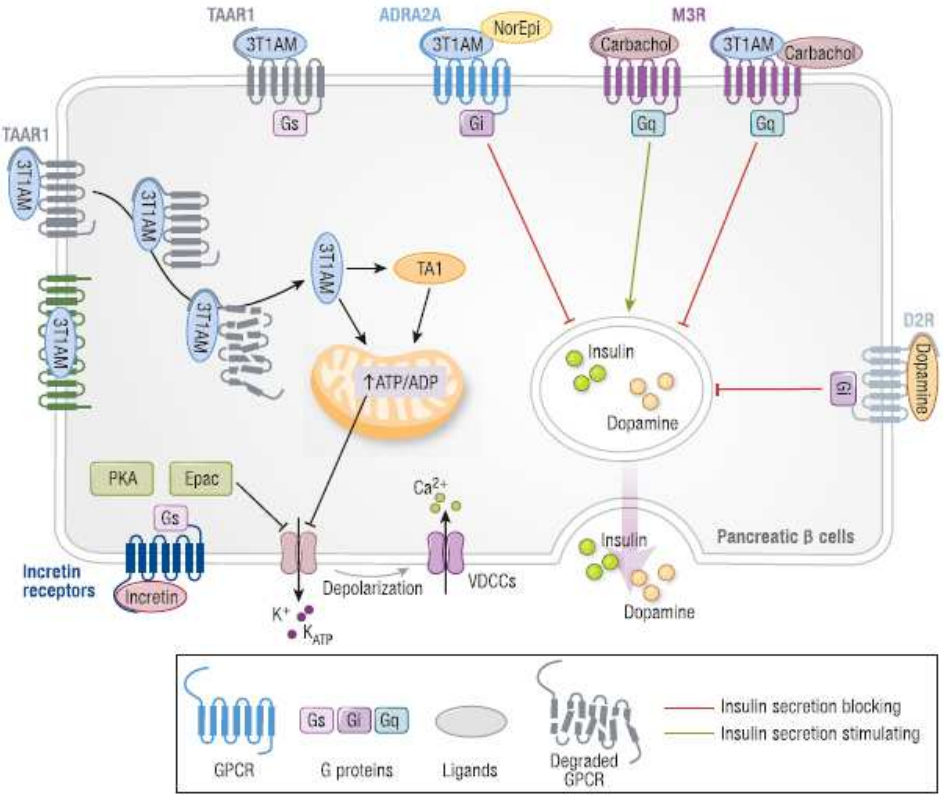

Figure 10. T_1AM-induced signalosome at pancreatic β cells (Köhrle 2019).

The first identified intracellular effector of T_1AM action in vitro is the mitochondrial F_0F_1-ATP synthase. Low concentrations of T_1AM increase mitochondrial respiration and cause a positive effect on mitochondrial energy production (Cumero 2012). In accordance with these data, T_1AM and its metabolite TA_1 reduce F_0F_1-ATP synthase function, decrease thereby the ATP/ADP ratio, and regulate mitochondrial energy metabolism, resulting in decreased insulin secretion (Lemphul 2018).

To summarize, T_1AM has a variety of GPCR targets that classify it as a multitarget ligand (Zucchi 2014) and the signaling mediated by T_1AM in various cell types is very complex and might depend on a variety of different parameters such as the expression of receptors, their possible heteromerization, the presence of different ligands, the availability of intracellular signaling proteins and the expression level of interacting proteins (Köhrle 2019). They exert a concentration-related and receptor-mediated function on target cells, various tissues, and in animals after exogenous administration of T_1AM or its metabolites.

1.2.4 Effects of T_1AM and TA_1

The exogenous T_1AM administration leads to different effects, including modification of cardiac function (Scanlan 2004; Chiellini 2007), thermoregulation (Scanlan 2004, Doyle 2007, Braulke 2008), energy metabolism (Braulke 2008; Manni 2012; Dhillo 2009) and neuromodulation (Saba 2010; Scanlan 2004; Zucchi 2014).

Regarding the effects of TA_1, exogenous administration of TA_1, at doses close to its endogenous levels, modified behaviour, including memory acquisition and reduced nociceptive thresholds and raised plasma glucose. All these effects were modulated by histamine H1 and H2 receptor antagonists (Musilli 2014).

In general, both T_1AM and TA_1 targets seem to overlap. These results let to the speculation that effects of T_1AM may be due, at least in part, to TA_1 production.

The first functional effects of T_1AM were described by Scanlan et al., demonstrating that a single i.p. injection of T_1AM (50 mg/kg) led to a rapid, drastic but transient decrease in body temperature of mice. This effect lasted for 6-8 hours after injection and during this period the mice became inactive, but reflexes were preserved and no compensatory homeostatic responses, such as shivering and piloerection, were observed (Scanlan 2004, Doyle 2007).
This hypothermia was confirmed in Djungarian hamsters (Phodopus sungorus) and probably occurs due to a decrease in metabolic rate (Braulke 2008).

Recently investigations have clarified that the observed hypothermia is not mediate by the activation of TAAR1 as the hypothermic response to T_1AM administration was still maintained in TAAR1 knockout mice (Panas 2010). Instead, this effect can be better characterized as anapyrexia, which is centrally mediated and causes vasodilatation without directly affecting peripheral Taar1 or ADRα2A (Gachkar 2017).

Furthermore, it was shown that TA_1, does not contribute to the thermoregulatory effects observed after T_1AM administration in mice, suggesting that oxidative deamination constitutes an important deactivation mechanism for T_1AM with possible implications for thermoregulatory functions (Musilli 2014).

Additionally, to the already cited hypothermic effects, in the heart, exogenous administration of T_1AM (50 mg/kg, i.p.) in mice resulted in modulation of cardiac functions. An immediate drop-in heart rate (bradycardia) was reported both in the conscious mouse and in the isolated perfused rat heart, while contractile performance was reduced in the working rat heart preparation (Scanlan 2004, Chiellini 2007) an effect that contrasts with the action of classical thyroid hormones (Scanlan 2004). Surprisingly, pretreatment with T_1AM reduced irreversible ischemic injury when T_1AM was tested both in *ex vivo* working rat heart and in cardiomyocyte preparations as model of ischemia-reperfusion injury (Frascarelli 2011, Frascarelli 2008, Chiellini 2007, Ghelardoni 2009).

It has been speculated that T_1AM produces a cardioprotective effect may triggering the transduction pathways involved in ischemic preconditioning, in which protein kinase C K^+(ATP)-dependent pathway and that this mechanism is probably linked to the modulation of mitochondrial permeability transition and/or ischemic arrest time (Hoefig 2016).

These effects might be specific for T_1AM considering that TA_1 seemed did not produce any cardiovascular effects (Musilli 2014).

Subsequently, many other effects have been reported, the most interesting being the induction of acute metabolic responses with actions on carbohydrates and lipids (Braulke 2008; Manni 2012; Manni 2013; Ghelardoni 2014) and it is emerging as a possible modulator of noradrenergic, dopaminergic and histaminergic systems and neurological effects (Saba 2010; Scanlan 2004; Zucchi 2014).

T_1AM modulates metabolic processes by decreasing insulin and increasing glucagon secretion, increasing gluconeogenesis (Klieverik 2009), and shifting to lipid catabolism, inducing effects associated with a decreased food intake, energy expenditure, metabolic rate, respiratory quotient (RQ)

and oxygen consumption (Chiellini 2007), just the opposite of what is typically expected for an effect of a TH-derived metabolite. These effects were dose-dependent and reversible (Scanlan 2004, Dhillo 2009, Braulke 2008).

As for the neurological effects, intracerebral T_1AM behaved as a neuromodulator, affecting adrenergic and/or histaminergic neurons. Intracerebral T_1AM administration favored prolearning and anti-amnestic effects, increased locomotor activity, protection from toxic injury, modulated sleep and feeding, and decreased the painthreshold (Saba 2010; Scanlan 2004; Zucchi 2014).
Several groups have demonstrated that T_1AM is present endogenously in the brain (Scanlan 2004; Saba 2010; Zucchi 2014) and that it reaches this organ after systemic or i.c.v. administration (Gompf 2010; Saba 2010; Chiellini 2012). Also, T_1AM interacts with catecholaminergic and serotoninergic systems, inhibiting rodent DAT, NET and SERT (Snead 2008), activating α2a adrenergic receptor and increasing isoprenaline-mediated activation of β2 adrenergic receptor (Regard 2007; Dinter 2015b; Bräunig 2018) and, in binding experiments, T_1AM acted as a competitive ligand of muscarinic receptors (Laurino 2016).
Although the most interesting molecular target of T_1AM is TAAR1, particularly at the level of the central nervous system (CNS), some of the elicited responses persisted in TAAR1 knock out animals (Khorle 2019). This suggests the existence of a complex signaling system with multiple molecular targets and downstream transduction pathways.

Snead et al. observed that T_1AM affected the response to catecholamines and other neurotransmitter, acting as a specific inhibitor of noradrenaline and dopamine re–uptake and vesicular monoamine transport, discovering a novel role for T_1AM as neuromodulator (Snead 2007). Furthermore, neuroprotective effects of T_1AM were also observed (Doyle 2007).

Several findings have led to consider T_1AM as an adrenergic blocking endogenous at level of the central noradrenergic system (Köhrle 2000).

Gompf and collaborators in 2010 observed that microinjections of T_1AM in locus coeruleus (LC), the major centre of adrenergic control in the central nervous system (CNS), activate the neurons in a dose dependent manner (Gompf 2010).

In 2013 Manni et al observed an enhancement of learning and memory after i.c.v. injections of T_1AM in mice with a mechanism that may implicate the activation of extracellular signal–regulated kinase (ERK) (Manni 2013) a member of the family of MAPKs. Activation of the ERK pathway induces the cAMP-responsive element binding protein (CREB) and other transcription factors, stimulating the

synthesis of proteins that are required for the stabilization of new memories (Kida 2002; Pittenger 2002) and the regulation of long-term synaptic plasticity (LTP) (Roberts 1999).

Starting from the assumption that if TA_1 may be the active end product of T_1AM, and assuming then that administration of TA_1 should reproduce some of the effects described for T_1AM, Musilli et al. studied the effect of i.c.v. of TA_1 on memory and pain (Musilli 2014). Authors observed that TA_1 effect on memory seems more composite than the one mediated by T_1AM. At a low dose the acid is able to produce amnesia while at higher dose stimulate learning without inducing memory consolidation, as instead observed for T_1AM (Bellusci 2017). Laurino et al. (Laurino 2015; Laurino 2018b; Laurino 2015b) demonstrated that T_1AM and TA_1 behavioural effects were dependent on the activation of the histaminergic system, with a mechanism which, however, remains to be clarified.

Studies using MAO inhibitors (Laurino 2015b; Manni 2012) revealed that effects and targets of TA_1 are at least in part distinct from those of its precursor T_1AM. Even if there are also overlapping targets with its precursor, as application of low concentrations of TA_1 increases itch and reduces pain thresholds, actions possibly linked to activation of aminergic GPCRs and/or transient receptor potential (TRPs) (Laurino 2015b). On the current knowledge, T_1AM presents an uncertain pharmacological profile, suggesting a role as a cell messenger, behaving as a hormone and/or a neuromodulator, with a function probably also mediated by the 3-iodothryoacetic acid (TA_1) (Laurino 2018b).

In general, both T_1AM and TA_1 targets seem to overlap. TA_1 can be virtually produced in every tissue, considering the wide distribution of MAOs (Laurino 2015b). The administration of TA_1 to rodents, favored memory retention and acquisition and produced hyperglycaemia. These results let to the speculation that effects of T_1AM may be due, at least in part, to TA_1 production.

T_1AM seems to also affect clearing pathway namely autophagy-lysosomal degradation of proteins, a process that has emerged as a potential target of therapeutic strategies developed to treat neurodegenerative conditions characterised by the aberrant accumulation of aggregation-prone proteins (Friedman 1995). Specifically, in cell cultures, T_1AM administration has been demonstrated to increase autophagy, possibly through the inhibition of phosphorylation of mTOR by the PI3K/AKT/mTOR pathway (Bellusci 2017).

In addition, previous studies have shown that administration of T_1AM is able to rescue β-Amyloid induced neuronal dysfunction in wild type mice (Accorroni 2017) and more recently, the protective effect of T_1AM against neuronal plasticity impairment, counteracting beta amyloid toxicity, has been

further confirmed in mouse model of Alzheimer's disease (AD) (Accorroni 2016), neurodegenerative condition characterised initially by memory impairment.

A common pathology shared by several neurodegenerative diseases is the accumulation of misfolded proteins. Given that autophagy is a cellular function that degrades abnormal proteins, including those that are misfolded, autophagy-inducing compounds are expected to mitigate the onset and progression of these diseases (Bellusci 2020).

We can speculate that T1AM might exert pleiotropic effects on energy metabolism and cell clearing pathways, which is likely to sustain neuroprotection.

1.2.5 Glutamatergic system

Glutamate is one the major excitatory neurotransmitter in the nervous system and as an amino acid and a neurotransmitter, has a large range of functions. One of the most known signaling cascade in the nervous system activated by glutamate is the long-term potentiation (LTP) postsynaptic signaling cascade. Long-term potentiation is considered one of the major cellular mechanisms that underlies learning and memory, mainly located in the hippocampus where involves activation of the glutamatergic pathway. It is a form of synaptic plasticity that consist in a persistent strengthening of the signal transmission between two neurons (Bliss 1973, Purves 2001).

When glutamate is released from the pre-synaptic neuron, it binds to several different receptors on the post-synaptic neuron leading to the activation of the LTP postsynaptic signaling cascade (Kumar 2011).

When an impulse on presynaptic fibers causes the release of glutamate, it binds to glutamate receptors (AMPA and kainate) at the postsynaptic membrane. This activation triggers the influx of Na+ or K+ into the postsynaptic cell, initiating postsynaptic depolarization (Voglis 2006) (Figure 12).

Membrane depolarization remove the Mg^{2+} ions that block ionotropic non-selective cationic glutamate receptors (NMDA), and its activation leads to the transient influx of Ca^{2+} into the cells. The magnitude of depolarization determines the amount of Ca^{2+} that will entry into the postsynaptic cell, defining the degree and duration of LTP. The rapid increase in intracellular Ca^{2+} concentration leads to the activation of several enzymes, specifically kinases, such as calcium/ calmodulin-dependent protein kinase II (CaMKII) and protein kinase C (PKC) (Kumar 2011).

The final phase of LTP require gene transcription and protein synthesis. A transient increase in intracellular Ca^{2+} stimulates Ca^{2+}-sensitive adenylyl cyclase enzymes (AC), which catalyze production of 3′,5′-cyclic adenosine monophosphate (cAMP). The increase of intracellular cAMP can

activate a group of protein kinases, including the protein kinase A (PKA), which will activate mitogen-activated protein kinases, specifically extracellular regulated kinase (ERK), that leads to the activation of transcription factors, such as cAMP-response element-binding protein (CREB), who is involved in the activation of cAMP-response element, which induces changes in gene transcription and triggers synthesis of new proteins (Kumar 2011).

Kainate receptors (KARs) are tetrameric complexes that result from the combinations of GluK1–GluK5 glutamate receptor subunits (Petrovic 2017). They are present at both pre- and postsynaptic membranes, where they mediate different roles modulating synaptic transmission, network activity and neuronal excitability. KARs are also implicated in processes, ranging from neuronal differentiation and development to neurodegeneration and cell death. Recently investigations discovered a NMDA-receptor-independent mechanism that allows an increase in AMPA receptor at the membrane level and drives LTP. This pathway passes through the activation of kainate receptors and the activation of the PKC (Petrovic 2017) (Figure 11).

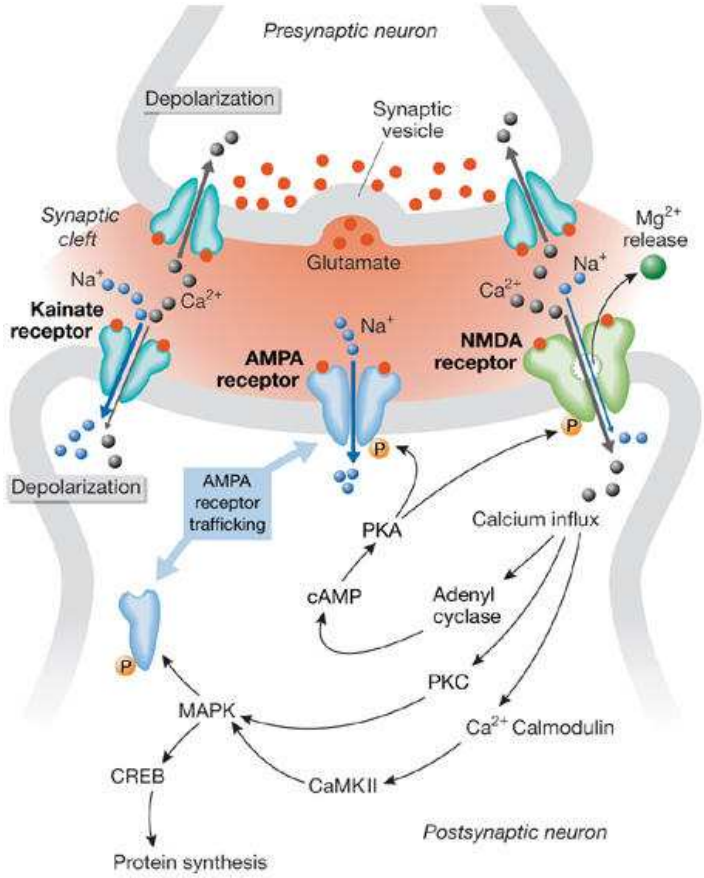

Figure 11. Glutamate receptors and synaptic plasticity (Voglis 2006).

Neuromodulators, such as serotonin, norepinephrine, dopamine, acetylcholine, and histamine can affect the induction of LTP and can control the strength of synaptic facilitation at Schaffer-collateral synapses (Kumar 2011).

LTP inhibition has been demonstrated to be a pathological change in Alzheimer's disease, in fact its impairment is associated with increased levels of soluble Aβ oligomers (Rowan 2003; Jang 2016). Aβ peptides are derived from the processing of amyloid precursor protein (APP) by two proteases, β-secretase and γ-secretase. The highly fibrillogenic Aβ 1-42, (produced via the amyloidogenic processing of APP) can trigger a neurotoxic cascade, thereby causing neurodegeneration and finally Alzheimer's disease (AD) (Yamada 2000).

Animal studies have supported a role of TH as neuroprotective agents against β-amyloid (Aβ) dependent neuronal impairment, which is assumed to be one of the pathophysiological mechanisms involved in AD (Accorroni 2020).

A novel insight in the complexity of TH signaling was provided by the discovery that TH derivatives represent additional chemical messengers. In particular, since T_1AM has been proposed as a memory enhancer as it induced pro-learning and antiamnestic effects in mice (Manni 2013, Laurino 2015), it has been investigated the effects of T_1AM on the early signs of neurodegeneration in models of Aβ toxicity on EC layer II (Accorroni 2020).

T_1AM and its receptor TAAR1 are present in the EC of WT and mhAPP mice. T_1AM counteracts Aβ-induced inhibition of LTP at the level of EC layer II, both when Aβ is acutely administered (Aβ 1-42 oligomers) and when it accumulates endogenously (mhAPP mice) (Accorroni 2020). This finding adds a novel issue to the discussions on the elusive links between TH signaling, Aβ effects and the pathophysiology of AD.

T_1AM neuroprotection may be achieved through the modulation of intracellular pathways counteracting cell stress signaling, leading to the increase in ERK 1/2 phosphorylation and cFos expression (Manni 2013; Bellusci 2017), that have been demonstrated to play a fundamental role in LTP mechanisms and in memory processes (Giese 2013; Minathoara 2015).

Furthermore, it has been suggested that some of T_1AM effects could be due to its oxidative product, 3-iodotyhyroacetic acid (TA_1) (Laurino 2015; Musilli 2014; Laurino 2018).

Recent investigation suggests that resveratrol (RSV), a polyphenolic phytoalexin produced by several plants, known to exhibit antioxidant and neuroprotective effects in several experimental models, can counteract Aβ-induced oxidative stress damage and memory loss associated to Aβ peptide accumulation (Rege 2015).

Chapter 2 Aim of the project

The focus of this project was on thyroid hormone derivates, mainly 3-Iodothyronamine T_1AM and 3-iodothyroacetic acid TA_1, a catabolite of T_1AM and their effects on different tissues.

Firstly, the effect of T_1AM on nervous tissue was analyzed. Starting from the evidence that T_1AM can have a putative role in neurotransmission, influencing memory and learning (Manni 2012), and counteracting beta-amyloid toxicity in mice (Pooler 2015), we decided to test this compound on two brain cell lines and evaluate its effects on the glutamatergic signaling cascade. To test this hypothesis two brain cancer cell lines were used as models: a hybrid line of cancer cells of mouse neuroblastoma and rat glioma (NG 108-15) and a human glioblastoma cell line (U-87 MG).
We first characterized cell lines, analyzing gene expression of glutamatergic receptors and several proteins involved in the glutamatergic postsynaptic cascade, then we evaluated the possible cytotoxicity and cellular uptake of T_1AM.
Cell lines were then treated with T_1AM in concentration ranging from 0.1 to 10 μM, alone or in combination with 10 μM resveratrol (RSV) and/or 10 μM amyloid β peptide (25-35). After treatment, we analyzed protein expression and phosphorylation of members of the glutamatergic postsynaptic signaling cascade. The possible metabolic effect, including glucose consumption, cAMP production and calcium concentration in cell lysates were assessed.

In the second part of the project, we extended investigations to 3-iodothyroacetic acid TA_1, a catabolite of T_1AM and of thyroid hormone, on the same cell lines we explored by infusion with T_1AM, assuming that TA_1 may either strengthen T_1AM effects or exert parallel actions, especially in brain tissue.

First, we assessed cytotoxicity and uptake of TA_1. Cell lines were then treated with TA_1, at concentration ranging from 0.1 to 10 μM. After treatment at the same conditions used for the previous experiments, we analyzed TA_1 effects on protein expression of members of the glutamatergic postsynaptic signaling cascade and cAMP production.

Chapter 3 Material and Methods

3.1 Chemicals

The 3-iodothyronamine (T_1AM) was purchased from Cayman Chemical (Ann Arbor, MI). TA_1 was kindly provided by Dr Thomas S Scanlan (Oregon Health and Science University, USA).
Resveratrol and amyloid β-Protein Fragment (25-35) were provided by Sigma-Aldrich (Saint Louis, MO, USA). Solvents for HPLC-MS/MS measurements were HPLC grade, and the other chemicals were reagent grade. Unless otherwise specified, all reagents were obtained from Sigma-Aldrich (St. Louis, MO, USA). The vehicle for T_1AM, TA_1, resveratrol and β-Protein Fragment (25-35), in the cell culture treatment, was dimethyl sulfoxide (DMSO). Primary antibody against GluR2, EphB2, NMDAR1, and secondary antibody were purchased from Cell Signaling (Danvers, MA, USA) CREB, pCREB (Ser133) were purchased from Thermo Fisher (Waltham, MA, USA), CAMKII, pCAMKII (Thr286), PKC were purchased from Santa Cruz Biotechnology (Dallas, TX, US).

3.2 Cell culture and treatments

NG 108-15 cell line, a hybrid cell line of mouse neuroblastoma and rat glioma, and U-87 MG cell line, from human malignant glioma, were obtained from Sigma-Aldrich (St. Louis, MO, USA). Cells were cultured in Dulbecco's Modified Eagle Medium (DMEM) supplemented with 10 % (vol/vol) of fetal bovine serum (FBS), 1 mM pyruvate, 4,5 g/L glucose, 100 U/mL penicillin, and 100 µg/mL streptomycin at 37 °C in a humidified atmosphere containing 5 % CO_2 and subcultured before confluence. Unless otherwise specified, cells were used after 4-5 passages in vitro.

To assess glucose uptake, cells were seeded in six-well plate (5×10^5 cells/well), with standard medium, grown to 80% of confluence and then washed twice with PBS before treatment. Cells were then exposed for 4 h to exogenous T_1AM (0.1-10 µM) or to the same T_1AM concentrations in presence of resveratrol (10 µM), or in presence of β-amyloid peptide 25-35 (10 µM), in 1 ml of the same DMEM base (phenol red free) supplemented with 0.5 mg/ml glucose. To evaluate resveratrol and β-Amyloid peptide 25-35 effects, a standard concentration of 10 µM was chosen for both. Control group was incubated with DMEM containing the same volume of vehicle. Glucose concentration was then evaluated in medium with a spectrophotometric assay kit (Sigma-Aldrich), reading the absorbance at 340 nm. Metabolite concentrations were referred to the total protein content of whole-cell lysates calculated using the Bradford method (Bradford 1976).

To assess protein expression, cells were seeded in six-well plates ($3x10^5$ cells/well) and grown to 80 % of confluence with standard medium. Cells were then exposed for 24 h to exogenous T_1AM and TA_1 (in a range from 0,1 µM to 10 µM) in presence/absence of 10 µM resveratrol (RSV) and/or 10 µM β-Amyloid peptide 25-35 (Aβ) in 2 mL of standard medium at 37 °C in 5 % CO_2. Control cells were incubated with supplemented DMEM containing DMSO. Aβ 25-35 is a neurotoxic fragment which rapidly accumulates in the brain; produced by the proteolytic cleavage of the peptide Aβ 1-40 by secretases, it can induce Alzheimer's disease in animal models (Deng 2016).

For Western-blot samples, we then removed the medium at the end of treatment, washed wells with sterile PBS and then cells were stored at -80°C until lysis. Cells in each well were lysed in ice-cold buffer (100 µl, pH 7.4) containing 20 mM Tris pH 7.5, 150mM NaCl, 1 mM ethylenediaminetetraacetic acid (EDTA), 1 mM EGTA, 25 mM sodium pyrophosphate, 1% Igepal CA-630, 1 mM sodium orthovanadate, 20 mM NaF, 1 mM phenylmethanesulfonyl fluoride (PMSF) and protease inhibitor cocktail was added to cells in well. After sonication, cell lysates were centrifuged at 10000xg for 10 minutes at 4°C to pellet cellular debris. The supernatant was collected and frozen to -80 °C. The protein concentration of the supernatant fraction was determined by the Bradford method (Bradford 1976).

3.3 Gene Expression Analysis

Expression of 8 genes (G*lur2, Nmdar1, Nmdar2b, Ephb2, Pkcα, Pkcγ, Sirt1, Erk1)* was evaluated in NG 108-15 and U-87 MG cell lines by real time PCR.

Real-time PCR samples was performed according to the manufacturer's instruction (Euroclone, Milan, Italy) and were obtained after removing medium from the 6 well plate and washed gently with PBS, 1mL of Eurogold Trisfast per well was added and then cells were stored at -80 °C until use.

To perform RNA isolation, 200µL of chloroform was added to each sample which were vigorously shaken for 15 s and then store at RT for 3 minutes. Samples were then centrifuged at 12000xg for 15 minutes at 4 °C, the aqueous phase was transferred to a new tube and 500 µL of isopropanol was added. Tubes were shaken, stored at RT for 10 minutes and centrifuged at 12000xg at 4 °C for 8 minutes. Pellets were then washed twice with 1 mL of 75 % ethanol and let dried. Then 50 µL of RNAase-free water were added and samples stored at -80 °C.

After resuspended RNA in RNAase free water, all samples were purified performing digestion with DNAase by RNA Clean & Concentrator (Zymo Reasearch, Irvine, CA, US). RNA concentration and purity were then analyzed using a Qubit RNA HS Assay kit (Life Technologies, Carlsbad, CA, USA) with a Qubit 1.0 fluorometer from Invitrogen (Waltham, MA, US).

1 µg of total RNA was then retrotranscribed in 20 µL (5 min at 25 °C, 20 min at 46 °C and 1 min at 95 °C) using iScript gDNA Clear cDNA Synthesis Kit (Bio-Rad Laboratories, Hercules, CA, USA). Expression of 8 genes (G*lur2, Nmdar1, Nmdar2b, Ephb2, Pkcα, Pkcγ, Sirt1, Erk1)* were evaluated in the two cell lines (NG 108-15 and U-87 MG) by real time PCR.

Relative quantity of gene transcripts was measured by real-time PCR on samples' cDNA using a SYBRGreen chemistry and iQ5 instrument (Bio-Rad). 4 µL of 2 µM primer solution was added to 10 µL SsoAdvanced Universal SYBR Green Supermix (Bio-Rad) in a 20 µL total volume reaction. The PCR cycle program consisted of an initial 30 s denaturation at 95 °C followed by 40 cycles of 10 s denaturation at 95°C and 15 s annealing/extension at 60 °C. For primers with low Ta, we used lower temperature for the annealing/extension step. Primers were designed with Beacon Designer Software v.8.20 (Premier Biosoft International, Palo Alto, CA, USA) with a junction primer strategy (Tables 1 and 2). For the hybrid cell line, we used ClustalW (Larkin 2007) to find the homology region where we designed the primer. In any case, negative control of retro-transcription was performed to exclude any interference from residual genomic DNA contamination.

3.4 Uptake of T_1AM and HPLC–MS/MS Assay Technique

To evaluate T_1AM uptake, cells were seeded in 24-well plate, ($8x10^4$ cells/well), and let grow until 80 % confluency. At the beginning of each experiment, the culture medium was removed, wells washed with PBS and cells were incubated with fresh medium supplemented with T_1AM or TA_1, at concentration ranging from 0.1 to 10 µM. The medium was then removed at specific time point from each well and frozen at −80°C until extraction.

For cell lysis, 100 µl of 0.1 M NaOH were used with consequent pH neutralization by adding 10 µl of 1 M HCl to each well. 390 µl MeOH were added before samples collected and then centrifuged for 10 min at 14,000 × g. The supernatants were evaporated under N_2 at 40°C and reconstituted with 50 µl of water/methanol (70/30 by volume) solution.

Cell medium was extracted using a liquid-liquid method with the addition of 1 mL of methyl tert-butyl ether (MTBE). The mixture quickly shaken and spun at 14,000 × g to separate the organic from aqueous phases, which was then collected. The extraction process was repeated twice, the organic phases were collected in the same tube which were then evaporated under a gentle stream of nitrogen at 40°C. Dried samples were reconstituted with 50 µL of water/methanol (70/30 by volume).

To assess distribution in cellular fractions, cells were treated in flasks with 10 µM T_1AM for 1h. The nuclear pellet was extracted by using a nuclear extraction kit (Abcam); the resulting cytoplasmic extract was centrifuged at 10000 x g for 30 min at 4°C to separate the mitochondrial and the cytosolic

fractions. Media, cell lysates and fractions were extracted following the same protocol mentioned above.

3.4.1 Instrumental layout and operative conditions

HPLC-MS-MS was performed using an AB Sciex API 4000 triple quadrupole mass spectrometer (Concord, ON, Canada), equipped with an electrospray (ESI) Turbo V ion source, coupled to an Agilent 1290 Infinity UHPLC system (Santa Clara, CA, USA).

Chromatographic separations were carried out using a 110 Å, 2x50 mm, 3µm particle size, Gemini C18 column (Phenomenex, Torrance, CA), protected by a C18 Security guard cartridge and thermostated in the column oven.

For data acquisition and system control an AB Sciex Analyst version 1.6.3 software was used.

1 µL of each sample were injected into the system and gradient chromatography were carried out with a flow rate of 400 µl min^{-1} using methanol (MeOH)/acetonitrile (ACN) (20/80 by volume) added with 0.1% formic acid (FA) as solvent A and water containing 0.1% FA as solvent B.

T_1AM and TA_1 selected reaction monitoring (SRM) mass spectrometry methods were used operating in positive and negative ion mode, respectively. For each compound, after the optimization of declustering potential (DP), collision energy (CE) and collision exit potential (CxP), three transitions were considered in the analysis. Based on the highest signal/noise ratios, one of them was used as quantifier (356→ 212 for T_1AM and 369 →127 for TA_1) and the other two as qualifiers (Table 2).

	Positive ion mode					Negative ion mode			
	Operative parameters					Operative parameters			
Analyte	SRM transition	DP	CE	CXP	Analyte	SRM transition	DP	CE	CXP
T_1AM	356 → 165	50	57	14	TA_1	369 →127	-28	-14	-11
	356 → 165		36	16		369 →197		-13	-11
	356 → 212		26	18		369 → 325		-8	-8

Table 2. SRM transition and operative parameters for T_1AM and TA_1. T_1AM in the positive ion mode and TA_1 in the negative ion mode. DP, Declustering potential; CE, collision energy; CXP, collision exit potential (Saba 2010).

3.5 Cell viability

Cell viability was assessed by using two different assays: crystal violet staining (Feoktistova 2016) and the 3-(4,5-dimethylthiazol-2-yl) 2,5-diphenyltetrazolium bromide (MTT) test (Mossmann 1983). Cells were seeded in 96-well microtiter plate at a density of 5,000–10.000 and treated the day after the seeding. Cells were treated with different concentrations T_1AM and/or resveratrol and/or β-Amyloid peptide 25-35, or with different concentrations of TA_1 and cell viability was determined 24 h after incubation. For the MTT test, 2,5-diphenyltetrazolium bromide (0.5 mg/ml) was added to the medium, and after 4 h an SDS–HCl solution (0.05 mg/ml) was used to solubilize the formed formazan salt. The absorbance of the solution after 18h was read at 570 nm in a microplate reader (BioRad Laboratories, Italy). Since the MTT test focuses on the mitochondrial function, we used also a different cell viability assay, the crystal violet staining that measure cell adherence (Mossmann 1983). In this technique the crystal violet binds to DNA and proteins of attached cells and is considered as an alternative index of viability (Mossmann 1983). For the crystal violet staining, after the treatment, cells were washed gently with PBS and stained 10 min at room temperature with crystal violet solution (0.2% crystal violet in 2% ethanol). The plate was then washed twice with deionized water, a 1% SDS solution was added to each well and the plate agitated until complete solubilization of the staining. In the end the absorbance was read at 570 nm.

3.6 Glucose consumption

To assess glucose uptake, cells were seeded in six-well plate (5×10^5 cells/well) and exposed for 4 h to exogenous T_1AM (0.1–10 μM), in presence/absence of Resveratrol and/or β-amyloid peptide 25-35 10 μM, in 1 mL of DMEM (phenol free) supplemented with 0.5 mg/mL glucose. Control cells were incubated with DMEM containing the same volume of vehicle. Cell culture medium was then collected, and glucose concentration was evaluated in medium with a spectrophotometric assay kit (Sigma-Aldrich).

3.7 cAMP and Calcium production

cAMP concentration was assessed in cell lysate with an ELISA assay kit (BioVision Incorporated, USA) according to manufacturer's instruction. Briefly cells were treated for 24 h T_1AM and TA_1 (0.1–10 μM). At the end of treatment, medium was removed, 0.1M HCl was added to each well (1 ml of 0.1 M HCl for every 35 cm2 of surface area) and cells incubated at RT for 20 minutes. Then cells were scraped, collected and centrifuged for 10 min at top speed. The cAMP concentration in

supernatant was spectrophotometrically evaluated, and results were normalized to total protein concentration in supernatant.

3.8 Western blotting

Western blotting was performed according to manufacturer's instructions (Biorad). In brief, 40 µg of proteins was subjected to SDS-PAGE (4-20% acrylamide separating gel, Criterion stain free TGX Biorad). The separated proteins were transferred to a polyvinylidene difluoride (PVDF) membrane (Millipore Corporation, Billerica, MA, USA), which was dried and then incubated with diluted antibody (1:1000) in 5 % w/v BSA, 1X TBS, 0,1 % Tween 20 at 4 °C with gentle shacking, overnight. Primary antibodies against CREB, pCREB, pERK, Sirt1, cFos, β-actin, EphB2, NMDAR1 and GluR1/2, and secondary antibodies were purchased from Cell Signaling (Danvers, MA, USA); CAMKII, pCAMKII, ERK were purchased from Santa Cruz Biotechnology (Dallas, TX, US).
Immunoblots were visualized by means of a chemiluminescence reaction (Millipore) by Image LabTM Software (Biorad) under a luminescent image analyzer (Chemidoc XSR+ Biorad). Only bands below the saturation limit were analyzed. The chemiluminescence was expressed in terms of volume of specific immunoreactive bands and the protein level was normalized to the total protein density in each lane, previously acquired. The trihalo compounds, included into the TGX stain free gel (Biorad), react with tryptophan residues in a UV-induced reaction, allowing total protein detection by fluorescence on membranes and on gels. This allowed us to normalize the results on total blotting protein, and to avoid the use of a housekeeping protein as loading control. Only bands below the saturation limit were analyzed.

3.9 Statistical Analysis

Results are expressed as the mean of replicas ± SEM. Differences between groups were analyzed by one-way ANOVA or two-way ANOVA, as detailed for each figure. In the experiments aimed at determining differences vs a single control group, Dunnett's post hoc test was applied. The threshold of statistical significance was set at $P < 0.05$. GraphPad Prism version 6.0 for Windows (GraphPad Software, San Diego, CA, USA) was used for data processing and statistical analysis.

Chapter 4 Results

4.1 Characterization

Both cell lines, NG 108-15 and U-87 MG, were characterized by real time PCR to evaluate the expression of receptors implicated in the glutamatergic postsynaptic pathway. The expression of NMDAR1, NMDAR2B, GLUR2, EPHB2, TAAR1 genes was evaluated using as housekeeping gene mouse TATA box binding protein (TBP) for NG 108-15 cells and Hypoxanthine phosphoribosyltransferase 1 (HPRT1) for U-87 MG cells.

The receptor expression was evaluated using real time PCR (Table 3). As shown in table 3, both cell lines expressed receptors implicated in glutamatergic postsynaptic pathway: NMDAR1, GLUR2, EPHB2. TAAR1, the putative T_1AM receptor, was expressed only in the U-87 MG cell lines. Other proteins, namely PKCA, SIRT1 and ERK1, implicated in the postsynaptic signaling were also expressed as revealed by Western blotting.

	Threshold cycle	
Gene	**NG 108-15**	**U-87 MG**
Nmdar1	21,84	32,72
Glur2	25,64	31,79
Ephb2	29,51	25
Taar1	--	35,01
Tbp	22,62	24,53

Table 3. Characterization of NG 108-15 and U-87 MG cell lines by using real time PCR. Values of the threshold cycle, compared to the housekeeping gene (TATA box binding protein, TBP, in NG 108-15 cells, and Hypoxanthine phosphoribosyltransferase 1, HPRT1, in U-87 MG cells).

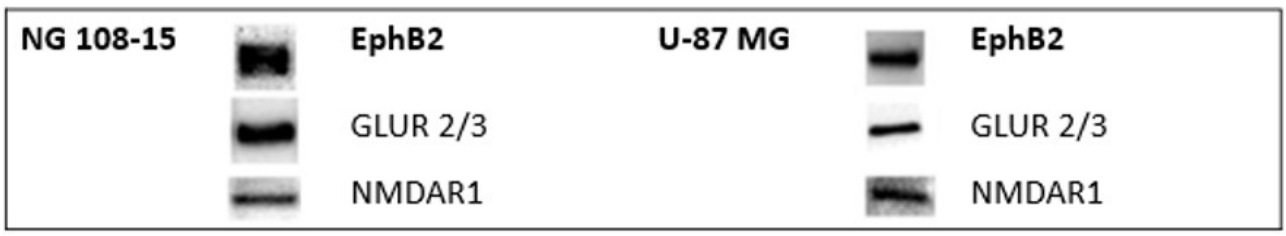

Figure 12. NG 108-15 and U-87 MG cell lines were characterized for expression of receptors implicated in synaptic plasticity by Western blot. Blots of NMDAR1, Glu 2/3, and EphB2 in NG 108-15 and U-87 MG cells.

4.2 Cellular uptake

4.2.1 Cellular uptake of T_1AM

We measured by HPLC MS/MS T_1AM uptake and TA_1 production in NG 108-15 and U-87 MG cell lines, in presence of FBS and T_1AM at concentrations of 0.1, 1 or 10 µM, in cell medium and lysate at the end of treatment (Instrument detection limits: T_1AM > 0.3 nM; TA_1 > 5 nM).

In medium used to treat NG 108-15 cells, after 24 hours, T_1AM was detectable only at the highest concentration of infusion (10 µM) and averaged 0.66 ± 0.14 nM, while its catabolite, TA_1, was detected starting from the lowest concentration, respectively at the following concentrations: 404 ± 21 nM (0.1 µM T_1AM); 2576 ± 272 nM (1 µM T_1AM); 4996 ± 97 nM (10 µM T_1AM). Similar results were obtained in U-87 MG cell line, where, in medium T_1AM was present in trace amounts (0.36 ± 0.01 nM, at 10 µM T_1AM), and TA_1 was, respectively 95 ± 6 nM (0.1 µM T_1AM), 2323 ± 66 nM (1 µM T_1AM), and 13214 ± 302 nM (10 µM T_1AM) (Table 4).

Cell lines	Medium (nM)					
	0.1 µM T_1AM		1 µM T_1AM		10 µM T_1AM	
	T_1AM	TA_1	T_1AM	TA_1	T_1AM	TA_1
NG 108-15	N.D.	404 ± 21 nM	N.D.	2576 ± 272 nM	0,66 ± 0,14 nM	4996 ± 97 nM
U-87 MG	N.D.	95±6 nM	N.D.	2323 ± 66 nM	0.36 ± 0.01 nM	13214 ± 302 nM

Table 4. Concentrations of T_1AM and of its catabolite TA_1, in cell medium, in NG 108-15 and U-87 MG after 24 hours of treatment with T_1AM at concentration ranging from 0,1 to 10 µM. Data represent mean ± SEM, n=3-4 per group. [p<0.0001 for TA_1 in medium and lysate in both cell lines (ANOVA)]. N.D., Not Detectable.

In NG 108-15 or U-87 MG cell lysates T_1AM was still measurable only at 10 µM T_1AM (10 ± 6 nM or 6 ± 0.3 nM respectively), and present in trace amounts at the other tested concentrations. Differently, TA_1 was clearly detectable at 1 or 10 µM T_1AM and averaged, respectively, as follow: in NG 108-15 cell lysate, 7.7 ± 0.2 nM (1 µM T_1AM); 91 ± 19 nM (10 µM T_1AM); in U-87 MG cell lysate, 22 ± 5 nM (1 µM T_1AM); 144 ± 80 nM (10 µM T_1AM); it was present in trace amount at 0.1 µM T_1AM in both cell lines (Table 5).

Cell lines	Lysate (nM)					
	0.1 µM T_1AM		1 µM T_1AM		10 µM T_1AM	
	T_1AM	TA_1	T_1AM	TA_1	T_1AM	TA_1
NG 108-15	N.D.	N.D.	N.D.	7.7 ± 0.2 nM	10 ± 6 nM	91 ± 19 nM
U-87 MG	N.D.	N.D.	N.D.	22 ± 5 nM	6 ± 0.3	144 ± 80 nM

Table 5. Concentrations of T_1AM and of its catabolite TA_1, in cell lysate, in NG 108-15 and U-87 MG cell lines after 24 hours treatment with T_1AM at concentration ranging from 0,1 to 10 µM. Data represent mean ± SEM, n=3-4 per group. [p<0.0001 for TA_1 in medium and lysate in both cell lines (ANOVA)]. N.D., Not Detectable.

T_1AM uptake and TA_1 production are shown in both cell lines, NG108-15 (Figure 13) and U-87 MG (Figure 14), in presence of FBS, in cell medium and lysate. Cells were treated for 0, 1, 2, 4, 24 hours with T_1AM, at concentrations 0,1, 1 and 10 µM. The concentration of T_1AM, or the production of its catabolite, TA_1, defined as peak area, were measured by LC-MS-MS in cell medium and lysate.

When NG 108-15 cells are exposed to 0,1 and 1 µM T_1AM, its concentration in the incubation medium decreased drastically and tended to zero after 2 and 3 hours, respectively (Figure 13 A and B). Instead, when cells are exposed to 10 µM T_1AM, its concentration decreased, reaching a steady state after 3 hours (Figure 13 C). T_1AM in cell lysate, instead, increased (Figure 13 A, B and C).

Medium and lysate were also assayed for T_1AM catabolite, TA_1. A considerable increase in TA_1 production was observed both in lysate and in medium, with an accumulation proportional to the decrease of T_1AM (Figure 13).

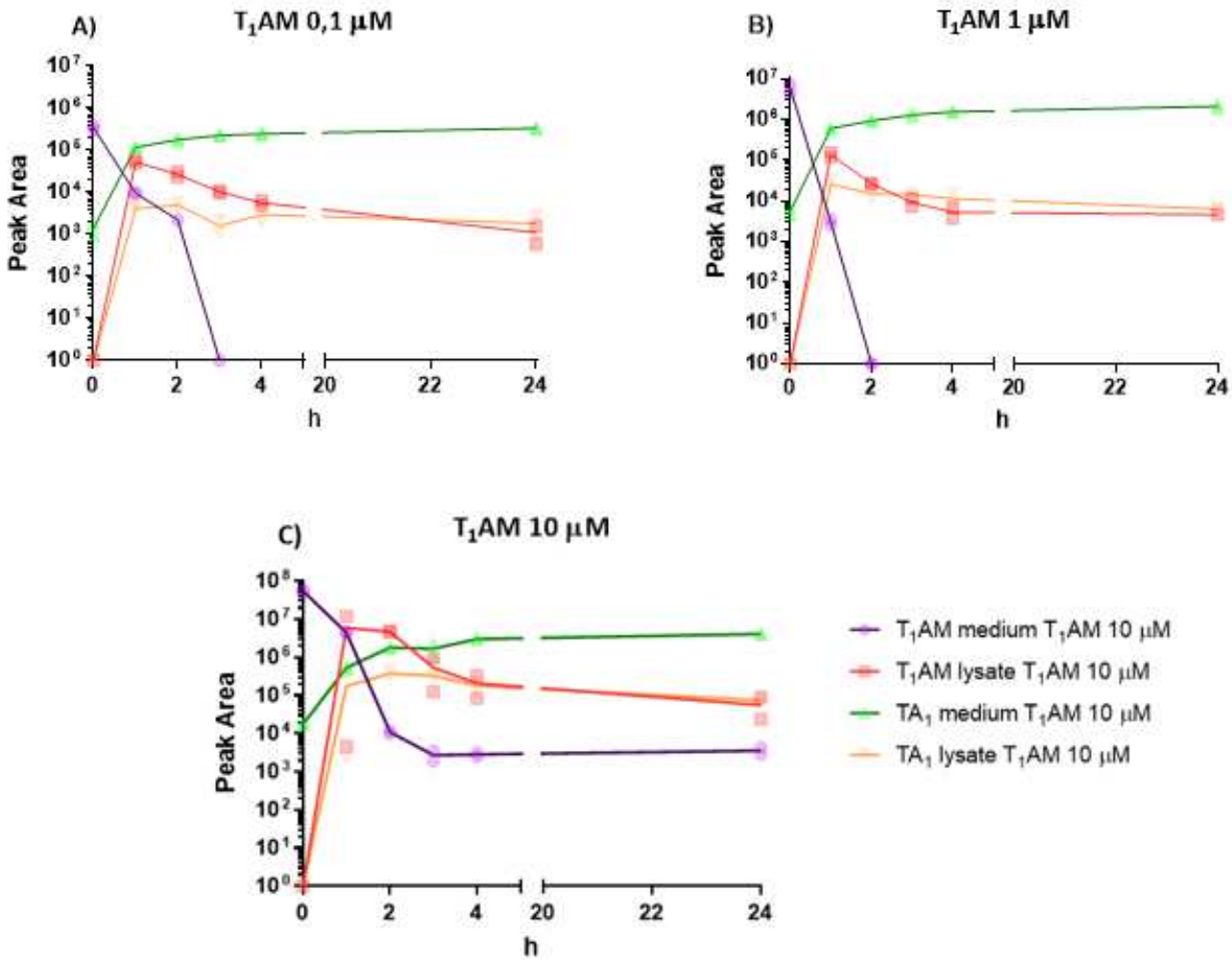

Figure 13. T_1AM cellular uptake was measured with LC-MS-MS in NG 108-15 cells in cell lysate and medium. Cells were treated for 0, 1, 2, 4 and 24 hours, with T_1AM 0,1 µM (A), 1 µM (B) and 10 µM (C). TA_1 production was evaluated in cell lysate and medium using TA_1 peak area.

Similar results were obtained in U-87 MG cell line (Figure 14) treated for 0, 1, 2, 4, 24 h with T_1AM at concentrations 0,1, 1 and 10 µM.

T_1AM concentration in cell medium, decreased and tended to zero after 2 and 4 hours of treatment with T_1AM 0,1 and 1 µM, respectively, while its concentration decreased and reached a steady state after about 4 hours when cells were treated with T_1AM at concentration of 10 T_1AM (Figure 14 C). T_1AM, instead, increased in cell lysate (Figure 14).

As previously observed in NG 108-15 cell line, a considerable increase in TA_1 production was observed both in lysate and in medium of U-87 MG cells, with an accumulation proportional to the decrease of T_1AM (Figure 14 A, B and C).

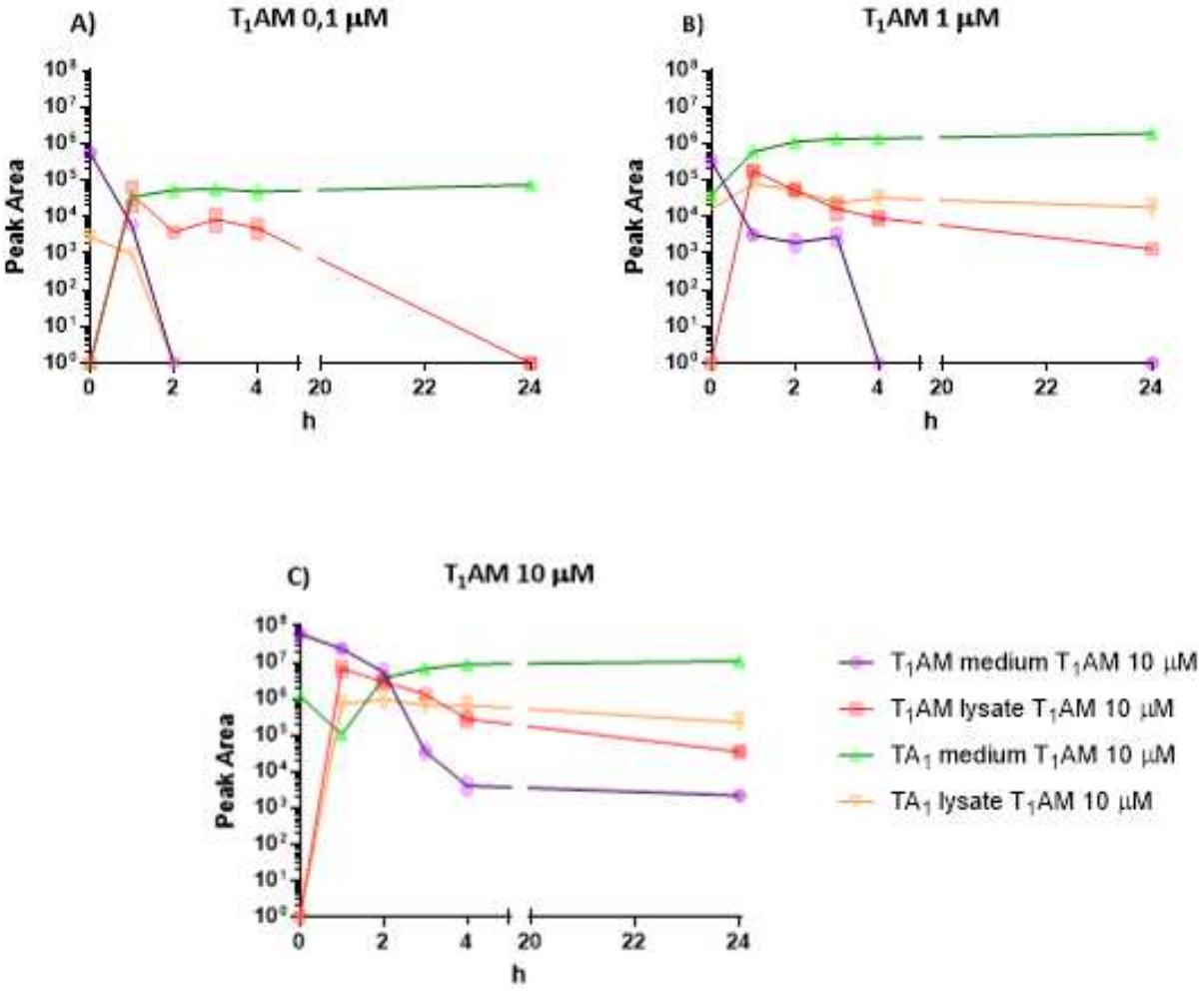

Figure 14. T_1AM cellular uptake was measured with LC-MS-MS in U-87 MG cells in cell lysate and medium. Cells were treated for 0, 1, 2, 4 and 24 hours, with T_1AM µM 0,1 (A), 1 µM (B) and 10 µM (C). TA_1 production was evaluated in cell lysate and medium using TA_1 peak area.

The values of the concentrations of T_1AM and of its catabolite, TA_1, in different cell fractions are summarized in Table 6 and expressed as µM and nM, respectively. The results showed a similar

T_1AM distribution in the two cell lines: T_1AM was detected in all fractions, albeit at a higher concentration in cytosol and nuclear fractions. Differently, TA_1 was measurable in all fractions of NG 108-15 cells, while in U-87 MG cells TA_1 was detected only in cytosol. Due to pellet resuspension, the concentrations of T_1AM and TA_1 in the mitochondrial and nuclear fractions might be underestimated. These results indicated a wide distribution of T_1AM in cell and confirmed that different experimental models may produce diverse behaviors.

Cell lines	Cytosolic fraction		Mitochondrial fraction		Nuclear fraction	
	T_1AM µM	TA_1 nM	T_1AM µM	TA_1 nM	T_1AM µM	TA_1 nM
NG 108-15	2.89 ± 0.13	205.3 ± 27.6	1.66 ± 0.1	18.6 ± 2.9	2.77 ± 0.07	46.5 ± 9.3
U-87 MG	2.62 ± 0.24	20.5 ± 0.9	0.54 ± 0.17	N. D.	1.63 ± 0.34	N. D.

Table 6. Concentrations of T_1AM and TA_1 in cellular fractions after 1 hour treatment with T_1AM (0,1 to 10 µM) in NG 108-15 and U-87 MG cell lines. Data represents mean of 3 values ± SEM, n=3 per group. [Within each row, $p<0.0001$ for T_1AM, and $p<0.001$ for TA_1 for differences among cellular fractions (ANOVA)]. N.D., Not Detectable.

To exclude any potential endogenous production of thyronamines or derivative catabolites, the same experimental procedure was repeated with supplemented DMEM in absence of exogenous T_1AM, incubated alone or in presence of cells: neither T_1AM nor TA_1 were revealed.

4.2.2 Cellular uptake of TA_1

We measured by HPLC MS/MS TA_1 uptake in NG 108-15 and U-87 MG cell lines, in presence of FBS and TA_1 at concentration of 0.1, 1 or 10 µM, in cell medium and lysate at the end of treatment. (Instrument detection limits: TA_1 > 5 nM).

Results in Figure 15 demonstrated that neither change in concentration nor further metabolism occurred during infusion in only medium.

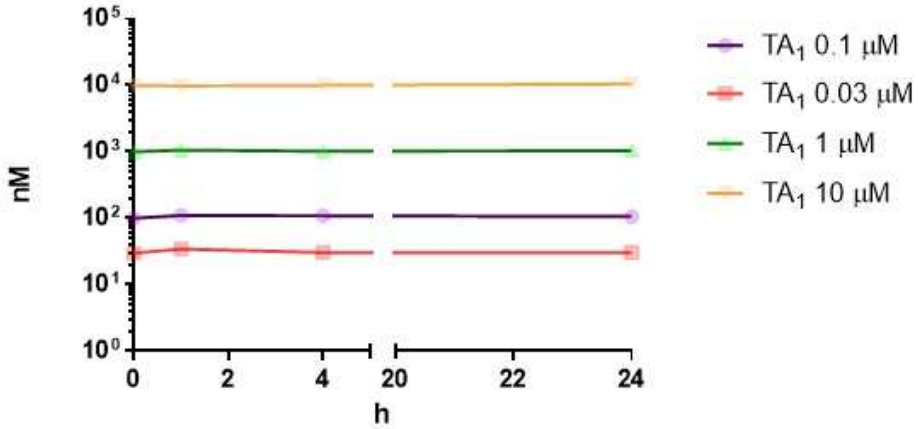

Figure 15. TA_1 uptake was measured with LC-MS-MS in only medium treated for 0, 1, 2, 4 and 24 hours, with TA_1 at concentration 0,1, 0,03, 1 and 10 µM. TA_1 was evaluated in medium using TA_1 peak area.

In presence of cells, TA_1 was taken up and even though only a slight reduction in medium concentration was recorded upon 24 hours of incubation, TA_1 was detectable in medium and cell lysate (Figure 16).

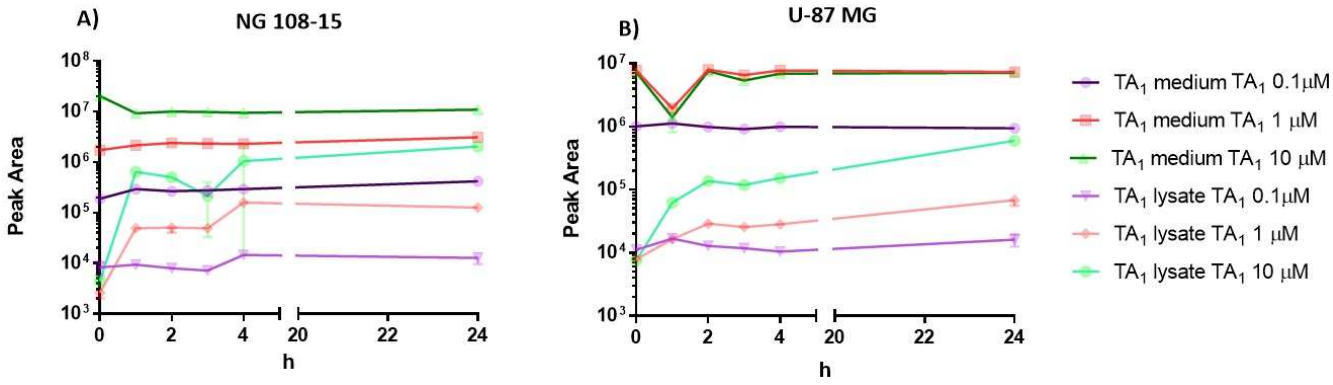

Figure 16. TA_1 cellular uptake was measured with LC-MS-MS in NG 108-15 (A) and U-87 MG (B)cell lines in cell lysate and medium. Cells were treated for 0, 1, 2, 4 and 24 hours, with TA_1 at concentration 0,1, 1 and 10 µM. TA_1 was evaluated in cell lysate and medium using TA_1 peak area.

As shown in table 7, in medium used to treat NG 108-15 cells, after 24h, TA_1 was detectable respectively at the following concentrations: 233 ± 18 nM (0.1 µM TA_1); 1795 ± 55 nM (1 µM TA_1); 5355 ± 175 nM (10 µM TA_1). Similar results were obtained in U-87 MG cell line where in medium TA_1 was present at the following concentrations: 135 ± 26 nM (0.1 µM TA_1); 1193 ± 140 nM (1 µM TA_1); 1520 ± 327 nM (10 µM TA_1).

In NG 108-15 or U-87 MG cell lysates, TA_1 was clearly detectable at 0,1, 1 and 10 µM TA_1 and averaged, respectively, as follow: in NG 108-15 cell lysate, 6,8 ± 1,9 nM (0,1 µM TA_1); 72,4 ± 6,9 nM (1 µM TA_1), reaching the high concentration of 995 ± 95 nM for 10 µM TA_1. In U-87 MG cell lysate, 1,6 ± 0,1 nM (0,1 µM TA_1); 15,4 ± 3,9 nM (1 µM TA_1), reaching the high concentration of 120 ± 22 nM for 10 µM TA_1 (Table 7).

Cell lines	Medium			Lysate		
	0,1 µM TA_1	**0,1 µM TA_1**	**0,1 µM TA_1**	**0,1 µM TA_1**	**0,1 µM TA_1**	**0,1 µM TA_1**
NG 108-15	233 ± 18 nM	1795 ± 55 nM	5355 ± 175 nM	6,8 ± 1,9 nM	72,4 ± 6,9 nM	995 ± 95 nM
U-87 MG	135 ± 26 nM	1193 ± 140 nM	1520 ± 327 nM	1,6 ± 0,1 nM	15,4 ± 3,9 nM	120 ± 22 nM

Table 7. Cellular uptake TA_1. Uptake was measured using LC-MS-MS in medium and in cell lysate.

In NG 108-15 or U-87 MG cell lysates, T_1AM was present in trace, maybe as impurity of TA_1, since neither T_1AM nor TA_1 were revealed in previous assessment of the experimental model.

4.3 Glucose consumption

To assess glucose consumption, NG 108-15 and U-87 MG cells were incubated for 4 hours in phenol red-free DMEM containing 0.5 mg/mL glucose. At the end of treatment, glucose concentration was assayed in the medium and results were expressed as the difference between the initial and the final concentrations, normalized to the total proteins content in cell lysates.

As indicated in Figure 17 A, a 20 % decrease in glucose consumption was observed upon 4 hours of treatment at 1-10 µM with T_1AM, in the NG 108-15 cell line (*p<0.05 vs control), while no significant changes were observed after treatment in U-87 MG cell line (Figure 17 B, p=NS vs control).

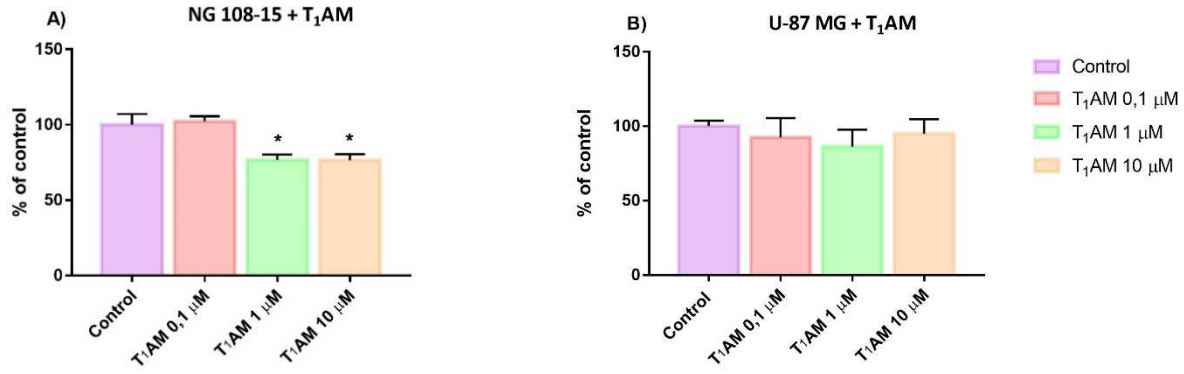

*Figure 17. Glucose consumption evaluated using a spectrophotometric assay kit after 4h of treatment with T_1AM 1-10 µM in NG 108-15 (A) and in U-87 MG cells (B). Results are the difference between the initial and the final glucose concentration in medium, normalized to the total content of proteins in cell lysate. Control cells were incubated with medium containing the same volume of vehicle. Values are mean 3-4 replicas ± SEM and are expressed as % of control. [One-way ANOVA and Dunnett's post-hoc test for multiple comparison, *p<0.05, vs control].*

By comparison, glucose consumption was not affected in cells exposed to T_1AM in combination with RSV 10 µM (Figure 18).

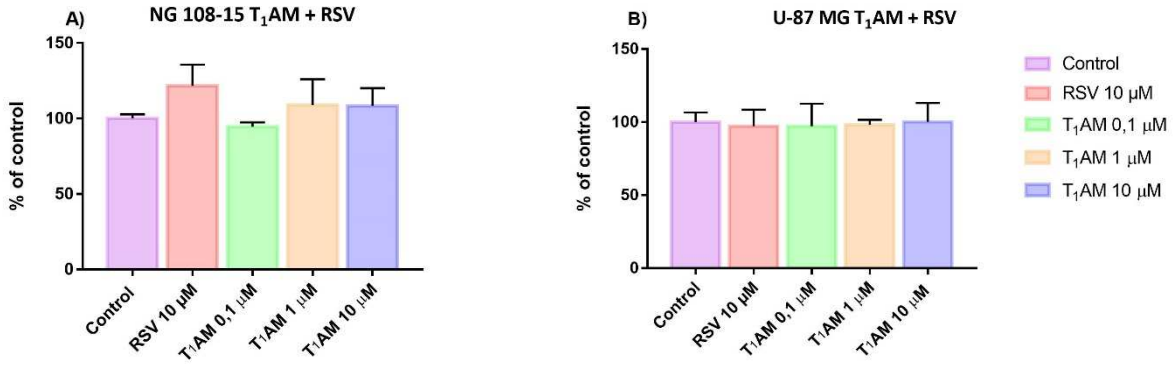

Figure 18. Glucose consumption was evaluated using a spectrophotometric assay kit after 4h of treatment with T_1AM 1-10 µM in combination with resveratrol (RSV) 10 µM in NG 108-15 cells (A) and in U-87 MG cells (B). Results are the difference between the initial glucose concentration in medium and the final concentration, normalized to the total content of proteins in cell lysate. Control cells were incubated with medium containing the same volume of vehicle. Values are mean of 3-4 replicas ± SEM and are expressed as % of control. [One-way ANOVA and Dunnett's post-hoc test for multiple comparison, p=NS].

In cells exposed to T_1AM in combination with β-amyloid peptide 25-35 10 µM, we observed a 20% increase of glucose consumption in NG 108-15 cells treated with 1 µM T_1AM and β-amyloid (Figure 19 A, *p<0.05 vs Control). Instead, in U-87 MG, a 20% decrease in glucose consumption was observed after infusion with β-amyloid 10 µM alone (Figure 19 B, *p<0,05 vs Control) and this effect seem to be restored after the treatment in combination with T_1AM (Figure 19 B, p=NS).

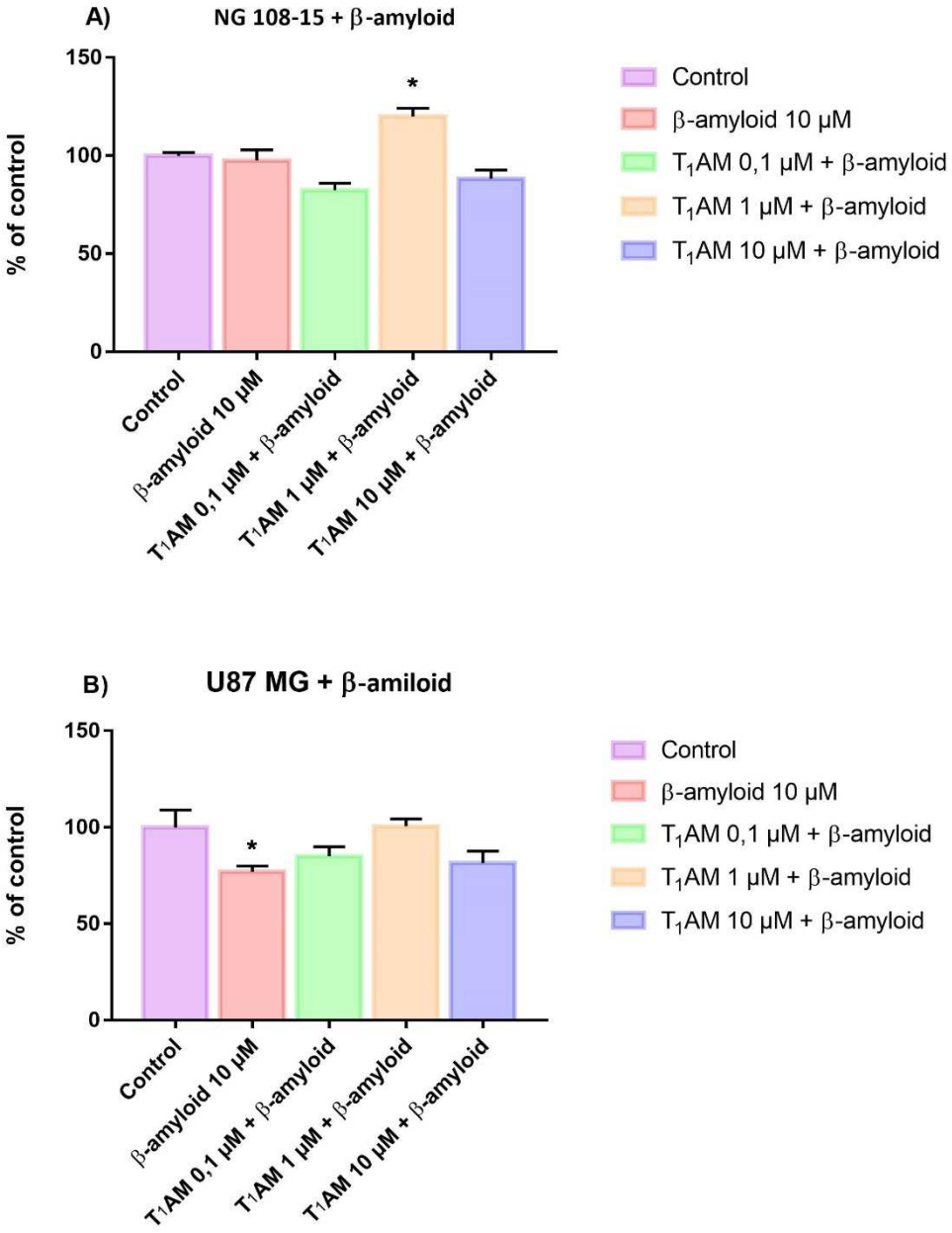

*Figure 19. Glucose consumption was evaluated using a spectrophotometric assay kit after 4h of treatment with T_1AM 1-10 µM in combination with 10 µM β-amyloid 23-35, in NG 108-15 cells (A) and in U-87 MG cells (B). Results are the difference between the initial and the final glucose concentration in medium, normalized to the total content of proteins in cell lysate. Control cells were incubated with medium containing the same volume of vehicle. Values are mean of 3-4 replicas ± SEM and are expressed as % of control. [One-way ANOVA and Dunnett's post-hoc test for multiple comparison, *p<0.05 vs Control].*

4.4 Calcium Assay and cAMP Assay

4.4.1 Effects of T_1AM

cAMP and Calcium intracellular concentration were evaluated using a cAMP assay kit and a Calcium assay kit, after 24h of treatment with T_1AM at concentration ranging from 0,1 µM to 10 µM. As shown in Figure 20, a significant decrease in intracellular calcium concentration was observed in NG 108-15 cell line at every concentration dose of T_1AM treatment (-40% at 0,1 µM T_1AM *p<0.05, -50% at 1 and 10 µM T_1AM, **p<0,01, ***p<0,001 vs Control), while no change in the intracellular calcium concentration was observed in U-87 MG (p=NS).

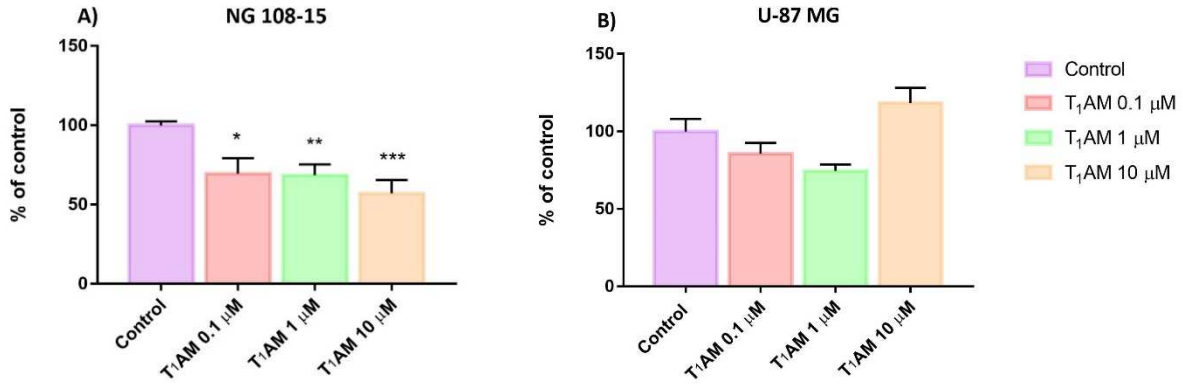

*Figure 20. Calcium intracellular concentration after 24h of treatment with T_1AM (0,1 to 10 µM), in NG 108-15 (A) and U-87 MG (B) cell lines. Calcium concentrations in each sample were normalized to the total content of proteins in cell lysates. All treatments received the same amount of vehicle. Control groups were incubated with medium containing the same volume of vehicle (DMSO). Data are plotted as means of 6-8 replicas ± SEM and expressed as % of control [one-way ANOVA and Dunnett's post hoc test for multiple comparison, *p<0.05, **p<0,01, ***p<0,001 vs Control].*

Instead, 0.1 µM and 10 µM T_1AM increased cAMP production of 90% in U-87 MG cell line (Figure 21 B, *p<0.05, **p<0,01 vs Control), while no change was observed in NG 108-15 cell line (Figure 21 A, p=NS)

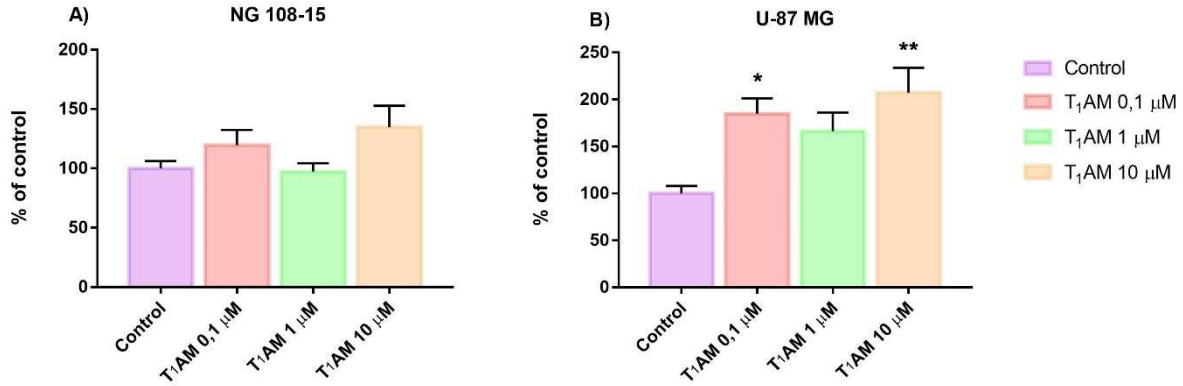

*Figure 21. cAMP concentration in NG 108-15 (A) and U-87 MG (B) cell lines after treatment with T_1AM. cAMP concentrations in each sample were normalized to the total content of proteins in cell lysates. All treatments received the same amount of vehicle. Control groups were incubated with medium containing the same volume of vehicle (DMSO). Data are plotted as means of 6-8 replicas ± SEM and expressed as % of control [one-way ANOVA and Dunnett's post hoc test for multiple comparison, *p<0,05, **p<0,01 vs Control].*

4.4.2 Effects of TA_1

The same experiment was repeated assessing cAMP concentration using a colorimetric assay kit, after 24 hours of treatment with TA_1 at concentration ranging from 0,1 µM to 10 µM.

As shown in Figure 22, no significative changes occurred in the intracellular cAMP concentration in NG 108-15 (Figure 22 A) or U-87 MG cells (Figure 22 B) (p=NS).

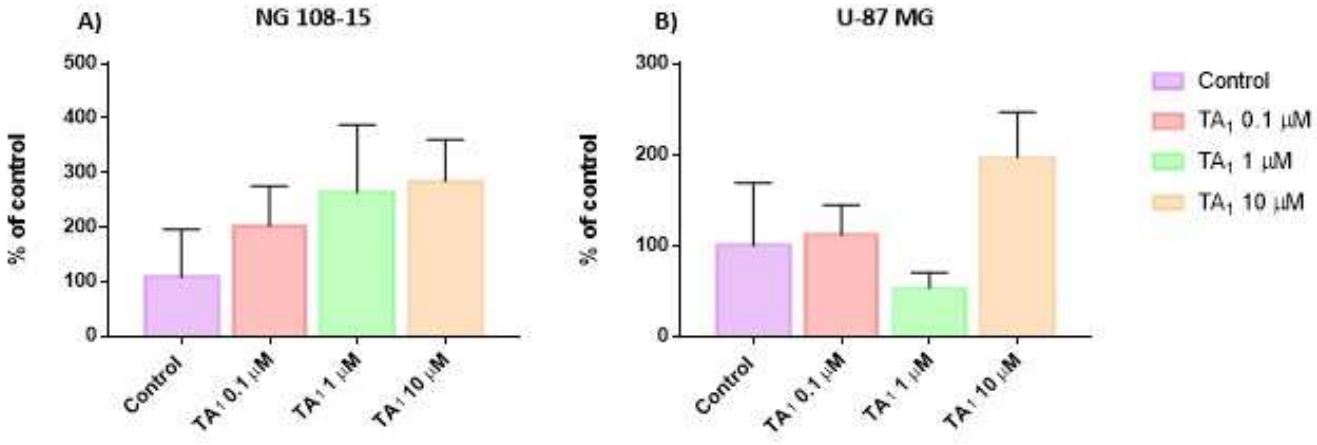

Figure 22. cAMP concentration in NG 108-15 (A) and U-87 MG (B) cell lines after treatment with TA_1. cAMP concentration in each sample was normalized to the total content of proteins in cell lysates. All treatments received the same amount of vehicle. Control groups were incubated with medium containing the same volume of vehicle (DMSO). Data are plotted as means of 6-8 replicas ± SEM and expressed as % of control [one-way ANOVA and Dunnett's post hoc test for multiple comparison, p=NS].

4.5 Cell viability

Cell viability was assessed by using two different assays: crystal violet staining (Feoktistova 2016) and the 3-(4,5-dimethylthiazol-2-yl) 2,5-diphenyltetrazolium bromide (MTT) test (Mossmann 1983).

4.5.1 MTT

4.5.1.1 MTT T_1AM

Cell viability was evaluated using MTT test in NG 108-15 and U-87 MG cells treated with different concentrations of T_1AM (ranging from 10 nM to 10µM) alone (Figure 23 A) and in association with Resveratrol RSV 10 µM (Figure 23 B) or β-amyloid peptide 25-35 10 µM (Figure 23 C).

Preliminary results indicated that 10 µM Aβ was able to significantly decrease cell viability without occurring a drastic reduction (data not shown).

In both cell lines, T_1AM showed a slightly but significant cytotoxic action starting from 0.1 µM (Figure 23 A, -10/15 %, *p<0.05 vs control), implying also a reduced oxidative metabolism, which is completely blunted if incubated with RSV (Figure 23 B).

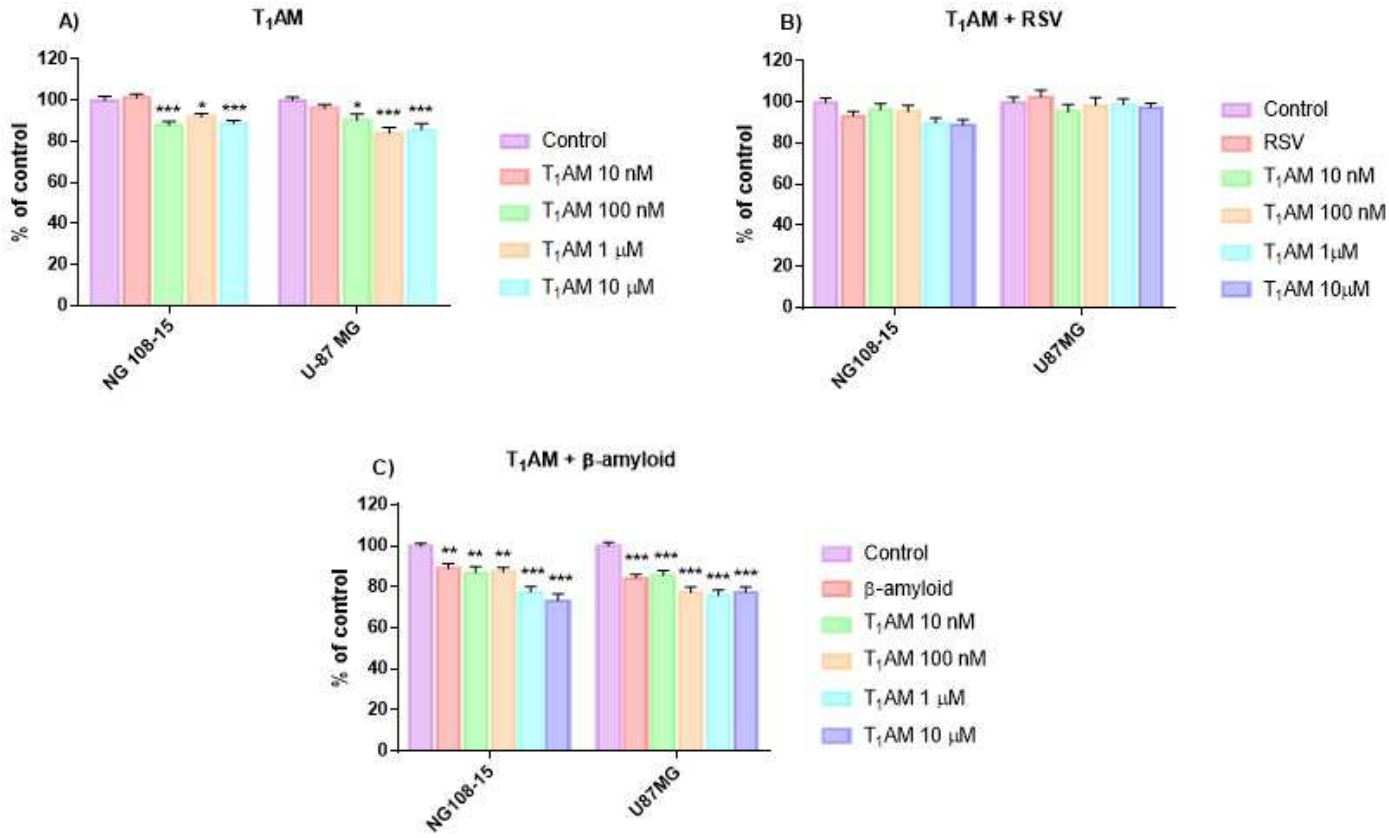

*Figure 23. Cell viability of NG 108-15 or U-87 MG cell lines after the treatment with T_1AM by using MTT test. In (A) cells, except for control, were treated with T_1AM at concentration ranging from 10 nM to 10 µM. Data are plotted as means of 6-8 replicas ± SEM, and expressed as % of control [one-way ANOVA and Dunnett's post hoc test for multiple comparison, *p<0,05, **p<0,01, ***p<0,001 vs Control]. In (B), except for control, medium was supplemented with 10 µM resveratrol (RSV) (p=NS). In (C), cells, except for control, were treated with 10 µM β-amyloid. Data are plotted as means of 6-8 replicas ± SEM and expressed as % of control [two-way ANOVA and Dunnett's post hoc test for multiple comparison, **p<0.01, ***p<0.001 vs Control].*

The infusion with β-amyloid peptide 25-35 10 µM was more cytotoxic, being viability significantly reduced from by about 10-15% in both cell lines, if compared to vehicle (Control) (Figure 23 C, **P<0,01 vs Control in NG 108-15 cells, ***P<0,001 vs Control in U-87 MG). Treatment with T_1AM (1-10 µM) in combination with β-amyloid leads to a 15-25% reduction in viability in both cell lines (Figure 23 C, -15 % p<0.01, -25 % p<0.001 vs control). U-87 MG cell line seemed more sensible to the treatment with β-amyloid peptide as compared to NG 108-15 cells.

4.5.1.2 MTT TA_1

Cytotoxic effects were evaluated using MTT test in cells treated with different concentrations of TA_1 ranging from 0,1 to 10 µM. TA_1 was not cytotoxic and a significant increase, about 50%, was measured after treatment with TA_1 at 0,1 µM and 10 µM (*p<0,05, **p<0,01) in U-87 MG cell line, while no change was observed in NG 108-15 cell line (Figure 24).

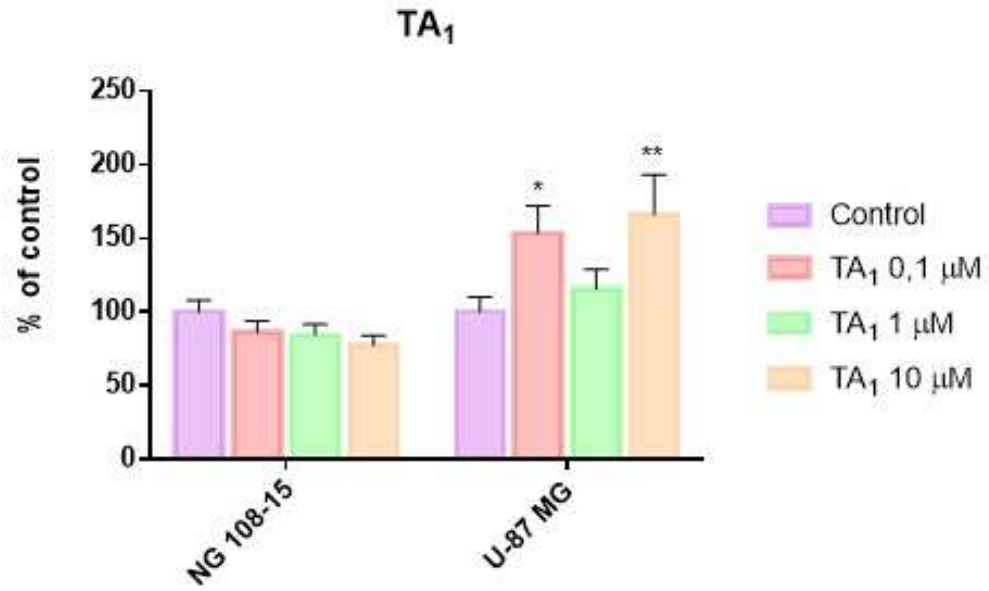

*Figure 24. Cell viability of NG 108-15 or U-87 MG cell lines after the treatment with TA_1 by using MTT test. Cells, except for control, were treated with TA_1 at concentration ranging from 0,01 µM to 10 µM. Control groups were incubated with medium containing the same volume of vehicle (DMSO). Data are plotted as means of 6-8 replicas ± SEM, and expressed as % of control [one-way ANOVA and Dunnett's post hoc test for multiple comparison, *p<0,05, **p<0,01 vs Control].*

4.5.2 Cristal Violet T_1AM

Since the MTT test focuses on the mitochondrial function, we used also a different cell viability assay, the crystal violet staining that measures cell adherence (Mossmann 1983).

Cells were treated with different concentrations of T_1AM (ranging from 10 nM to 10 µM) alone (Figure 25 A) and in association with Resveratrol (RSV) at concentration of 10 µM (Figure 25 B) or β-amyloid peptide 25-35 at concentration of 10 µM (Figure 25 C).

Our results indicated the absence of the marked cytotoxic effect observed previously in both cell lines using MTT test to assess cell viability, in fact we observed an increase in viability at T_1AM 0,1 µM (+25%, *p<0,05 vs Control) in NG 108-15 cells, while no changes were observed in U-87 MG cell lines (p=NS vs Control) (Figure 25 A).

In NG 108-15 cell line, a significant reduction in viability occurred only at T_1AM 0,1 μM in combination with RSV (Figure 25 B, -20%, p<0,01 vs Control), an effect that appeared reverted at higher concentration of treatment.

The infusion with β-amyloid does not appear cytotoxic, being viability increased in NG 108-15 cell line if compared to vehicle (Figure 25 C, p<0,05 vs Control).

Further investigations are needed to understand the reason for such contradictory results.

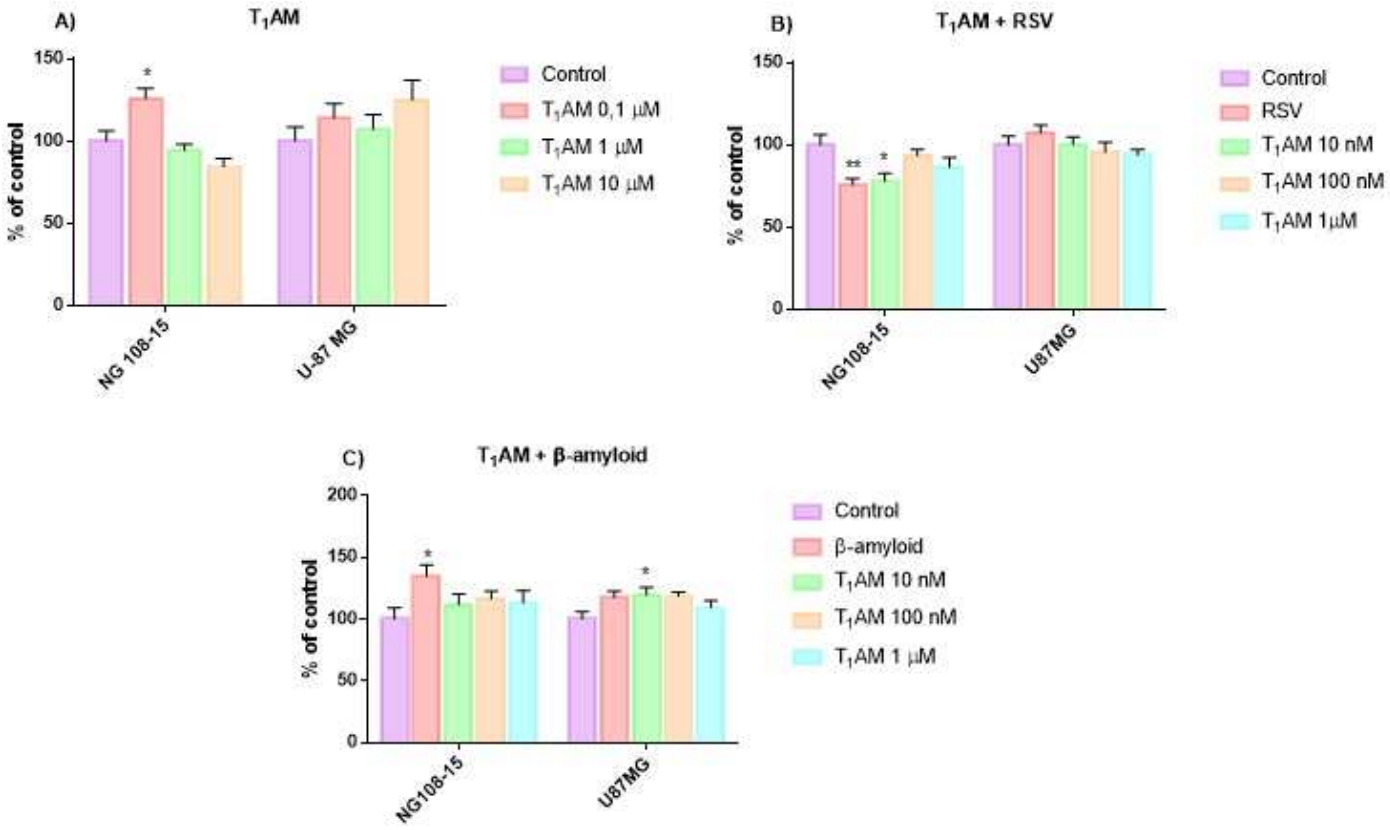

*Figure 25. Cell viability of NG 108-15 or U-87 MG cell lines after the treatment with T_1AM by using Cristal violet staining. In (A) cells, except for control, were treated with T_1AM at concentration ranging from 0,1 μM to 10 μM. In (B), except for control, medium was supplemented with 10 μM resveratrol (RSV). In (C), cells, except for control, were treated with 10 μM β-amyloid. Data are plotted as means of 6-8 replicas ± SEM, and expressed as % of control [one-way ANOVA and Dunnett's post hoc test for multiple comparison, *p<0,05 vs Control].*

4.6 Protein Expression

4.6.1 Effects of T_1AM

We investigated changes in expression and post-translational modifications of some proteins involved in the glutamatergic postsynaptic signaling, in NG 108-15 (Figure 26) and U-87 MG cells (Figure 27), upon infusion of T_1AM. Western blotting analyses were performed after 24 hours of treatment with T_1AM ranging from 0.1 to 10 µM, resulting in different effects according to the cell line.
The major effect highlighted in both cell lines was an increase in the phosphorylation of members of the signaling cascade, even though on different target proteins.

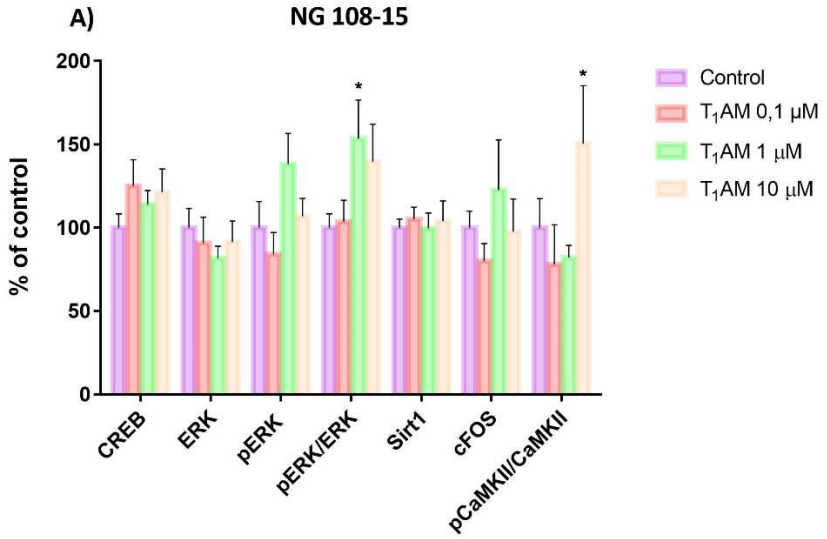

*Figure 26. Western blot to evaluate expression and post-translational modifications after treatment with T_1AM at concentration ranging from 0,1 µM to 10 µM in NG 108-15 cell line. Data are plotted as means of 3-4 replicas ± SEM, and expressed as % of control [one-way ANOVA, Dunnett's post hoc test for multiple comparison, *p<0,05 vs Control].*

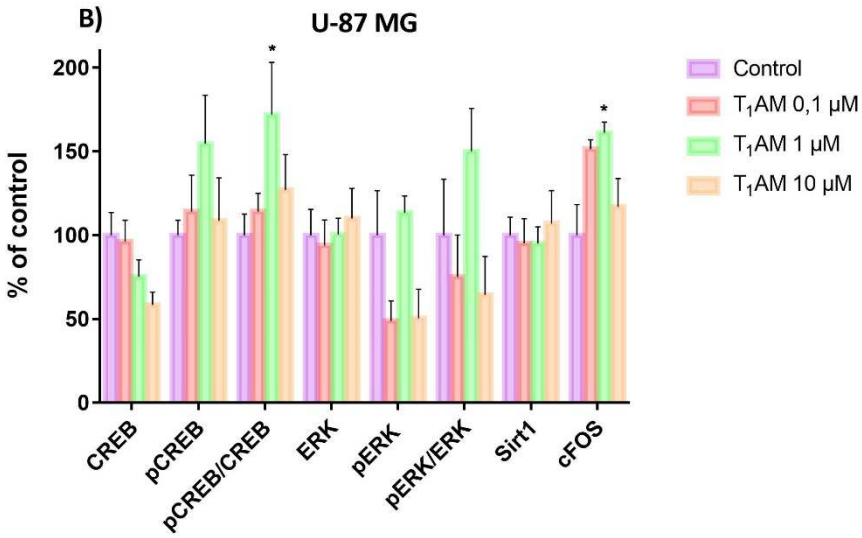

*Figure 27. Western blot to evaluate expression and post-translational modifications after treatment with T_1AM at concentration ranging from 0,1 µM to 10 µM in U-87 MG. Data are plotted as means of 3-4 replicas ± SEM, and expressed as % of control [one-way ANOVA and Dunnett's post hoc test for multiple comparison, *p<0,05 vs Control].*

In the NG 108-15 an increase in phosphorylation of ERK and CaMKII was observed at the highest T_1AM concentrations (Figure 28 C, 1 µM T_1AM, pERK/ERK + 60 %, *p<0.05 vs Control; Figure 29, 10 µM T_1AM, pCAMKII/CAMKII + 50 %, *p<0.05 vs control).

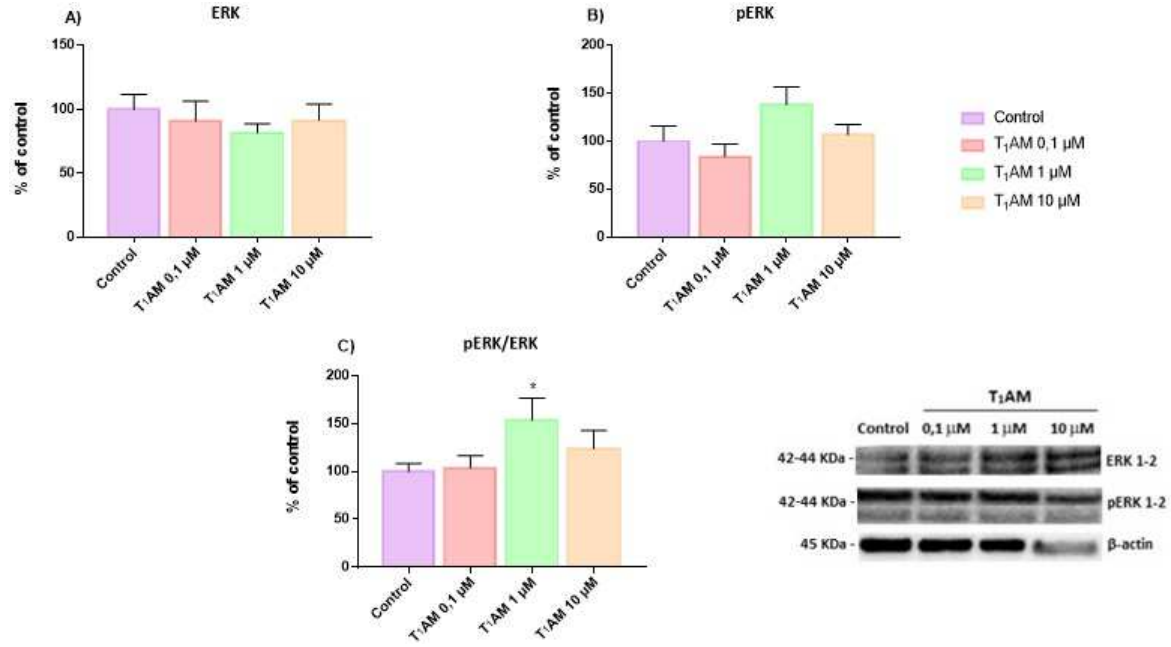

*Figure 28. Western blot to evaluate expression and post-translational modifications after the treatment with T_1AM in NG 108-15 cell line. (A) ERK expression (B) pERK expression. Data are plotted as means of 3-4 replicas ± SEM, and expressed as % of control [one-way ANOVA, Dunnett's post hoc test for multiple comparison, p=ND vs Control]. (C) ERK phosphorylation. Results are shown as the ration between the phosphorylated protein and the total expressed protein. Data are plotted as means of 3-4 replicas ± SEM and expressed as % of control [one-way ANOVA, Dunnett's post hoc test for multiple comparison, *p<0.05 vs Control].*

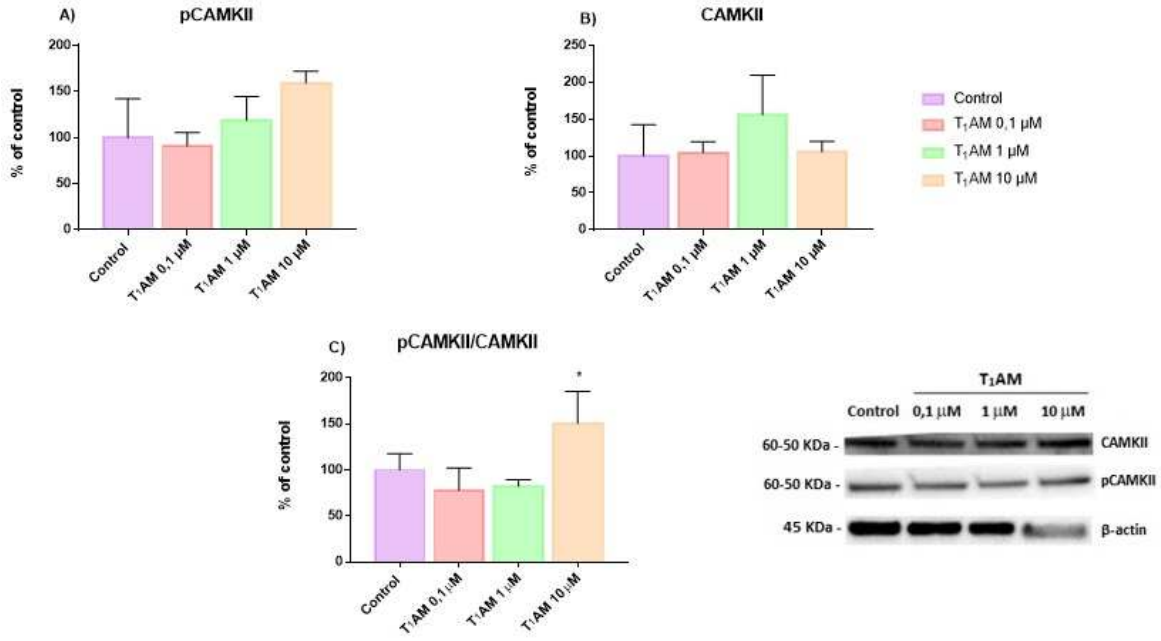

*Figure 29. Western blot to evaluate expression and post-translational modifications after the treatment with T_1AM in U-87 cell line. (A) CAMKII expression (B) pCAMKII expression. Data are plotted as means of 3-4 replicas ± SEM, and expressed as % of control [one-way ANOVA, Dunnett's post hoc test for multiple comparison, p=ND vs Control]. (C) CAMKII phosphorylation. Results are shown as the ration between the phosphorylated protein and the total expressed protein. Data are plotted as means of 3-4 replicas ± SEM and expressed as % of control [one-way ANOVA, Dunnett's post hoc test for multiple comparison, *p<0.05 vs Control].*

In U-87 MG, T_1AM induced the phosphorylation of the transcriptional factor CREB at 1 µM (Figure 30 C, pCREB/CREB + 70 %, *p<0.01 vs control) and an increase in expression of cFOS at 1 µM (Figure 31, cFOS, + 60% *p<0,01 vs control).

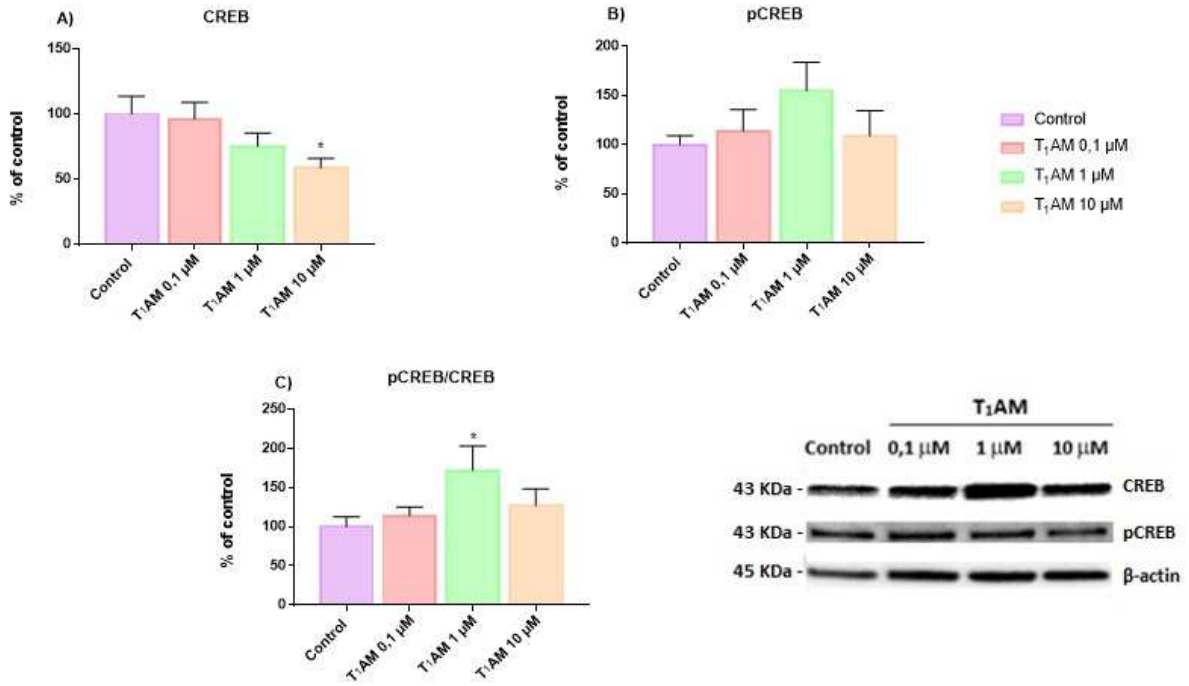

*Figure 30. Western blot to evaluate expression and post-translational modifications after the treatment with T_1AM in U-87 cell line. (A) CREB expression (B) pCREB expression. Data are plotted as means of 3-4 replicas ± SEM, and expressed as % of control [one-way ANOVA, Dunnett's post hoc test for multiple comparison, *p<0,05 vs Control]. (C) CREB phosphorylation. Results are shown as the ration between the phosphorylated protein and the total expressed protein. Data are plotted as means of 3-4 replicas ± SEM [one-way ANOVA, Dunnett's post hoc test for multiple comparison, *p<0.05 vs Control].*

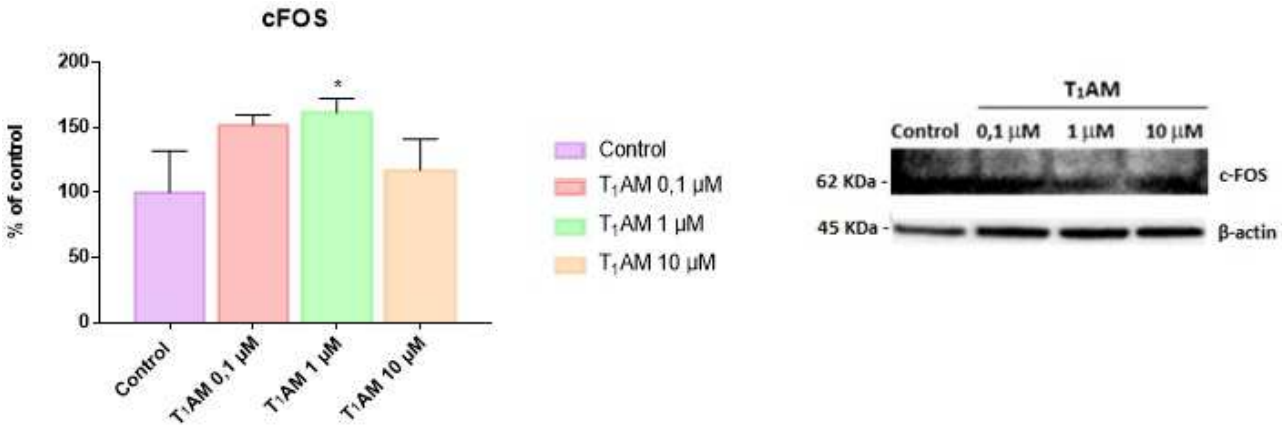

*Figure 31. Western blot to evaluate expression and post-translational modifications after the treatment with T_1AM in U-87 cell line. cFOS expression. Data are plotted as means of 3-4 replicas ± SEM and expressed as % of control. [One-way ANOVA, Dunnett's post hoc test for multiple comparison, *p<0.05 vs Control].*

Expression or post-translational modifications of other proteins were not affected.

4.6.2 Effects of TA_1

We also investigated changes in expression and post-translational modification of some proteins involved in the glutamatergic postsynaptic signaling, upon infusion of TA_1 in U-87 MG and NG 108-15 cell lines, resulting in different effects according to the cell line.

Western-blot analysis were performed after 24 hours of treatment with TA_1 at concentration of 0.1, 1 and 10 µM.

Western blot analysis indicated that in U-87 MG, upon infusion of pharmacological doses of TA_1, neither the expression of Sirtuin 1, (p=NS) nor the expression of ERK or post-translational modifications of ERK were changed (ERK, pERK, pERK/total ERK, p=NS) (Figure 32).

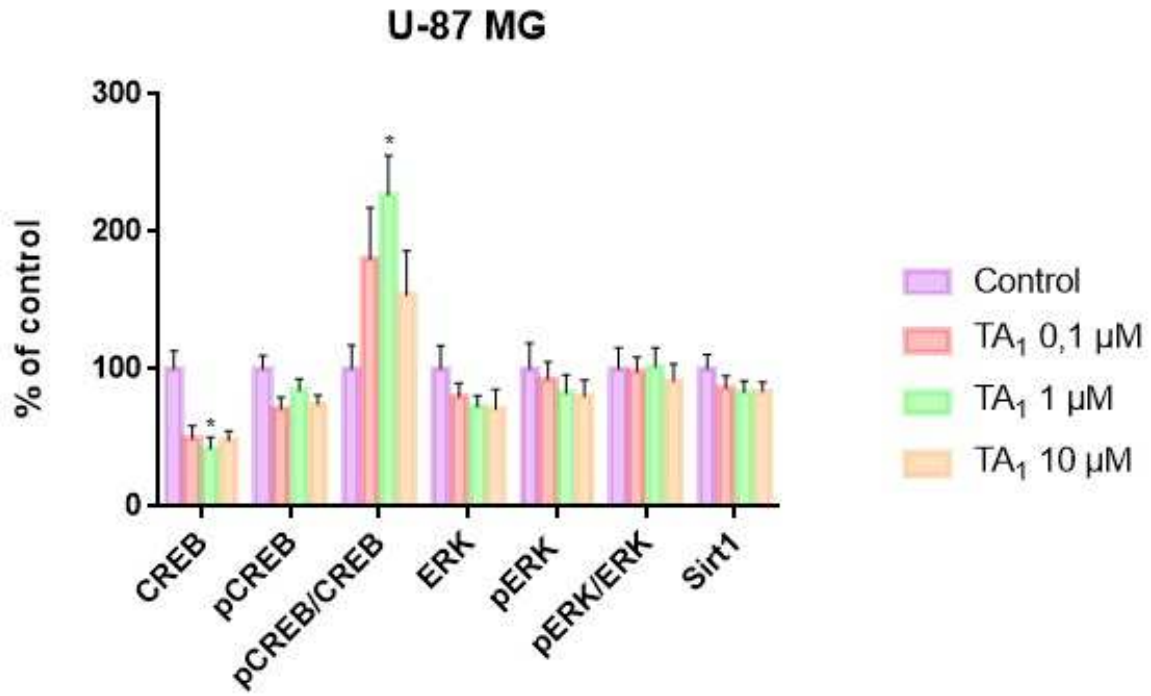

*Figure 32. Western blot to evaluate expression and post-translational modifications after treatment with TA_1 at concentration ranging from 0,1 µM to 10 µM in U-87 MG. Data are plotted as means of 3-4 replicas ± SEM, and expressed as % of control [one-way ANOVA, Dunnett's post hoc test for multiple comparison, *p<0,05, **p<0,01 vs Control].*

Instead, it was observed that TA_1 induced the phosphorylation of the transcriptional factor cAMP response element-binding protein (CREB) (+ 220%, *p<0,05, pCREB/total CREB vs control, Figure 33 C).

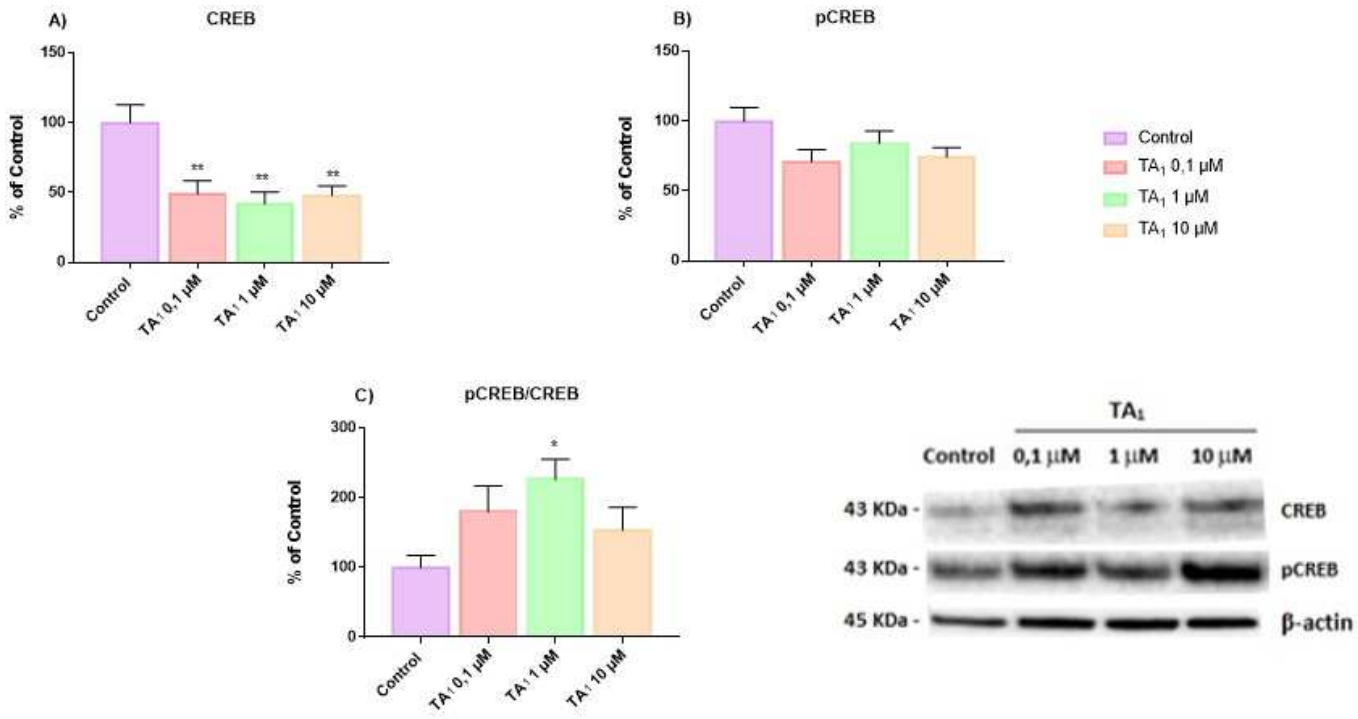

*Figure 33. Western blot to evaluate expression and post-translational modifications after the treatment TA_1 in U-87 cell line. (A) CREB expression (B) pCREB expression. Data are plotted as means of 3-4 replicas ± SEM, and expressed as % of control [one-way ANOVA, Dunnett's post hoc test for multiple comparison **p<0,01 vs Control]. (C) CREB phosphorylation. Results are shown as the ration between the phosphorylated protein and the total expressed protein. Data are plotted as means of 3-4 replicas ± SEM [one-way ANOVA, Dunnett's post hoc test for multiple comparison, *p<0.05].*

Preliminary analysis on protein expression and post-translational modification in NG 108-15 cells indicated that no modifications of ERK (pERK/total ERK, p=NS) were occurred (Figure 34).

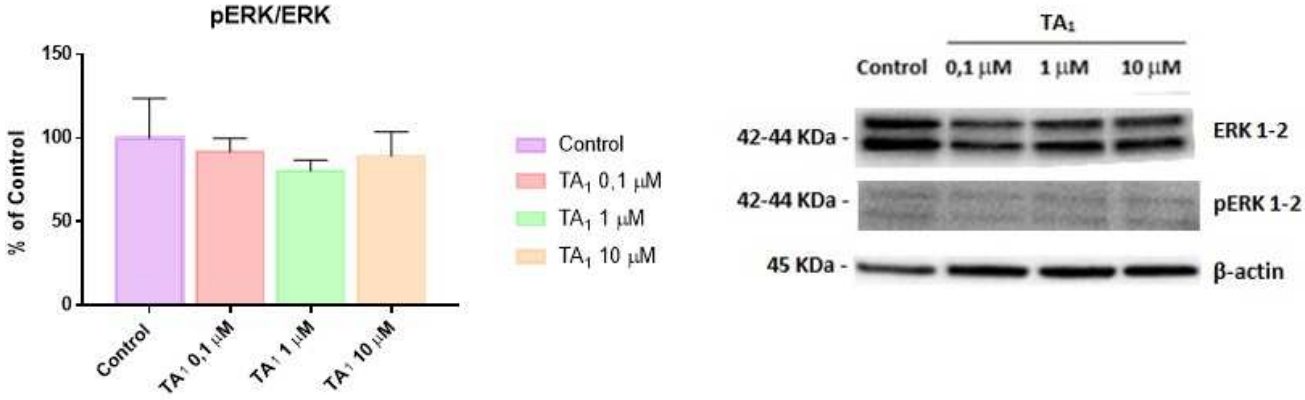

Figure 34. Western blot to evaluate expression and post-translational modifications after the treatment with TA_1 in NG 108-15 cell line. ERK. Results are shown as the ration between the phosphorylated protein and the total expressed protein. Data are plotted as means of 3-4 replicas ± SEM [one-way ANOVA, Dunnett's post hoc test for multiple comparison, p=NS].

Chapter 5 Discussion

In this project we firstly characterized the experimental model and then we evaluated the effects of T_1AM and TA_1 on postsynaptic glutamatergic system.

Our results indicated that NG 108-15 and U-87 MG cell lines expressed the main receptors of glutamatergic postsynaptic pathway, namely NMDAR1, GLUR2, EPHB2, but not NMDAR2B. TAAR1, the putative T_1AM receptor, was expressed only by U-87 MG cells, making NG 108-15 cell line a potential negative control for effects that can be mediated by this receptor.

To complete the validation of our models, we assessed the uptake of exogenous T_1AM and TA_1 production in cell medium and lysate at the end of treatment with T_1AM at different concentrations.

We observed that T_1AM, incubated in standard cell culture medium supplemented with FBS, was absorbed by U-87 MG and NG 108-15 cell lines, and catabolized to TA_1, one of the major T_1AM catabolites, indicating a strong metabolism of T_1AM, after 24 hours of infusion.

We observed that after 1 hour of treatment T_1AM was wide distributed into the cell, reaching extensively even the nucleus. Differently, TA_1 was measurable in all fractions of NG 108-15 cells, while in U-87 MG cells TA_1 was detected only in cytosol. These results indicated a wide distribution of T_1AM in cell and confirmed that different experimental models may produce diverse behaviors.

To exclude any potential endogenous production of thyronamines or derivative catabolites, the same experimental procedure was repeated with supplemented DMEM in absence of exogenous T_1AM, incubated alone or in presence of cells: neither T_1AM nor TA_1 were revealed.

The last step of cell characterization was to test T_1AM cytotoxicity. T_1AM showed a slight cytotoxic effect in both NG 108-15 and U-87 MG cells, as revealed from the MTT test, implying also a reduced oxidative metabolism. This effect increased in presence of β-amyloid 10 μM suggesting that in our models T_1AM did not counteract β-amyloid toxicity (Accorroni 2019, Tozzi 2021), but reduced by resveratrol, especially in NG 108-15 cells, indicating that this polyphenol may have a positive effect rescuing the decrease in cytotoxicity mediated by T_1AM and β-amyloid.

Since the MTT test focuses on the mitochondrial function, we used also a different cell viability assay, the crystal violet staining that measure cell adherence (Mossmann 1983), obtaining contradictory results, as compared to the previous ones.

Either NG 108-15 or U-87 MG cell lines expressed proteins associated to the glutamatergic system and they may be considered a simple *in vitro* model to evaluate T_1AM effects on its intracellular signaling cascade.

We investigated changes in expression and post-translational modifications of some of these proteins upon infusion of T_1AM and we showed that T_1AM was able to induce phosphorylation of nuclear factor CREB and increase the expression of cFOS in U-87 MG cells, while it was able to induce phosphorylation of CaMKII and ERK in NG 108-15 cell. These results indicated that infusion with exogenous T_1AM might alter the glutamatergic signaling cascade, albeit with different effects, depending on the in vitro model used.

CaMKII is a kinase activated by calcium ion, a key mediator in connecting transient calcium influx to neuronal plasticity, and its autophosphorylation at Thr-286 induces a persistent activation (Magupalli 2013). This kinase phosphorylates and activates different substrates, including the extracellular regulated kinase (ERK), a point of convergence of signals activated of long-term potentiation induction (Lynch 2004). ERK, in turn, leads to the activation of transcription factors, among them CREB and cFos, triggering the synthesis of new proteins. The transcriptional factor CREB is the heart of the glutamatergic signaling cascade, its activation at the end of the cascade leads to the transcription of factors fundamental for memory consolidation (Kida 2012). The observed increase of phosphorylation, induced by T_1AM may underly its prolearning effects.

Even though our hypothesis is not fully sustained by the increase of second messengers, namely cAMP and Ca^{2+}, whose concentration was almost unchanged, except for a significant decrease in intracellular calcium concentration in NG 108-15 cell line and an increase cAMP production in U-87 MG cell line, we can hypothesize that a crosstalk among pathways might occur.

Glucose is the main energetic substrate for the brain. Differences between cell lines were encountered in glucose consumption as well, that was slightly decreased after 4 hours by T_1AM from 1 μM in the hybrid cell line, while in presence of β-amyloid only 1 μM T_1AM increased glucose consumption, demonstrating a bell-shape dose-response as already observed in phosphorylation of ERKs and CREB and in other studies (Grandy 2007, Manni 2013), while U-87 MG cells were not affected. Assadi-Porter *et al*. (Assadi-Porter 2018) demonstrate that T_1AM can act as a regulator of both glucose and lipid metabolism in mice through Sirtuin-mediated pathways.

Both cell lines were tested for Sirtuin1 expression after T_1AM infusion, but no differences were observed, thus we can assume that in this model the metabolic effect is mediated by different pathway, but additional experiment will be needed to identify the specific signaling involved.

Both cell lines analyzed shared similar receptor pattern, except for TAAR1, which was not found in NG 108-15 line: this might account for difference in sensitivity towards exogenous T_1AM.

Notably most of significant effects was recorded at T_1AM 10 μM, which was the only concentration detectable after 24h in medium and lysate after 24 h. This indicated that effects could be attributable

to T_1AM rather than to its catabolite TA_1, even if more experiments will be needed to confirm this hypothesis.
Our biochemical observations are partially consistent with previous results (Bellusci 2017, Manni 2013): differences may be attributed to different circumstances, such as environmental conditions, cell stages/passages, subcellular localization, experimental models, and procedures.

In the second part of our investigations, we evaluated the effects of TA_1 one of the major products of oxidative deamination of T_1AM. TA_1, as previously observed in infusion with T_1AM, can be taken up by cells, while at low concentrations (0,1-1 μM) no further metabolism occurred, being the compound completely recovered. Differently, at 10 μM, TA_1 was further catabolized since it was recovered only partially, but only in presence of cells. No further metabolism was observed in supplemented DMEM when it is not exposed to cell metabolism, indicating that the metabolism was induced by the presence of cellular enzymes. It seems, in fact, that TA_1 is produced by oxidative deamination of phenylethylamine side chain of T_1AM forming an aldehydic intermediate which then can be further oxidized to 3-iodothyroacetic acid (TA_1) by the ubiquitously expressed NAD-dependent aldehyde dehydrogenase (Lorenzini 2017).
TA_1 did not affect cell viability, this could be explained by considering that no further oxidative deamination occurred in presence of TA_1 and consequently there was no production of hydrogen peroxide, ammonia or other compounds which are usually produced by MAO catalysis and can alter redox state of cell and induce cytotoxicity (Laurino 2018).
The results observed in presence of T_1AM were not repeated by TA_1 infusion. In fact, phosphorylation of proteins which were affected by T_1AM were unchanged by TA_1, except for the increase in phosphorylation of CREB, that occurs in U-87 MG at TA_1 1 μM.
This indicate that the effect produced by T_1AM were not influenced by the production of TA_1, in fact our preliminary results suggest that, in our experimental models, TA_1 does not seem to mimic T_1AM's effects, as well as widely described in literature.
In conclusion, we first characterized two brain cell models and then we tested the biochemical effects of T_1AM on the glutamatergic post synaptic cascade at pharmacological doses. These lines are unlimited auto-replicative source, easier to culture, albeit they suffer from the limitations induced by a cancer cell line. For this reason, the assessment of the overall effects of T_1AM should be extended to primary cell lines (astrocytes or primary hippocampal cells), and then to *in vivo* experimental models, which are more relevant and reflective of the original environment.

T_1AM demonstrates a very complex pharmacology, and an alteration in these signaling molecules or phosphorylation could not be its only primary effect, but also other mechanisms may be implicated.

However, T_1AM may emerge as a pharmacological agent in therapeutic strategies directed at improving biological processes mediated by the glutamatergic system.

Publications

Accorroni A, Rutigliano R, Sabatini M, Frascarelli S, Borsò M, Novelli E, **Bandini L**, Ghelardoni S, Saba A, Zucchi R and Origlia N. Exogenous 3-Iodothyronamine Rescues the Entorhinal Cortex from β-Amyloid Toxicity. *Thyroid*; 30(1): 147-160, 2020.

di Leo N, Moscato S, Borso' M, Sestito S, Polini B, Bandini L, Grillone A, Battaglini M, Saba A, Mattii L, Ciofani G and Chiellini G. Delivery of Thyronamines (TAMs) to the Brain: A Preliminary Study. *Molecules;* 26(6):1616, 2021.

Rutigliano G, **Bandini L**, Sestito S and Chiellini G. 3-Iodothyronamine and Derivatives: New Allies Against Metabolic Syndrome?. *Internal Journal of Molecular Sciences*; 21(6): 2005, 2020.

Sacripanti G, Lorenzini L, **Bandini L**, Frascarelli S, Zucchi R and Ghelardoni S. 3-Iodothyronamine and 3,5,3′-triiodo-L-thyronine reduce SIRT1 protein expression in the HepG2 cell line. *Hormone Molecular Biology and Clinical Investigation;* 41(1), 2020.

Saponaro F, Rutigliano G, Sestito S, **Bandini L**, Storti B, Bizzarri R and Zucchi R. ACE2 in the Era of SARS-CoV-2: Controversies and Novel Perspectives. *Frontiers in Molecular Biosciences*; 7: 588618, 2020.

References

Accorroni A, Rutigliano G, Sabatini M, Frascarelli S, Borsò M, Novelli E, Bandini L, Ghelardoni S, Saba A, Zucchi R and Origlia N. Exogenous 3-Iodothyronamine Rescues the Enthorinal Cortex from β-Amyloid Toxicity. *Thyroid;* 30(1): 147-160, 2019.

Accorroni A, Criscuolo C, Sabatini M, Donzelli R, Saba A, Origlia N and Zucchi R. 3-Iodothyronamine and trace amine-associated receptor 1 are involved in the expression of long-term potentiation in mouse entorhinal cortex. *European Thyroid Journal;* 5, 2016.

Accorroni A, Chiellini G and Origlia N. Effects of Thyroid Hormones and their Metabolites on Learning and Memory in Normal and Pathological Conditions. *Current Drug Metabolism;* 18: 225-236, 2017.

Accorroni A, Rutigliano G, Sabatini M, Frascarelli S, Borsò M, Novelli E, Bandini L, Ghelardoni S, Saba A, Zucchi R and Origlia N. Exogenous 3-Iodothyronamine Rescues the Entorhinal Cortex from b-Amyloid Toxicity. *Thyroid;* 30(1): 147-160, 2020.

Agretti P, De Marco G, Russo L, Saba A, Raffaelli A, Marchini M, Chiellini G, Grasso L, Pinchera A, Vitti P, Scanlan TS, Zucchi R and Tonacchera M. 3-Iodothyronamine metabolism and functional effects in FRTL5 thyroid cells. *Journal of Molecular Endocrinology;* 47(1): 23-32, 2011.

Assadi-Porter FM, Reiland H, Sabatini M, Lorenzini L, Carnicelli V, Rogowski M, Selen Alpergin ES, Tonelli M, Ghelardoni S, Saba A, Zucchi R and Chiellini G. Metabolic reprogramming by 3-iodothyronamine (T_1AM): a new perspective to reverse obesity through co-regulation of sirtuin 4 and 6 expression. *Internal Journal of Molecular Sciences;* 19(5): 1535; 2018.

Bartalena L and Robbins J. Thyroid hormone transport proteins. *Clinics in Laboratory Medicine;* 13(3): 583-598, 1993.

Bellusci L, Laurino A, Sabatini M, Sestito S, Lenzi P, Raimondi L, Rapposelli S, Biagioni F, Fornai F, Salvetti A, Rossi L, Zucchi R and Chiellini G. New insights into the potential roles of 3-iodothyronamine (T_1AM) and newly developed thyronamine-like TAAR1 agonists in neuroprotection. *Frontiers in Pharmacology;* 8: 905, 2017.

Bellusci L, Runfola M, Carnicelli V, Sestito S, Fulceri F, Santucci F, Lenzi P, Fornai F, Rapposelli S, Origlia N, Zucchi R and Chiellini G. Endogenous 3-Iodothyronamine (T_1AM) and Synthetic Thyronamine-Like Analog SG-2 Act as Novel Pleiotropic Neuroprotective Agents through the Modulation of SIRT6. *Molecules;* 25: 1054, 2020.

Bergh JJ, Lin HY, Lansing L, Mohamed SN, Davis FB, Mousa S and Davis PJ. Integrin aVb3 contains a cell surface receptor site for thyroid hormone that is linked to activation of mitogen-activated protein kinase and induction of angiogenesis. *Endocrinology;* 146(7): 2864-2871, 2005.

Bernal J, Guadaño-Ferraz A and Morte B. Thyroid hormone transporters-functions and clinical implications. *Nature Reviews Endocrinology;* 11(7): 406-417, 2015.

Bianco AC, Salvatore D, Gereben B, Berry MJ and Larsen PR. Biochemistry, cellular and molecular biology, and physiological roles of the iodothyronine selenodeiodinases. *Endocrine Reviews;* 23(1): 38-89, 2002.

Bliss TV and Lomo T. Long-lasting potentiation of synaptic transmission in the dentate area of the anaesthetized rabbit following stimulation of the perforant path. *The Journal of Physiology;* 232(2): 331-56, 1973.

Bradford MM. A rapid and sensitive method for the quantification of microgram quantities of protein utilizing the principle of protein-dye binding. *Analytical Biochemistry;* 72: 248-54, 1976.

Braulke LJ, Klingenspor M, DeBarber AE, Tobias SC, Grandy DK, Scanlan TS and Heldmaier G. 3-Iodothyronamine: a novel hormone controlling the balance between glucose and lipid utilisation. *Journal of Comparative Physiology B;* 178(2): 167-77, 2008.

Bräunig J, Dinter J, Höfig CS, Paisdzior S, Szczepek M, Scheerer P, Rosowski M, Mittag J, Kleinau G and Biebermann H. The Trace Amine-Associated Receptor 1 Agonist 3-Iodothyronamine Induces Biased Signaling at the Serotonin 1b Receptor. *Frontiers in Pharmacology;* 9: 222, 2018.

Brent GA. Mechanisms of thyroid hormone action. *Journal of Clinical Investigation;* 122(9): 3035-3043, 2012.

Chiamolera MI, Sidhaye AR, Matsumoto S, He Q, Hashimoto K, Ortiga-Carvalho TM and Wondisford FE. Fundamentally Distinct Roles of Thyroid Hormone Receptor Isoforms in a Thyrotroph Cell Line Are due to Differential DNA Binding. *Molecular Endocrinology;* 26: 926-939, 2012.

Chiellini G, Frascarelli S, Ghelardoni S, Carnicelli V, Tobias SC, DeBarber A, Brogioni S, Ronca-Testoni S, Cerbai E, Grandy DK, Scanlan TS and Zucchi R. Cardiac effects of 3-iodothyronamine: a new aminergic system modulating cardiac function. *Faseb Journal;* 21(7): 1597-608, 2007.

Chiellini G, Erba P, Carnicelli V, Manfredi C, Frascarelli S, Ghelardoni S, Mariani G and Zucchi R. Distribution of exogenous [125I]-3-iodothyronamine in mouse in vivo: relationship with trace amine-associated receptors. *The Journal of Endocrinology;* 213: 223-230, 2012.

de Escobar GM, Obregon MJ and del Rey FE. Iodine deficiency and brain development in the first half of pregnancy. *Public Health Nutrition*; 10(12A): 1554-1570, 2007.

Doyle KP, Suchland KL, Ciesielski TMP, Lessov NS, Grandy DK, Scanlan TS and Stenzel-Poore MP. Novel thyroxine derivatives, thyronamine and 3-iodothyronamine, induce transient hypothermia and marked neuroprotection against stroke injury. *Stroke;* 38(9): 2569-76, 2007.

Cumero S, Fogolari F, Domenis R, Zucchi R, Mavelli I and Contessi S. Mitochondrial F_0F_1-ATP synthase is a molecular target of 3-iodothyronamine, an endogenous metabolite of thyroid hormone. *British Journal of Pharmacology;* 166(8): 2331-2347, 2012.

Davis PJ, Davis FB and Cody V. Membrane receptors mediating thyroid hormone action. *Trends in Endocrinology and Metabolism;* 16: 429-435, 2005.

Davis PJ, Leonard JL and Davis FB. Mechanisms of nongenomic actions of thyroid hormone. *Frontiers in Neuroendocrinology;* 29(2): 211-218, 2008.

Davis PJ, Davis FB, Mousa SA, Luidens MK and Lin HY. Membrane receptor for thyroid hormone: Physiologic and pharmacologic implications. *Annual Review of Pharmacology and Toxicology;* 51: 99-115, 2011.

Davis PJ, Goglia F and Leonard JL. Nongenomic actions of thyroid hormone. *Nature Reviews of Endocrinology;* 12(2): 111-121, 2016.

DeBarber AE, Geraci T, Colasurdo VP, Hackenmueller SA and Scanlan TS. Validation of a liquid chromatography-tandem mass spectrometry method to enable quantification of 3- iodothyronamine from serum. *Journal of Chromatography A,* 1210(1): 55-59, 2008.

Deng H and Mi MT. Resveratrol Attenuates Aβ 25-35 Caused Neurotoxicity by Inducing Autophagy Through the TyrRS-PARP1-SIRT1 Signaling Pathway. *Neurochemical Research;* (9): 2367-79, 2016.

Dhillo WS, Bewick GA, White NE, Gardiner JV, Thompson EL, Bataveljic A, Murphy KG, Roy D, Patel NA, Scutt JN, Armstrong A, Ghatei MA and Bloom SR. The thyroid hormone derivative 3-iodothyronamine increases food intake in rodents. *Diabetes Obesity and Metabolism;* 11: 251-260, 2009.

Dinter J, Mühlhaus J, Wienchol CL, Yi C-X, Nürnberg D, Morin S, Grüters A, Köhrle J, Schöneberg T, Tschöp M, Krude H, Kleinau G and Biebermann H. Inverse Agonistic Action of 3-Iodothyronamine at the Human Trace Amine-Associated Receptor 5. *PLoS One;* 10(2): e0117774, 2015.

Dinter J, Mühlhaus J, Jacobi SF, Wienchol CL, Cöster M, Meister J, Hoefig CS, Müller A, Köhrle J, Grüters A, Krude H, Mittag J, Schöneberg T, Kleinau G and Biebermann H. 3-iodothyronamine differentially modulates α-2A-adrenergic receptor-mediated signaling. *Journal of Molecular Endocrinology;* 54: 205-216, 2015b.

Di Jeso B and Arvan P. Thyroglobulin From Molecular and Cellular Biology to Clinical Endocrinology. *Endocrine Reviews;* 37(1): 2-36, 2016.

Dratman MB. On the mechanism of action of thyroxin, an amino acid analog of tyrosine. *Journal of Theoretical Biology;* 46(1): 255-270, 1974.

Dunn JT and Dunn AD. Update on intrathyroidal iodine metabolism. *Thyroid;* 11: 407-414, 2001.

Feoktistova M, Geserik P and Leverkus M. Crystal violet assay for determining viability of cultured cells. *Cold Spring Harbor Protocols*; (4), 2016.

Fekete C and Lechan RM. Central regulation of hypothalamic-pituitary-thyroid axis under physiological and pathophysiological conditions. *Endocrine Reviews;* 35(2): 159-194, 2014.

Frascarelli S, Ghelardoni S, Chiellini G, Galli E, Ronca F, Scanlan TS and Zucchi R. Cardioprotective effect of 3-iodothyronamine in perfused rat heart subjected to ischemia and reperfusion. *Cardiovascular Drugs and Therapy;* 25(4): 307-313, 2011.

Frascarelli S, Ghelardoni S, Chiellini G, Vargiu R, Ronca-Testoni S, Scanlan TS, Grandy DK and Zucchi R. Cardiac effects of trace amines: Pharmacological characterization of trace amine-associated receptors. *European Journal of Pharmacology;* 587(1-3): 231-236, 2008.

Friedman TC, Loh YP, Cawley NX, Birch NP, Huang SS, Jackson IM and Nillni EA. Processing of prothyrotropin-releasing hormone (Pro-TRH) by bovine intermediate lobe secretory vesicle membrane PC1 and PC2 enzymes. *Endocrinology;* 136: 4462-447, 1995.

Gachkar S, Oelkrug R, Martinez-Sanchez N, Rial-Pensado E, Warner A, Hoefig CS, López M and Mittag J. 3-Iodothyronamine induces tail vasodilation through central action in male mice. *Endocrinology;* 158(6): 1977-1984, 2017.

Galli E, Marchini M, Saba A, Berti S, Tonacchera M, Vitti P, Scanlan TS, Iervasi G and Zucchi R. Detection of 3-iodothyronamine in human patients: a preliminary study. *The Journal of Clinical Endocrinology and Metabolism;* 97(1): E69-74, 2012.

Gereben B, McAninch EA, Ribeiro MO and Bianco AC. Scope and limitations of iodothyronine deiodinases in hypothyroidism. *Nature Reviews Endocrinology;* 11(11): 642-652, 2015.

Ghelardoni S, Suffredini S, Frascarelli S, Brogioni S, Chiellini G, Ronca-Testoni S, Grandy DK, Scanlan TS, Cerbai E and Zucchi R. Modulation of cardiac ionic homeostasis by 3-iodothyronamine. *Journal of Cellular and Molecular Medicine;* 13(9B): 3082-3090, 2009.

Ghelardoni S, Chiellini G, Frascarelli S, Saba A and Zucchi R. Uptake and metabolic effects of 3-iodothyronamine in hepatocytes. *Journal of Endocrinology;* 221(1): 101-110, 2014.

Giese KP and Mizuno K. The roles of protein kinases in learning and memory. *Learning and Memory;* 20: 540-552, 2013.

Gompf HS, Greenberg JH, Aston-Jones G, Ianculescu AG, Scanlan TS and Dratman TB. 3-Monoiodothyronamine: The rationale for its action as an endogenous adrenergic-blocking neuromodulator. *Brain Research;* 1351: 130-140, 2010.

Grandy DK. Trace amine-associated receptor 1-Family archetype or iconoclast? *Pharmacology and Therapeutics;* 116(3): 355-90; 2007.

Hackenmueller SA and Scanlan TS. Identification and quantification of 3-iodothyronamine metabolites in mouse serum using liquid chromatography-tandem mass spectrometry. *Journal of Chromatography A;* 1256: 89-97, 2012.

Hart ME, Suchland KL, Miyakawa M, Bunzow JR, Grandy DK and Scanlan TS. Trace amine-associated receptor agonists: synthesis and evaluation of thyronamines and related analogues. *Journal of Medicinal Chemistry;* 49(3): 1101-1112, 2006.

Hetzel BS. Iodine and neuropsychological development. *The Journal of Nutrition*; 130(2S Suppl): 493S-495S, 2000.

Hoefig CS, Köhrle J, Brabant G, Dixit K, Yap B, Strasburger CJ and Zida W. Evidence for extrathyroidal formation of 3-iodothyronamine in humans as provided by a novel monoclonal antibody-based chemiluminescent serum immunoassay. *The Journal of Clinical Endocrinology and Metabolism;* 96(6): 1864-1872, 2011.

Hoefig CS, Zucchi R and Köhrle J. Thyronamines and derivatives: Physiological relevance, pharmacological actions and future research directions. *Thyroid;* 26(12): 1656-1673, 2016.

Hoefig CS, Wuensch T, Rijntjes E, Lehmphul I, Daniel H, Schweizer U, Mittag J and Köhrle J. Biosynthesis of 3-Iodothyronamine From T_4 in Murine Intestinal Tissue. *Endocrinology;* 156(11): 4356-4364, 2015.

Hoefig CS, Renko K, Piehl S, Scanlan TS, Bertoldi M, Opladen T, Hoffmann GF, Klein J, Blankenstein O, Schweizer U and Köhrle J. Does the aromatic L-amino acid decarboxylase contribute to thyronamine biosynthesis? *Molecular and Cellular Endocrinology;* 349: 195-201, 2012.

Hoermann R, Midgley JE, Larisch R and Dietrich JW. Homeostatic Control of the Thyroid-Pituitary Axis: Perspectives for Diagnosis and Treatment. *Frontiers in Endocrinology;* 6: 177, 2015.

Ianculescu AG, Giacomini KM and Scanlan TS. Identification and Characterization of 3-Iodothyronamine Intracellular Transport. *Endocrinology;* 150: 1991-1999, 2009.

Ianculescu AG, Friesema EC, Visser TJ, Giacomini KM and Scanlan TS. Transport of thyroid hormones is selectively inhibited by 3-1190 iodothyronamine. *Molecular Biosystems;* 6: 1403-1410, 2010.

Jang SS and Chung HJ. Emerging Link between Alzheimer's Disease and Homeostatic Synaptic Plasticity. *Neural Plasticity;* 2016: 1-19, 2016.

Khajavi N, Reinach PS, Slavi N, Skrzypski M, Lucius A, Strauss O, Köhrle J and Mergler S. Thyronamine induces TRPM8 channel activation in human conjunctival epithelial cells. *Cell signalling;* 27: 315-325, 2015.

Khajavi N, Mergler S and Biebermann H. 3-Iodothyronamine, a novel endogenous modulator of transient receptor potential melastatin 8? *Frontiers in Endocrinology (Lausanne);* (8): 198, 2017.

Kida S, Josselyn SA, Peña de Ortiz S, Kogan JH, Chevere I, Masushige S and Silva AJ. CREB required for the stability of new and reactivated fear memories. *Nature Neuroscience;* (5): 348-355, 2002.

Kida S. A Functional Role for CREB as a Positive Regulator of Memory Formation and LTP. *Experimental Neurobiology;* 21(4): 136-40; 2012.

Klieverik LP, Foppen E, Ackermans MT, Serlie MJ, Sauerwein HP, Scanlan TS, Grandy DK, Fliers E and Kalsbeek A. Central effects of thyronamines on glucose metabolism in rats. *The Journal of Endocrinology;* 201: 377-386, 2009.

Köhrle J. The deiodinase family: Selenoenzymes regulating thyroid hormone availability and action. *Cellular and Molecular Life Sciences;* 57(13-14): 1853-1863, 2000.

Köhrle J. The Colorful Diversity of Thyroid Hormone Metabolites. *European Thyroid Journal;* 8(3): 115-129, 2019.

Köhrle J and Biebermann H. 3-Iodothyronamine - A Thyroid Hormone Metabolite With Distinct Target Profiles and Mode of Action. *Endocrine Reviews;* 40(2): 602-630, 2019.

Kumar A. Long-term potentiation at CA3–CA1 hippocampal synapses with special emphasis on aging, disease, and stress. *Frontiers in Aging Neuroscience;* 3(7), 2011.

la Cour JL, Christensen HM, Köhrle J, Lehmphul I, Kistorp C, Nygaard B and Faber J. Association Between 3-Iodothyronamine (T_1AM) Concentrations and Left Ventricular Function in Chronic Heart Failure. *The Journal of Clinical Endocrinology and Metabolism;* 104(4): 1232-1238, 2019.

Langouche L, Lehmphul I, Perre SV, Köhrle J and Van den Berghe G. Circulating 3-T_1AM and 3,5-T_2 in Critically Ill Patients: A Cross-Sectional Observational Study. *Thyroid;* 26(12): 1674-1680, 2016.

Larkin MA, Blackshields G, Brown NP, Chenna R, McGettigan PA, McWilliam H, Valentin F, Wallace IM, Wilm A, Lopez R, Thompson JD, Gibson TJ and Higgins DG. Clustal W and Clustal X version 2.0. *Bioinformatics;* 23(21): 2947-8, 2007.

Laurino A, De Siena G, Saba A, Chiellini G, Landucci E, Zucchi R and Raimondi L. In the brain of mice, 3iodothyronamine (T_1AM) is converted into 3iodothyroacetic acid (TA_1) and it is included within the signaling network connecting thyroid hormone metabolites with histamine. *European Journal of Pharmacology;* 761: 130-4, 2015.

Laurino A, De Siena G, Resta F, Masi A, Musilli C, Zucchi R and Raimondi L. 3-iodothyroacetic acid, a metabolite of thyroid hormone, induces itch and reduces threshold to noxious and to painful heat stimuli in mice. *British Journal of Pharmacology;* 172: 1859-1868, 2015b.

Laurino A, Matucci R, Vistoli G and Raimondi L. 3-Iodothyronamine (T_1AM), a novel antagonist of muscarinic receptors. *European Journal of Pharmacology;* 793: 35-42, 2016.

Laurino A, Landucci E and Raimondi L. Central Effects of 3-Iodothyronamine Reveal a Novel Role for Mitochondrial Monoamine Oxidases. *Frontiers in Endocrinology;* (9): 290; 2018.

Laurino A, Landucci E, Resta F, De Siena G, Pellegrini-Giampietro DE, Masi Mannaioni G and Raimondi L. Anticonvulsant and neuroprotective effects of the thyroid hormone metabolite

3-iodothyroacetic acid. *Thyroid;* 28: 1387-1397, 2018b.

Lee JS, Jang BS, Chung CM, Choi I, Kim JG and Park SH. In vivo molecular imaging of [125I]-labeled 3-iodothyronamine: a hibernation-inducing agent. *Applied Radiation and Isotope;* 73: 74-78, 2013.

Lynch MA. Long-term potentiation and memory. *Physiological Reviews;* 84(1): 87-136; 2004.

Lorenzini L, Ghelardoni S, Saba A, Sacripanti G, Chiellini G and Zucchi R. Recovery of 3-Iodothyronamine and Derivatives in Biological Matrixes: Problems and Pitfalls. *Thyroid;* 27(10): 1323-1331; 2017.

Lucius A, Khajavi N, Reinach PS, Köhrle J, Dhandapani P, Huimann P, Ljubojevic N, Grotzinger C and Mergler S. 3-Iodothyronamine increases transient receptor potential melastatin channel 8 (TRPM8) activity in immortalized human corneal epithelial cells. *Cellular signalling;* 28(3): 136-147, 2016.

Luongo C, Dentice M and Salvatore D. Deiodinases and their intricate role in thyroid hormone homeostasis. *Nature Reviews Endocrinology;* 15(8): 479-488, 2019.

Manni ME, De Siena G, Saba A, Marchini M, Dicembrini I, Bigagli E, Cinci L, Lodovici M, Chiellini G, Zucchi R and Raimondi L. 3-Iodothyronamine: a modulator of the hypothalamus-pancreas-thyroid axes in mice. *British Journal of Pharmacology;* 166(2): 650-658, 2012.

Manni ME, De Siena G, Saba A, Marchini M, Landucci E, Gerace E, Zazzeri M, Musilli C, Pellegrini-Giampietro D, Matucci R, Zucchi R and Raimondi L. Pharmacological effects of 3-iodothyronamine (T_1AM) in mice include facilitation of memory acquisition and retention and reduction of pain threshold. *British Journal of Pharmacology;* 168(2): 354-62; 2013.

Magupalli VG, Mochida S, Yan J, Jiang X, Westenbroek RE, Nairn AC, Scheuer T and Catterall WA. Ca2+-independent Activation of Ca2+/Calmodulin-dependent Protein Kinase II Bound to the C-terminal Domain of CaV2.1 Calcium Channels. *The Journal of Biological Chemistry;* 288(7): 4637-4648, 2013.

Matuszewski BK, Constanzer ML and Chavez-Eng CM. Strategies for the assessment of matrix effect in quantitative bioanalytical methods based on LC-MS-MS. *Analytical Chemistry*; 75: 3019-30, 2003.

Minatohara K, Akiyoshi M and Okuno H. Role of Immediate-Early Genes in Synaptic Plasticity and Neuronal Ensembles Underlying the Memory Trace. *Frontiers in Molecular Neuroscience;* 8: 78, 2015.

Moreno JC, Klootwijk W, Van Toor H, Pinto G, D'Alessandro M, Lèger A, Goudie D, Polak M, Grüters A and Visser TJ. Mutations in the Iodotyrosine Deiodinase Gene and Hypothyroidism. *New England Journal of Medicine;* 358(17): 1811-1818, 2008.

Moreno M, Giacco A, Di Munno C and Goglia F. Direct and rapid effects of 3,5-diiodo- L-thyronine (T_2). *Molecular and Cellular Endocrinology;* 458: 121-126, 2017.

Mosmann T. Rapid colorimetric assay for cellular growth and survival: application to proliferation and cytotoxicity assays. *Journal of Immunological Methods;* 65(1-2): 55-63, 1983.

Mullur R, Liu YY, and Brent GA. Thyroid hormone regulation of metabolism. *Physiological Reviews;* 94(2): 355-382, 2014.

Musilli C, De Siena G, Manni ME, Logli A, Landucci E, Zucchi R, Saba A, Donzelli R, Passani MB, Provensi G and Raimondi L. Histamine mediates behavioural and metabolic effects of 3-iodothyroacetic acid, an endogenous end product of thyroid hormone metabolism. *British Journal of Pharmacology;* 171(14): 3476-3484, 2014.

Oetting A and Yen PM. New insights into thyroid hormone action. *Best Practice and Research Clinical Endocrinology and Metabolism;* 21(2): 193-208, 2007.

Ortiga-Carvalho TM, Sidhaye AR and Wondisford FE. Thyroid hormone receptors and resistance to thyroid hormone disorders. *Nature Reviews Endocrinology;* 10(10): 582-91, 2014.

Ortiga-Carvalho TM, Chiamolera MI, Pazos-Moura CC and Wondisford FE. Hypothalamus-pituitary-thyroid axis. *Comprehensive Physiology;* 6(3): 1387-1428, 2016.

Feldt-Rasmussen U and Rasmussen AK. Thyroid hormone transport and actions. *Pediatric and Adolescent Medicine;* 11: 80-103, 2007.

Palha JA. Transthyretin as a thyroid hormone carrier: Function revisited. *Clinical Chemistry and Laboratory Medicine;* 40(12): 1292-1300, 2002.

Panas HN, Lynch LJ, Vallender EJ, Xie Z, Chen GL, Lynn SK, Scanlan TS and Miller GM. Normal thermoregulatory responses to 3-1255 iodothyronamine, trace amines and amphetamine-like psychostimulants in trace amine associated receptor 1 knockout mice. *Journal of Neuroscience Research;* 88(9): 1962-9, 2010.

Petrovic MM, Viana da Silva S, Clement JP, Vyklicky L, Mulle C, González-González IM and Henley JM. Metabotropic action of postsynaptic kainate receptors triggers hippocampal long-term potentiation. *Nature Neuroscience;* 20: 529-539, 2017.

Piehl S, Heberer T, Balizs G, Scanlan TS, Smits R, Koksch B and Köhrle J. Thyronamines are isozymespecific substrates of deiodinases. *Endocrinology;* 149(6): 3037-45, 2008.

Piehl S, Hoefig CS, Scanlan TS and Köhrle J. Thyronamines - Past, Present, and Future. *Endocrine Reviews;* 32: 64-80, 2011.

Pietsch CA, Scanlan TS and Anderson RJ. Thyronamines Are Substrates for Human Liver Sulfotransferases. *Endocrinology;* 148: 1921-1927, 2007.

Pittenger C, Huang YY, Paletzki RF, Bourtchouladze R, Scanlin H, Vronskaya S and Kandel EL. Reversible inhibition of CREB/ATF transcription factors in region CA1 of the dorsal hippocampus disrupts hippocampus-dependent spatial memory. *Neuron;* 34: 447-462, 2002.

Purves D, Augustine GJ, Fitzpatrick D, Hall WC and Lamantia A. Neuroscience. 2nd edition. *Sinauer Associates Inc,* 2001.

Refetoff S. Thyroid Hormone Serum Transport Proteins. *MDText.com, Inc.,* 2000.

Regard JB, Kataoka H, Cano DA, Camerer E, Yin L, Zheng Y-W, Scanlan TS, Hebrok M and Coughlin SR. Probing cell type–specific functions of Gi in vivo identifies GPCR regulators of insulin secretion. *The Journal of Clinical Investigation;* 117: 4034-4043, 2007.

Rege SD, Geetha T, Broderick TL and Babu JR. Resveratrol Protects β Amyloid-Induced Oxidative Damage and Memory Associated Proteins in H19-7 Hippocampal Neuronal Cells. *Current Alzheimer Research;* 12(2): 147-56, 2015.

Roberts EB and Ramoa AS. Enhanced NR2A subunit expression and decreased NMDA receptor decay time at the onset of ocular dominance plasticity in the ferret. *Journal of Neurophysiology;* 81(5): 2587-91; 1999.

Rowan MJ, Klyubin I, Cullen WK and Anwyl R. Synaptic plasticity in animal models of early Alzheimer's disease. *Philosophical Transactions of the Royal Society of London B Biological Sciences;* 358: 821-828, 2003.

Roy G, Placzek E and Scanlan TS. ApoB-100-containing lipoproteins are major carriers of 3-iodothyronamine in circulation. *The Journal of Biological Chemistry;* 287: 1790-1800, 2012.

Rutigliano G, Accorroni A and Zucchi R. The case for TAAR1 as a modulator of central nervous system function. *Frontiers in Pharmacology;* 8: 987, 2018.

Rutigliano G, Bandini L, Sestito S and Chiellini G. 3-Iodothyronamine and Derivatives: New Allies Against Metabolic Syndrome? *International Journal of Molecular Sciences;* 21(6): 2005, 2020.

Saba A, Chiellini G, Frascarelli S, Marchini M, Ghelardoni S, Raffaelli A, Tonacchera M, Vitti P, Scanlan TS and Zucchi R. Tissue distribution and cardiac metabolism of 3-iodothyronamine. *Endocrinology;* 151(10): 5063-5073, 2010.

Sacripanti G, Nguyen NM, Lorenzini L, Frascarelli S, Saba A, Zucchi R and Ghelardoni S. 3,5-Diiodo-l-Thyronine Increases Glucose Consumption in Cardiomyoblasts Without Affecting the Contractile Performance in Rat Heart. *Frontiers in Endocrinology;* 9:282, 2018.

Saponaro F, Sestito S, Runfola M, Rapposelli S and Chiellini G. Selective Thyroid Hormone Receptor-Beta (TRβ) Agonists: New Perspectives for the Treatment of Metabolic and Neurodegenerative Disorders. *Frontiers in Medicine (Lausanne);* 7: 331, 2020.

Scanlan TS, Suchland KL, Hart ME, Chiellini G, Huang Y, Kruzich PJ, Frascarelli S, Crossley DA, Bunzow JR, Ronca-Testoni S, Lin ET, Hatton D, Zucchi R and Grandy DK. 3-Iodothyronamine is an endogenous and rapid-acting derivative of thyroid hormone. *Nature Medicine;* 10(6): 638-42, 2004.

G.C. Schussler. The thyroxine-binding proteins. *Thyroid;* 10(2):141-149, 2000.

Snead AN, Santos MS, Seal RP, Miyakawa M, Edwards RH and Scanlan TS. Thyronamines inhibit plasma membrane and vesicular monoammine transport. *ACS Chemical Biology*; 2(6): 390-8, 2007.

Snead AN, Miyakawa M, Tan ES and Scanlan TS. Trace amine-associated receptor 1 (TAAR1) is activated by amiodarone metabolites. *Bioorganic and Medicinal Chemistry Letters*; 18: 5920-5922, 2008.

Song Y, Ruf J, Lothaire P, Dequanter D, Andry G, Willemse E, Dumont JE, Van Sande J and De Deken X. Association of duoxes with thyroid peroxidase and its regulation in thyrocytes. *The Journal of Clinical Endocrinology and Metabolism*; 95: 375-382, 2010.

Tai SSC, Sniegoski LT and Welch MJ. Candidate reference method for total thyroxine in human serum: Use of isotope-dilution liquid chromatography-Mass spectrometry with electrospray ionization. *Clinical Chemistry*; 48(4): 637-642, 2002.

Tai SSC, Bunk DM, White VE and Welch MJ. Development and evaluation of a reference measurement procedure for the determination of total 3,3,5-triiodothyronine in human serum using isotope-dilution liquid chromatography-tandem mass spectrometry. *Analytical Chemistry*; 76(17): 5092-5096, 2004.

Tozzi F, Rutigliano G, Borsò M, Falcicchia C, Zucchi R and Origlia N. T_1AM-TAAR1 signalling protects against OGD-induced synaptic dysfunction in the entorhinal cortex. *Neurobiology of Disease*; 151: 105271, 2021.

Vancamp P, Butruille L, Demeneix BA and Remaud S. Thyroid Hormone and Neural Stem Cells: Repair Potential Following Brain and Spinal Cord Injury. *Frontiers in Neuroscience*; 14: 875, 2020.

van der Spek AH, Fliers E and Boelen A. The classic pathways of thyroid hormone metabolism. *Molecular and Cellular Endocrinology*; 458: 29-38, 2017.

Venditti P, Napolitano G, Di Stefano L, Chiellini G, Zucchi R, Scanlan TS and Di Meo S. Effects of the thyroid hormone derivatives 3-iodothyronamine and thyronamine on rat liver oxidative capacity. *Molecular and Cellular Endocrinology*; 341(1-2): 55-62, 2011.

Visser TJ. Metabolism of thyroid hormone. *New Comprehensive Biochemistry*; 18: 81-103, 1988.

Voglis G and Tavernarakis N. The role of synaptic ion channels in synaptic plasticity. *EMBO Reports;* 7(11): 1104-1110, 2006.

Wirth EK, Sheu SY, Chiu-Ugalde J, Sapin R, Klein MO, Mossbrugger I, Quintanilla-Martinez L, Hrabe de Angelis M, Krude H, Riebel T, Rothe K, Köhrle J, Schmid KW, Schweizer U and Gruters A. Monocarboxylate transporter 8 deficiency: altered thyroid morphology and persistent high triiodothyronine/thyroxine ratio after thyroidectomy. *European Journal of Endocrinology*; 165: 555-561, 2011.

Yamada K and Nabeshima T. Animal models of Alzheimer's disease and evaluation of antidementia drugs. *Pharmacology and Therapeutics*; 88: 93-113, 2000.

Yen PM. Physiological and Molecular Basis of Thyroid Hormone Action. *Physiological Review*; 81(3): 1097-1142, 2001.

Zimmermann MB, Jooste PL and Pandav CS. Iodine-deficiency disorders. *Lancet*; 372(9645): 1251-1262, 2008.

Zucchi R, Accorroni A and Chiellini G. Update on 3-iodothyronamine and its neurological and metabolic actions. *Frontiers in Physiology*; 5: 402, 2014.

Zucchi R, Rutigliano G and Saponaro F. Novel thyroid hormones. *Endocrine*; 66(1): 95-104, 2019.